THREE DIMENSIONAL RECONSTRUCTION OF BONE SHAPES FOR COMPUTER AIDED DESIGN OF PROSTHESES SOCKETS

by

David G. Cooper

B.Sc. (Kinesiology), Simon Fraser University, 1979

A THESIS SUBMITTED IN PARTIAL FULFILLMENT OF

THE REQUIREMENTS FOR THE DEGREE OF

MASTER OF SCIENCE, KINESIOLOGY

in the Department

of

Kinesiology

SIMON FRASER UNIVERSITY

April 1986

APPROVAL

NAME: David Gow COOPER

DEGREE: M.Sc. Kinesiology

TITLE OF THESIS: Three Dimensional Reconstruction of Bone Shapes for Computer Aided Design of Prostheses Sockets

EXAMINING COMMITTEE:

Chairman: Professor M.V. Savage

Dr. James B. Morrison
Senior Supervisor

Dr. Arthur E. Chapman

Mr. James Foort

Dr. Geoffrey R. Fernie
West Park Hospital
Toronto, Ontario

Date Approved: 15 April 1986

PARTIAL COPYRIGHT LICENSE

I hereby grant to Simon Fraser University the right to lend my thesis, project or extended essay (the title of which is shown below) to users of the Simon Fraser University Library, and to make partial or single copies only for such users or in response to a request from the library of any other university, or other educational institution, on its own behalf or for one of its users. I further agree that permission for multiple copying of this work for scholarly purposes may be granted by me or the Dean of Graduate Studies. It is understood that copying or publication of this work for financial gain shall not be allowed without my written permission.

Title of Thesis/Project/Extended Essay

Three dimensional reconstruction of bone shapes for computer aided design of prostheses sockets

Author:

(signature)

David Gow Cooper

(name)

April 15/86

(date)

ABSTRACT

The objectives of this thesis were to develop and test procedures for modelling from selected anthropometric measures the size, shape and relative orientations of the bones that are contained within below knee artificial limb sockets.

Bone distribution is one of the primary determinants of socket shape. Pressure on the bone must be kept to a minimum while maintaining close contact to avoid excessive movement between the socket and the residual limb. A computer-aided display and sculpting system for design of sockets has been developed. This system reproduces the external surface shape of the residual limb from anthropometric measures. The procedures resulting from this thesis project will be used to assist in the design process by identifying and locating internal structures relative to the external shape.

Bone shapes of the tibia, fibula, patella and femur were generated by reproduction of cross section images by Computerized Tomography (CT). Images were produced at 4mm and 8mm intervals along the length of the bones. These images were digitized and transformed to a three dimensional computer image of each bone.

Uniform dilation, orthogonal, nonorthogonal and non-homogeneous procedures were developed for transforming the CT reference bone shapes to the shapes of amputees' bones.

The bone shapes from 6 amputees were reconstructed from the reference shapes. The actual bone shapes of the amputees were also measured directly by CT scan reconstruction. The transformed shapes were then compared with the directly measured shapes for determination of shape replication accuracy.

The scaling procedures did not consistently generate bone shapes that were more accurate than the original reference shapes. This is believed to be due to the considerable nonhomogeneous shape differences between bones of the same type. The most consistant scaling improvement was for the patella, which also demonstrated the least degree of nonhomogenity between bones. Some of the nonhomogeneous features between bones were identified. It is probable that improved nonhomogeneous scaling algorithms could replicate these shape differences.

ACKNOWLEDGEMENTS

First, I would like to express my appreciation for the guidance and tolerance of my colleagues in the Medical Engineering Resource Unit. As always, Jim Foort provided inspiration and support whenever it was needed. Carl Saunders provided assistance which helped relieve the frustrations associated with computers. Marg Bannon, Tom Steinke, Sylvia Mosterman and Blake Johnson all contributed to an environment which made this project possible and enjoyable.

I am indebted to the six amputees and to Blake Johnson who provided the reference shapes. Without the assistance of these gentlemen, the project would not have been possible. Their patience and cooperation is greatly appreciated.

The guidance of Dr. Morrison, Dr. Chapman and James Foort greatly enhanced the quality of this study. I am grateful for the profound effect they have had on my scholastic, research and design endeavors.

A special thank you to my wife Darcy. Her support and encouragement helped get me through the tough parts. More importantly, she covered for me on the home front. Her contribution was substantial.

Table of Contents

	Page
Title	i
Approval	ii
Abstract	iii - iv
Acknowledgements	v
Table of contents	vi- vii
List of tables	viii
List of figures	ix - x
Text	
Introduction	1
Review	4
Socket design and production	5
Socket types	5
Socket shape determinantes	7
Automated socket manufacture	11
Shape sensing techniques	13
a) Mechanical	13
b) Three-dimensional digitizers	14
c) Stereometric	15
d) Radiographic	24
e) Magnetic resonance imaging	28
Variability of bone geometry	29
Objectives	32
Methods	33
Reference bone shapes	34
Reference shape acquisition	34
Data format	35
Scaling procedures	37
Generation of transformation matrices	38
Scaling of the Patella	43
Scaling of the Fibula	44
Scaling of the Tibia	44
Scaling of the Femur	45
Testing the scaling procedure	47
Selection of subjects	47
Shape comparisons	48
Nonhommogenity of bone shapes	52
Positioning and orientation error calc.	53
Data acquisition error analysis	54

Page

Results 55
Subject description 56
Data acquisition errors 67
Digitizing variability 67
Computerized tomography 67
Reference point measurement 67
Comparison of amputees to reference shapes 69
Comparison of scaled reference bone shapes to amputee bone shapes 76
Bone positioning 86

Discussion 88

Conclusions 99

Appendices

I Bone shape variability plots 101

II Comparison plots for the scaling procedures giving the best results for each bone 125

III Bone shape comparison algorithm 149

Bibliography 153

List of Tables

		Page
1.	Subject demographics	56
2.	Subject residual limb and body dimensions and body weight	57
3.	Dimensions of the reference subject	58
4.	Reference point measurement variability	68
5.	Comparison of amputee to reference bone shapes .	70
6.	Comparison of scaled tibia to amputee bone shape as acquired by Computerized Tomography ..	77
7.	Comparison of scaled fibula to amputee bone shape as acquired by Computerized Tomography ..	78
8.	Comparison of scaled patella to amputee bone shape as acquired by Computerized Tomography ..	79
9.	Comparison of scaled femur to amputee bone shape as acquired by Computerized Tomography ..	80
10.	Positioning error	87

List of Figures

		Page
1.	The Patellar-Tendon-Bearing prosthesis without cosmetic cover	6
2.	Cross sections of the PTS socket	9
3.	Pressure sensitive areas on the below knee residual limb	9
4.	The stereophotography configuration	17
5.	The rasterstereographic configuration	19
6.	Schematic of Yamashita's Light Spot System	21
7.	The moire topography apparatus configuration ..	22
8.	CT scan x-ray source and sensor configuration	25
9.	Sample CT scan at the tibial condyle level	36
10.	The alignment and calibration jig that attached to the subject's limb	36
11.	Overview of the scaling procedure used to calculate the bone shapes	38
12.	The cylindrical coordinate system used when comparing bone shapes	49
13.	The dependence of mean difference and standard deviation on positioning of cross sections relative to each other	52
14.	The femur, patella, tibia and fibula reference shapes	59
15.	The bone shapes of subject JD, reconstructed from CT data	61
16.	The bone shapes of subject EH, reconstructed from CT data	62
17.	The bone shapes of subject BW, reconstructed from CT data	63
18.	The bone shapes of subject GS, reconstructed from CT data	64

Page

19. The bone shapes of subject FD, reconstructed from CT data 65

20. The bone shapes of subject DL, reconstructed from CT data 66

21. Reference point measurement variability verses order of measurement 68

22. Amputee tibia minus reference tibia 72

23. Amputee fibula minus reference fibula 73

24. Amputee patella minus reference patella 74

25. Amputee femur minus reference femur 75

26. Amputee minus uniform dilation tibia 82

27. Amputee minus uniform dilation fibula 83

28. Amputee minus uniform dilation patella 84

29. Amputee minus uniform dilation femur 85

INTRODUCTION

A lower limb prosthesis for below knee amputations consists of an artificial foot, a socket interface to the residual limb, a pylon connecting the foot to the socket in a specified orientation and a cosmetic cover. The socket, which is the concern of this project, has several built in features dependent on residual limb tissues and ambulation forces. The forces generated during ambulation must be distributed over areas of tissue tolerant of repetitive loading. To provide the necessary pressure distribution, the socket shape is different from the unloaded residual limb shape. The socket volume is reduced in areas that can take repetitive loading such as the muscles and patellar tendon, and is increased in the non-tolerant areas such as bone, (Barclay, 1969). Some prosthetic techniques constrict the proximal portion of the residual limb above the femoral condyles to provide suspension during non-weight bearing periods, (Lyquist, 1969). When the socket is put on the residual limb, soft tissues are distorted to accommodate the socket shape. To be applicable for prolonged use without severe discomfort the socket must fit the individual patient extremely well. Therefore, sockets are predominantly custom made.

It is estimated that there are between 250,000 and 300,000 amputees in North America, (Leavitt et al, 1972; Philadelphia, 1976). Below knee amputees constitute a substantial proportion of the amputee population. Estimates for western countries range between 37 and 64 per cent of amputations, (Ebskov, 1983;

Mandrup-Poulsen et al, 1982; Boontje, 1984).

Computer aided socket design (CASD) procedures are being developed at the Medical Engineering Resource Unit (MERU), University of British Columbia. These procedures are specific to below knee amputations. They involve modification of a standard socket shape to that necessary for the individual amputee. In its present format, the socket shape is scaled using several girth, length and circumference measurements of the residual limb. After scaling, local areas of the socket shape are modified interactively using a graphics cursor for input. The modifications account for non-homogeneous residual limb variations. The system is completed by a Computer Numerically Controlled (CNC) milling machine which carves the socket mould over which the socket is vacuum formed. This system is currently producing functional sockets on a limited experimental basis.

The CASD procedure is functioning with little information on the bone geometry of the residual limb; only girth and length measurements. As bone geometry and location are primary determinants of socket shape, information as to bone distribution in the amputees' residual limbs could greatly improve socket design procedures. The basis of this study was to develop and test a procedure for estimating the size, shape and relative orientation of the bones contained within the sockets used by below knee amputees.

The calculated bone shapes will automatically determine certain aspects of the socket shape. Graphic display of bone distribution within the residual limb in the interactive shape

modification program will aid the prosthetist by providing visual clues as to the internal structure of the residual limb. He will know exactly where to provide relief around bony protuberances, and he will know where he may cut away without infringing on the bone. This will reduce the time necessary to make the modifications and increase their accuracy.

REVIEW

The review section is in three parts. It begins with background information on socket design techniques, looking first at the various socket types, then the determinants of socket shape and a description of automated socket manufacturing procedures.

The second part covers techniques that could be used for determining the bone shapes in vivo. Techniques suitable for measuring the position of external landmarks, necessary for scaling bone shapes, and techniques for measuring bone shapes directly, are reviewed.

Finally, a knowledge of the variability of bone shapes is essential to understand the type and range of bone geometries that must be processed. The limited number of investigations on this subject are presented.

Socket Design and Production

Socket Types

A mosaic in the Cathedral of Lescar, France, depicts an amputee supported at the knee by a wooden pylon. This mosaic is believed to be from the Gallo-Roman era about 500 BC, it is the earliest recorded lower limb prosthesis, (Gardner, 1970). The socket was likely fashioned out of wood, the dominant technique up to about 25 years ago when plastics became popular. Some sockets are still carved out of wooden blocks.

The sculpting procedures used to obtain socket shapesare very much an artisan activity. Not surprisingly, the shapes produced by different prosthetists vary considerably, depending on individual preferences. Surgical procedures also vary, resulting in differences in residual limb shapes. None the less, there is one generalized technique for below knee socket design that is followed almost universally. It is the Patellar-Tendon-Bearing (PTB) socket developed at Berkeley by Radcliffe and Foort, (1961). The PTB prosthesis (figure 1) is so named because the majority of weight bearing was thought to be by the patellar tendon which is well suited for the purpose. The PTB socket is a replica of the residual limb, deformed in specified areas to transmit forces in a manner suitable for ambulation and comfortable to the amputee.

Since introduction of the PTB socket there have been a number of variants. One that survived was the Patellar-Tendon Supra-Condylar Suspension Socket (PTS). It was introduced in 1964 by Fajal, (Pierquin et al, 1964, 1965, figure 2).

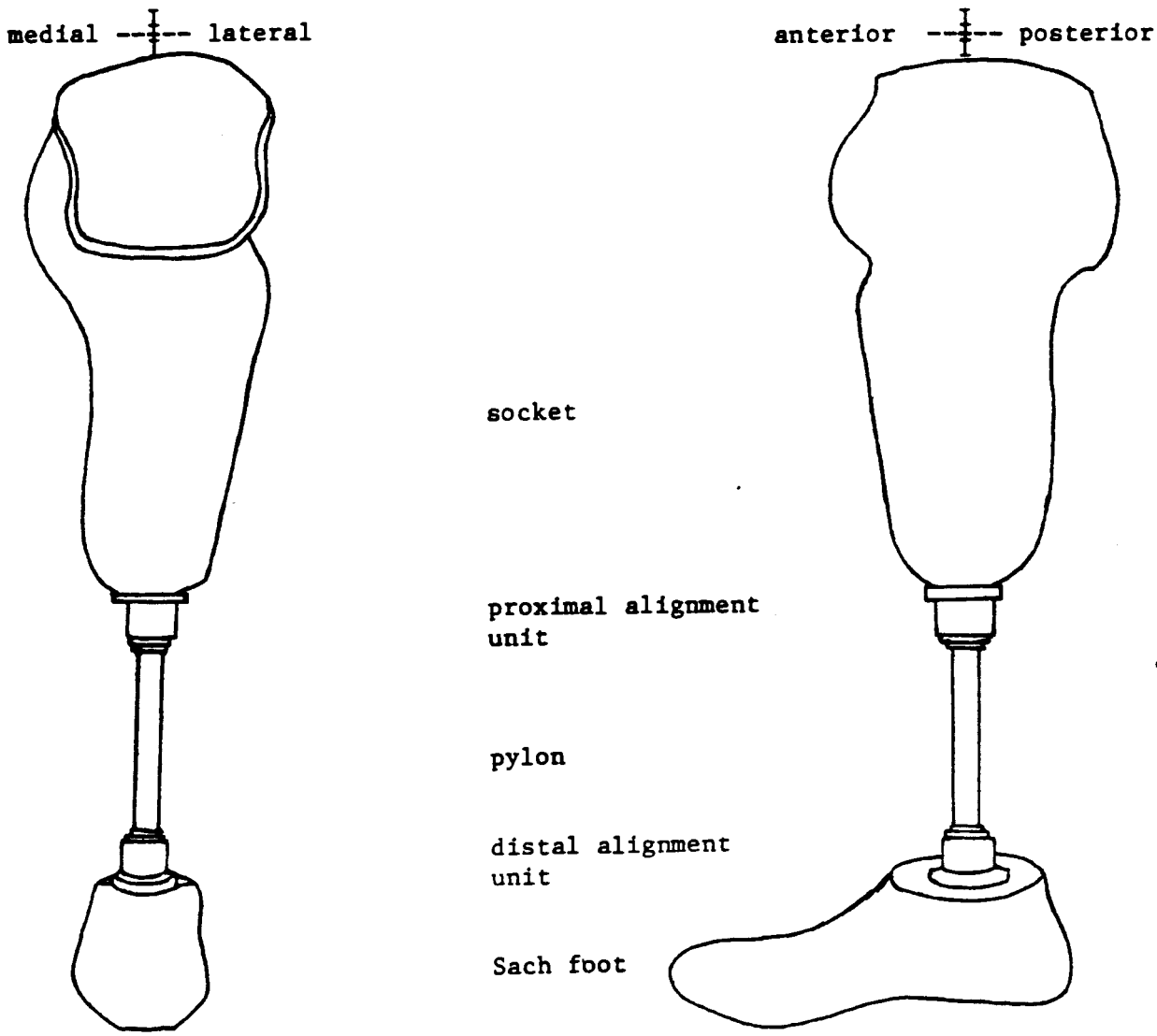

Figure 1: The Patellar-Tendon-Bearing prosthesis, without cosmetic cover.

The PTS socket encloses the entire patella and a major part of the femoral condyles whereas the PTB socket extends to mid patella and only slightly proximal to the mid level of the femoral condyles. The PTS socket improved suspension by hooking over the superior edges of the patella and femoral condyles, and distributed lateral forces over a larger area. Many modern day sockets are a compromise of these two types. They are like a PTS socket but do not enclose the patella.

Another variant is prefabricated sockets of standard shape. These were first introduced by Foort in 1967. They consisted of a range of 19 left and 19 right below knee sockets with a 1/8 inch increment between socket radii. The original prefabricated sockets did not follow the nonhomogeneous shape changes of a maturing stump. Though some developers (Breakey, 1973) have addressed this problem, prefabricated sockets remain suitable for new amputations only. They are appropriate for about 75% of the new below knee population.

There have been several other variants to the PTB socket such as wedge inserts for suspension (Kuhl 1966) and an air cushion total contact socket (Wilson et al 1968, 1984). Both of these are based on modifications of the original PTB principles but have played a minor role in the clinical setting.

Socket Shape Determinants

Bone distribution is most critical in terms of tolerances that must be maintained in contact areas. Pressure on the bone must be kept to a minimum while maintaining close contact to

avoid excessive movement between the socket and the residual limb. Figures 2 and 3 demonstrate the dependence of socket shape on bone distribution. Except for the hamstring tendons all the pressure sensitive areas are where the bone is near the surface. The socket must fit these areas intimately.

In conventional techniques, prosthetists derive the socket shape by casting the residual limb shape in plaster bandages. This negative cast is used to form a positive cast which is modified to form a mould over which the socket is made. The modifications change the cast shape such that pressures between the socket and residual limb are distributed in a modified configuration.

When shaping the mould, the prosthetist usually does not modify the cast in areas corresponding to bony areas. These are the tibial crest, the medial tibial flare, the inferior surfaces of the tibial condyles, the patella and the femoral condyles and epicondyles, (Barclay, 1969). Exceptions to this are the areas over the tibial tubercle and fibular head which may be increased slightly to provide pressure relief. Reductions in socket volume are made on the medial side from below the tibial flare to within 2.5 centimeters of its distal end, and on the lateral side from just below the fibular head to within 1 centimeter of its distal end. These reductions in volume provide stabilization of the residual limb relative to the socket.

Most patients can bear from 15 percent to 45 percent of their weight on the stump end when wearing their socket, (Katz et al, 1979). The shape of the distal end of the socket is

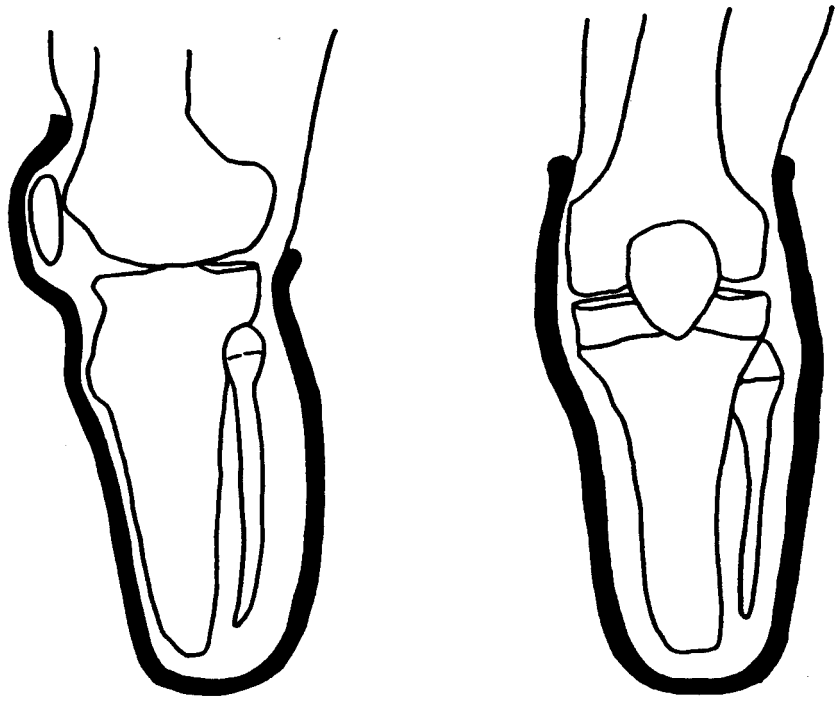

Lateral View Anterior View

Figure 2: Cross sections of the PTS socket.

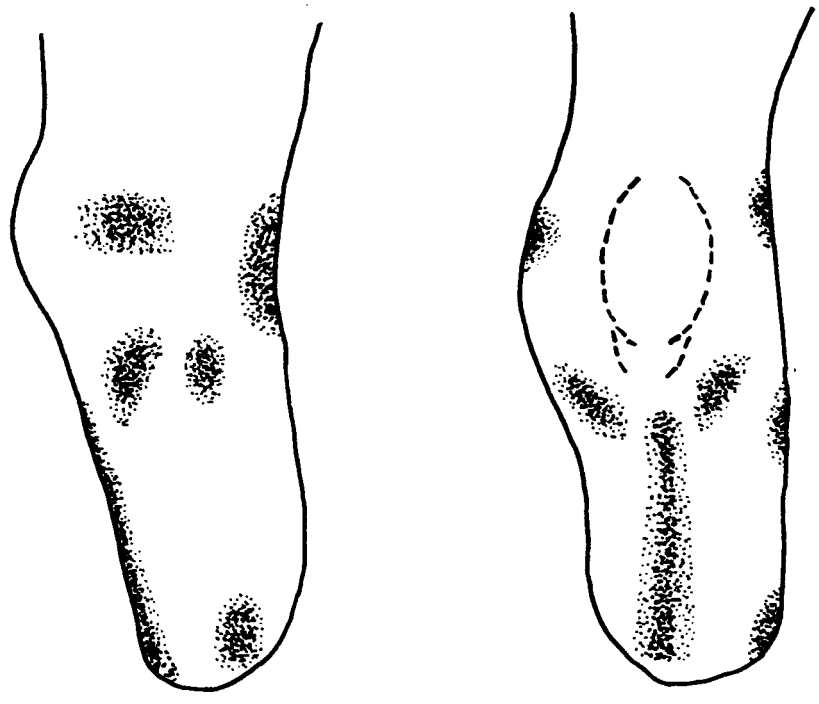

Lateral View Anterior View

Figure 3: Pressure sensitive areas on the below knee residual limb.

critical such that it provides some support without applying too much pressure to the end of the tibia and fibula. Most of the amputee's weight is supported by the medial tibial flare and the patellar tendon, (Barclay,1979).

In PTB sockets there is a reduction in volume in the area of the patellar tendon to transfer more weight bearing to the tendon, this is called the patellar bar. The prosthetist locates the patellar bar during the casting procedure by pressing in on either side of the tendon with both thumbs as the plaster wrap hardens. This locating technique is not available in the CASD procedures. The location of the tubercle and distal aspect of the patella are essential for this procedure. This requires that not only the bones' shape be determined within 1 or 2 millimeters, but also their orientation relative to each other. In the PTS socket, a similar reduction in socket volume is done over the medial femoral condyle to keep the socket on during swing phase while walking.

Sockets are designed in a specified amount of knee flexion, usually with a thigh-shank angle of 10 to 20 degrees, (Lyquist, 1969). Therefore, the relative position of bones is only required in one static position.

Muscle is secondary to bone distribution in determining socket shape. Being a viscoelastic material the muscle can be shaped by the socket to a limited extent. Thus, the major concern for muscle is that the appropriate socket volume is provided in a fairly standard shape. Any gaps between the socket and residual limb will enable movement between them. This leads

to an inefficient transfer of the forces during ambulation, poor suspension during swing phase and discomfort due to chafing. Too small a socket volume results in discomfort or an inability to put the socket on. To get the correct socket volume, traditional prosthetic practices involve taking several circumferential measurements down the full length of the residual limb and matching the socket mould to these.

Automated Socket Manufacture

The computer-aided display and sculpting system for use in prosthetics being developed at MERU is the only one of its kind, (Saunders and Fernie 1984, Saunders et al 1984, Saunders and Dean 1984, Saunders et al 1985). This system has been designed, as much as possible, to be compatable with current prosthetic practices. The system software allows systematic modification of a reference socket shape using techniques analogous to those used by a prosthetist working with rasps and plaster.

The first stage in the Computer Aided Socket Design (CASD) package is the recording of amputee stump measurements. On the basis of these measurements the reference socket shape is scaled in size longitudinally and transversely. The operator may then view the scaled primitive socket and make interactive fine modifications to it. As the prosthetist sculpts the primitive socket the CASD software keeps track of each modification by storing the modification particulars on disk. Once the prosthetist has completed his modifications the fully modified socket shape is also stored.

A second program converts the socket data into a series of commands which instruct a computer-numerically-controlled (CNC) milling machine to carve a positive model of the designed socket. The Rapidform (Lawrence et al 1981) microprocessor-controlled vacuum former for prosthetics is then used to produce the final polypropylene socket.

There are 3 principal benefits to the automated prosthetic procedures. First, there is a reduction in the time required to produce a socket from 3 to 4 hours to less than 2 hours. Second, every time an amputee requires a socket, averaging once every 2 years, his current socket shape is stored and available for minor modifications. Third, automation of the shape management process will capture the important aspects of current artisan methods and overcome their inefficiencies.

Shape Sensing Techniques

Human proportionality modelling is a long standing tradition. Polykeitos in 750 B.C. arbitrarily constructed a canon showing ideal proportions, which he had produced by combining the most aesthetically pleasing parts of 23 males, (Ross et al, 1982). His resultant sculpture has been used by artists as a model for centuries. Though subjective, this artisan approach is a form of shape sensing. Actually, the shape handling practices of prosthetists today are not very far removed from the techniques Polykleitos would have used in 750 B.C.. However, shape sensing, as applied to the human body, has advanced considerably. There are several techniques worth consideration.

a) Mechanical

Shapes can be described by a series of points that lie on the surface of the shape. The number of points required to describe the shape is dependent on the complexity of the shape and on its application. A flat surface can be described precisely by a few points while during development of the MERU CAD/CAM system it was found that at least 2,000 points are required to give a reasonable approximation of a socket shape shape. Mechanical shape sensors measure these points directly. This is usually done by touching the point in question with a stylus, then noting the position of the stylus through the orientation of some mechanical linkage to an arbitrary origin. The location of each point must be described by three cartesian

or cylindrical coordinates.

Obviously, this technique cannot be used to measure in vivo bone shapes. But, it can be used to measure external landmarks that are used in scaling procedures.

To measure a complex shape using a mechanical sensor is slow and tedious. Two days were required to measure a socket shape by this technique at the MERU. For that reason alone this technique does not lend itself to clinical application. However, the mechanism and its application are rather unsophistocated. Therefore, it does lend itself to limited number applications and when only simple shapes need be described.

b) Three Dimensional Digitizers

Three dimensional digitizers permit direct coordinate input into computers. Their principle application is for data input to computer aided design systems. There are several commercially available digitizers designed for small rigid objects which have limited applicability to clinical situations.

The most common type of 3-D digitizer is a stylus on a mechanical linkage that is instrumented to keep track of where the stylus point is in space. The instrumentation is usually potentiometers. For example, the Space Tablet by Micro Control Systems, comes with either 3 or 4 arms and respectively 3 or 4 potentiometers. The working volume is a sphere quadrant of approximately 16 inch radius. Three noncommercial digitizers of this type that are more appropriate for digitizing body parts are the Bio-Curve Tracer, (Kondraske et al, 1984), which has an

extended working volume, the MERU Anthropometer, (Saunders 1986, Saunders et al 1986), and a self propelled system for digitizing hand shapes by Saito and Oshima (1984).

The MERU Anthropometer has 5 rotational joints using optical encoders rather than potentiometers. A micro processor is used to calculate and store the coordinates of the stylus. After data collection is completed, the data is down loaded to a host computer. During measurement procedures an internal speech synthesizer "speaks" a preprogrammed sequence of instructions, via headphones, to the operator.

Another type of 3-D digitizer is one using a magnetic position and tracking system. This system was originally designed for military targeting purposes where the fighter pilots head position was monitored to determine the line-of-sight to a target, (Raab et al, 1979). This technology has been adapted into a three dimensional digitizer and a space tracker with clinical applicability; both are marketed by the Polhemus Navigation Sciences Division of McDonnell Douglas Electronics Co.

A third type of 3-D digitizer is a vector stereograph. These have been produced in various formats. One, as reported by Pynsent et al, (1983), consisted of 3 multiturn potentiometers mounted at the apices of a triangle with sides of approximately 1.5 meters. The potentiometers were connected to constant-torque spring-loaded bobbin reels wound with nylon thread. The free ends of the thread were brought together at a plastic pointer. The position of the pointer in space was determined through

computer monitoring of the 3 potentiometers.

c) Stereometric

Contact-free measurements of body surfaces are mainly performed using stereometric techniques based on distance measurements by triangulation. The most common of these techniques is stereophotography, though more recently rasterstereography and moire topography are gaining greater acceptance as shape measurement tools in the clinical setting.

Stereophotography

In stereophotography 2 photographs of the surface in question are taken simultaneously, (figure 4). The position of a point on the surface can be calculated from the known location of the cameras and the position of the image of the point on each film. Video cameras and landmark markers may be used to enable automated data processing.

Advantages of stereophotography are that it does not require extensive amounts of equipment, it has an acceptable accuracy, (Ayoub et al 1970, Pierrynowski and Morrison 1980, 1985), it is suitable for motion analysis and it is well known and understood.

There are two drawbacks to this technique. Each point to be located must be visible and identifiable on both films. Stereophotography is suitable for biomechanical analyses since the spatial relationship of a limited number of landmarks is required. The landmarks can be marked on the subject such that

they are visible during subsequent analysis. The same is not true if sufficient points to describe an anatomical shape are required. Identifying a large number of points is not practical. Since the points in question must be visible to both cameras, if points on more than one side of the object are required then additional equipment and more complicated analysis are necessary. If a point to be measured is in a concavity then the separation of the cameras is limited to ensure the point can be seen by both. As the cameras become closer together sensitivity to digitizing errors is increased. This is true of all triangulation techniques.

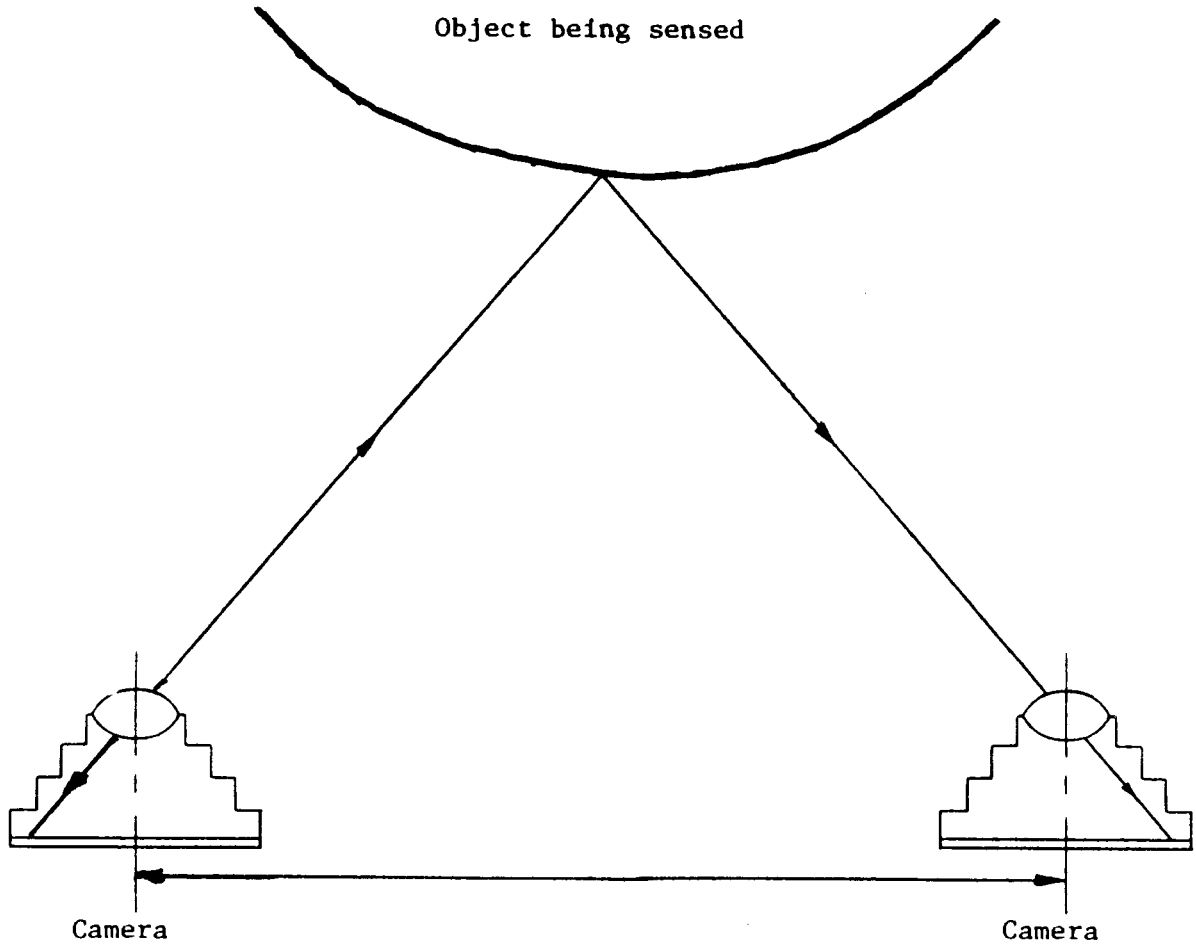

Figure 4: The stereophotography configuration.

Rasterstereography

Rasterstereography is very similar to stereophotography except that one of the cameras is replaced by a projector with a raster diapositive, (figure 5). The raster is in the form of a grid of known increment. The raster makes one of the film images of the stereophotographic technique a constant. This simplifies analysis to a single camera image. Identification of common points from the raster and film is possible by determination of the row and column numbers of the raster intersections. Thus, measurement of the many points necessary to describe a shape is possible. The resolution of measurement is dependent on the spacing on the grid. In addition, due to the simple image pattern, automatic processing of the image pattern is relatively simple. It is also possible to use a line raster rather than a grid, (Hierholzer and Frobin, 1981). The accuracy of this technique is reported to be in the order of 0.5 millimeters.

The concept of rasterstereography resulted from discussions concerning improvements of moire topography, (presented below). First results obtained with this rasterstereographic method were published by Frobin and Hierholzer in 1978.

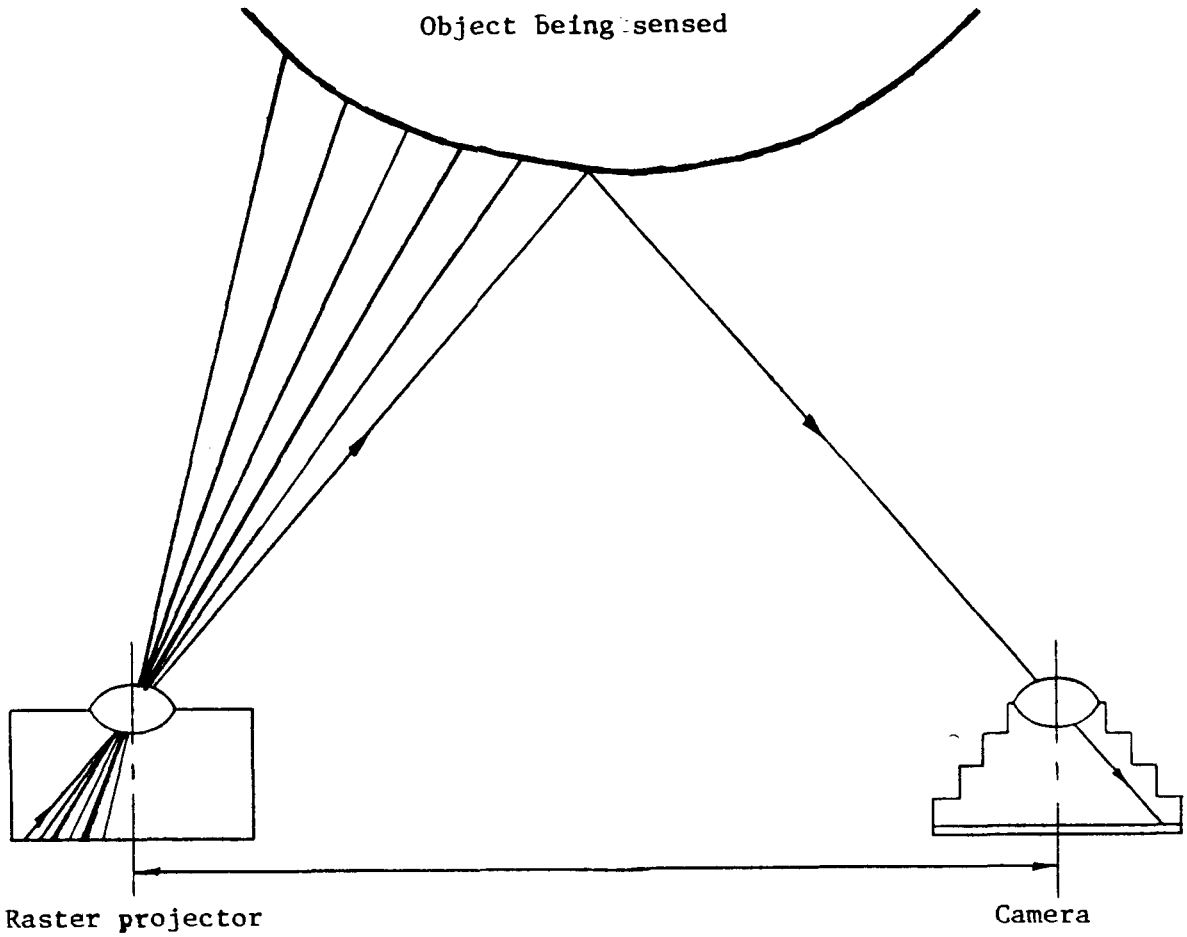

Figure 5: The rasterstereographic configuration.

Light Spot and Light Streak

Rasterstereography may be further reduced to a single line of light and even to a spot projected on to the surface. The light streak method was proposed as early as 1970 by Criuckshank, (Condie 1973) and by Condie in 1973 and Joel in 1974. Considering a spot first, if it moves over the surface in a predicatable fashion the entire shape can be calculated. This was originally done by Yamashita et al, 1982. Yamashita placed the object to be sensed on a rotory table, (figure 6). A light

spot from a laser was directed onto the surface of the shape. This spot was moved vertically in fixed increments by a stepper-motor controlled mirror. The spot was observed by a horizontally mounted linear array sensor which was placed a known distance from the laser mirror. A cylindrical lens was used to focus the light onto the axis of the sensor. As the rotary table turned the horizontal position of the spot was monitored by the linear sensor. Sufficient information was available to calculate all 3 cylindrical coordinates of the light spot. Yamashita's system has a reported accuracy of 1 millimeter.

Fernie developed the first practical light streak shape sensor for full circumferential sensing (Saunders and Fernie, 1984). The light streak rotates around the object rather than the object rotating. Video cameras view the streak from an angle and the position of the video image is obtained in digital form. Eight cameras are used evenly spaced around the object to give a sensing time of less than 1.6 seconds. This apparatus was designed specifically for sensing residual limb shapes. The shapes may be represented by up to 17,280 sets of cylindrical coordinates. The advantage of Fernie's system is that it measures the shape around the entire object in a very short time. Its disadvantage is that it cannot define the distal end of the residual limb.

The only commercially avilable light spot or streak system is ISIS (Instrumentation for Shape Investigation). ISIS, developed at Oxford University (Turner-Smith et al 1982), uses the light streak method but is restricted to one vantage point

rather than around the entire object. ISIS was designed primarily for back shape data acquisition.

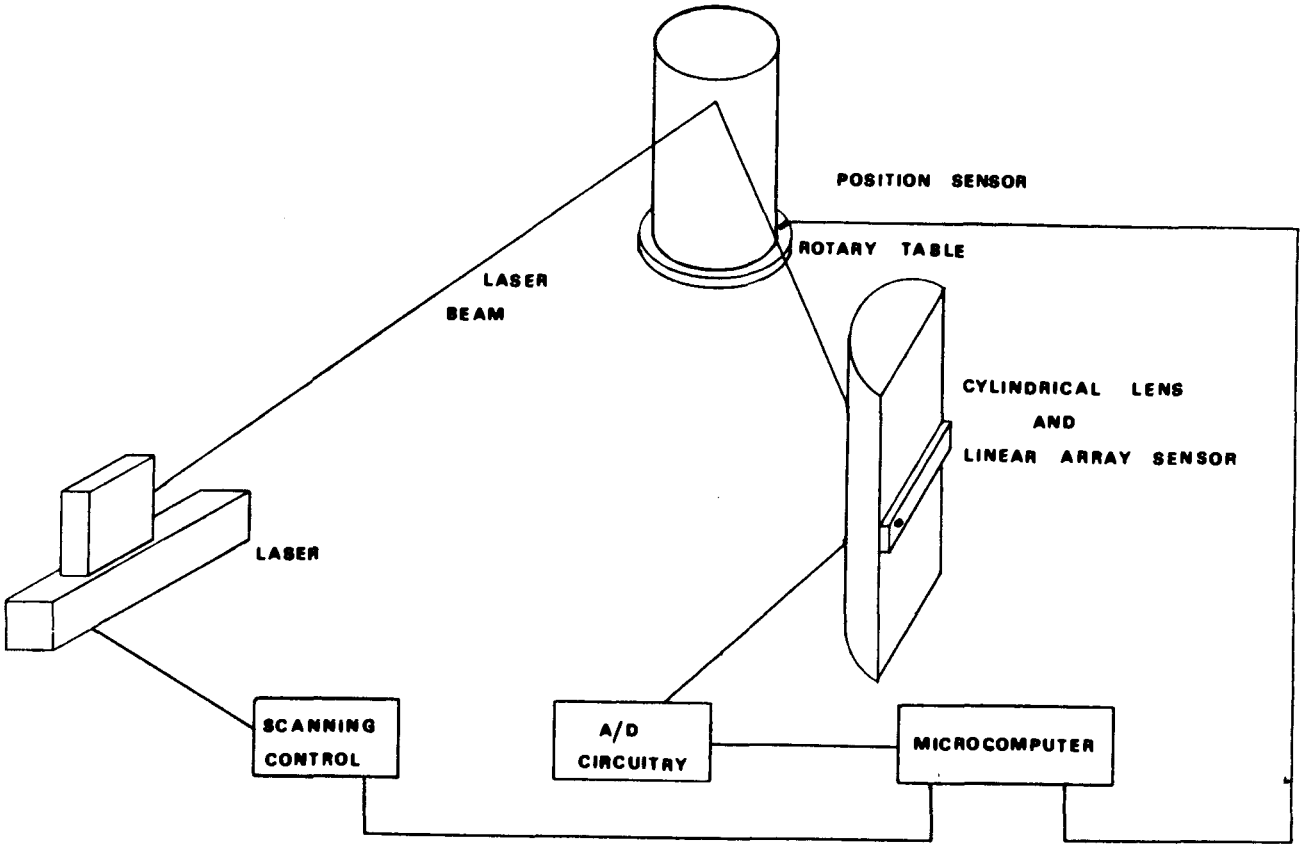

Figure 6: Schematic of Yamashita's Light Spot System.

Moire Topography

Moire topography is an optical interference technique that has been used extensively in the clinical setting. A point source of light casts the shadow of a grating or screen on the object to be viewed, (figure 7). When the object is viewed through the grating from a point other than the position of the light a fringe pattern resembling contour lines can be seen. The

interrelationship of the grating and its shadow is uniquely determined by the geometry of the system. If the positions of the system components are closely controlled, objective data can be extracted from the moire pattern.

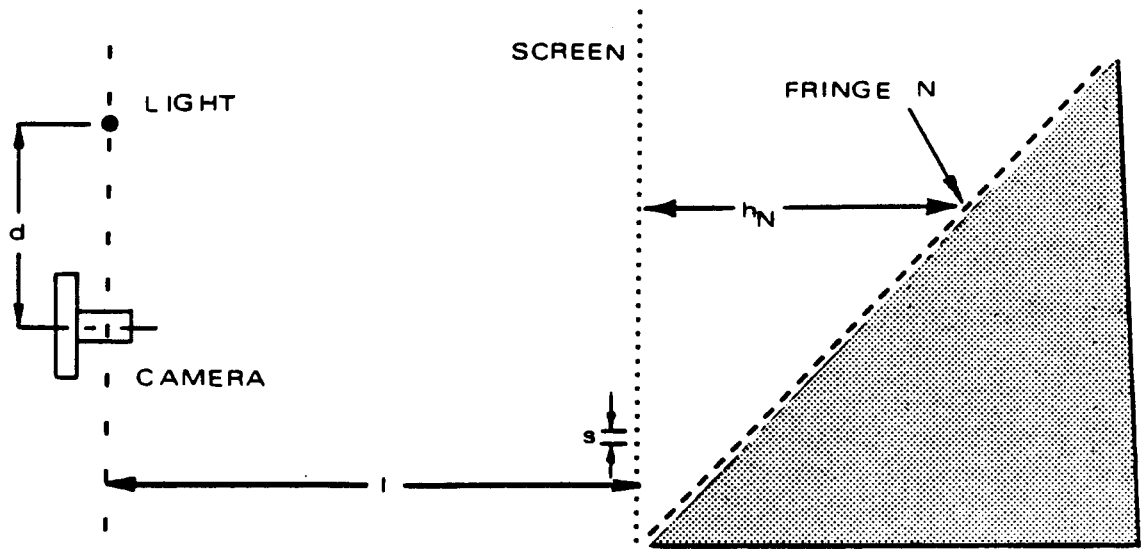

Figure 7: The moire topography apparatus configuration.

h_N = distance between Nth fringe and screen

N = fringe number

d = distance between camera or viewport and light

l = distance between camera and screen

s = centre to centre spacing of screen lines

The fringe pattern may be processed immediately by an observer, but usually a photograph is taken to obtain a permanent record. The photograph may be checked for recognizable patterns or a more sophisticated analysis may be performed with the aid of computers. This requires the data to be in numerical form. This is the major shortcoming of the moire technique. Manual digitization of the fringe pattern is slow and automated digitization is costly.

Shadow Moire techniques were initially used as a method of stress analysis of rigid materials called the oblique shadow method, (Theocaris, 1967). The first applications of this technique to the human body were in 1970 (Meadows et al, 1970; Takasaki, 1970). Since that time the technique has gained wide popularity in the field of medicine and in the garmet industry. It has proven to be very effective for the one-off measurement of unstable soft objects such as the human body (Takasaki, 1982).

The most extensive use of moire topography has been in the screening and monitoring of scoliosis among school children. The most successful applications have been in Japan, (Ohtsuka et al, 1981; Harada et al, 1981 & 1982). In a similar manner the posture of Japanese adults has been investigated, (Suzuki et al, 1981). Other applications to the human body include: replication of shoe lasts, (Saunders, 1981); investigation of chest wall deformities, (Kawamura et al, 1982); facial assymetries, (Mehta, 1981); and assisting during facial reconstructive surgery, (Windischbauer, 1982).

Problems associated with moire measurement of the human body include: the optically translucent nature of the skin; the inability to identify convex and concave surfaces without prior knowledge of the shape and the time necessary to objectively process the moire patterns.

d) Radiography

The advantage of radiographic techniques is that they can give shape information about internal structures. This is necessary if in vivo bone shapes are to be measured rather than scaled. Their disadvantage, which precludes their use on a routine basis, is the damaging effect of the radiation on body tissues. There are two radiographic techniques that are commonly used for shape data acquisition, stereoradiography and Computerized Tomography.

Stereoradiography

Stereoradiography utilizes the same principles as stereophotogrammetry except radiographs are used rather than photographs. This requires the position of the subject to be changed relative to the X-ray equipment such that 2 radiographs are taken at right angles to each other. With controlled positioning of the subject common X-ray equipment can be used for this purpose.

As with stereophotogrammetry, this technique is suitable for measuring the location of a limited number of points that can be easily identified on both radiographs, but it is not

practical as a general shape data acquisition tool.

Computed Tomography

Computed Tomography (CT) generates cross sections of body segments showing the internal and external structures. In CT scanning a fan beam of x-rays is passed through the patient. The amount of transmitted radiation is detected and recorded by an array of crystalline detectors placed opposite the radiation source. A large number of individual measurements are made and recorded in a computer as the x-ray source is rotated about the patient, (figure 8). The image is reconstructed by using a summation technique for each pixel, (Morgan 1983). This information is then displayed as a gray scale image.

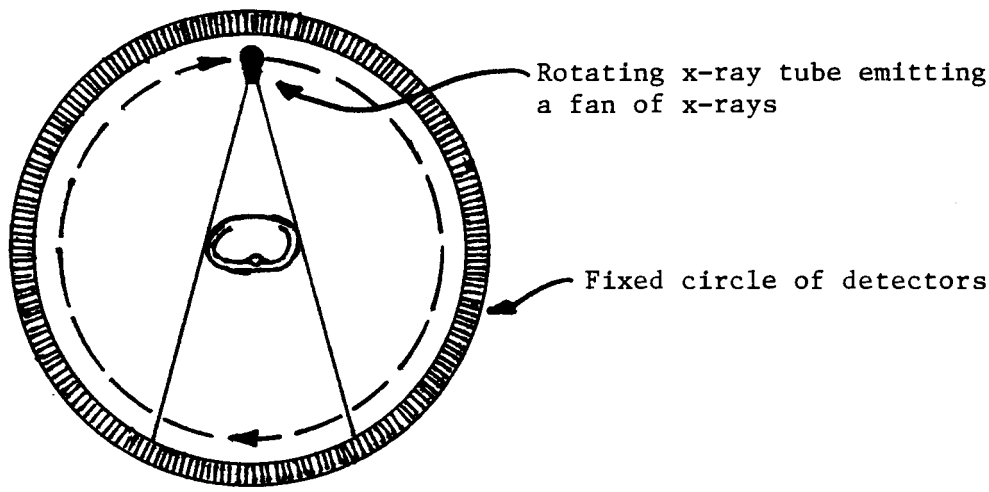

Figure 8: CT scan x-ray source and sensor configuration.

The image reconstruction techniques used in CT were developed for use in radio astronomy, electron miscroscopy and optics, (Hendee 1979). In 1961, Oldendorf (1961) explored the principle of CT. Shortly thereafter, Kuhl et al (1963) developed emission and transmission CT imaging systems and described the application of these systems to brain imaging (Kuhl et al 1966). The first commercial clinical unit for head imaging was introduced by EMI Ltd. in 1974 (Hounsfield 1973). In the same year, Ledley et al (1974) announced the development of a whole body CT scanner. By 1977, 16 or so commercial companies were marketing more than 30 models of CT scanners.

The CT measured cross sections can be linked to form the shape of the object being studied. Thus, it is a very practical shape data acquisition tool. Its main drawback is the amount of radiation exposure necessary to acquire the shape of large objects. The cross sections, or `slices', have a thickness, typically 4 to 8 millimeters for clinical applications. The slices are a summation through that thickness. A greater resolution is obtained by using thinner slices at a greater frequency. But, as the thickness of the scan decreases the exposure of the skin to radiation increases. Using the minimum exposure to delineate the shape of bone tissue in the lower limb, a 4 millimeter thick slice gives a skin dose of 3.6 mGrays, (Li, 1984). For comparison the skin dose for an anterior and a lateral plain radiograph of the knee, tibia and fibula would be approximately 1.2 to 1.5 mGray.

One of the disadvantages of using this technique is the

long time it takes to obtain all the cross sections to describe a shape. It may take as long as 40 minutes to scan from the knee to the ankle at 4 millimeter intervals. The possibility of the subject moving between scans has to be taken into consideration.

Several computer programs have been developed for three dimensional display of CT scans, (Herman, 1984, Latamore, 1983, Udupa, 1983). Notable among them is a commercial system resulting from the work of Vannier and colleagues, (1983, 1985). Initially developed for the skull they have extended their methods to include the pelvis, hip, hand and wrist. These three dimensional reconstructions are used mainly for viewing purposes. Some interactive manipulation programs have been developed to enable the surgeon to enhance the image. These include dislocation of the hip and separation of the carpals.

These high resolution modelling programs require scans at a 2 millimeter interval. At this exposure the thyroid would receive approximately 30 rads (radiation absorbed dose), the eye lense would receive approximately 75 rads. Cataract formation occurs with exposures between 150-200 rads. By comparison 3 standard skull x-rays provides an average exposure of 300 millirads. If high resolution is required, CT scans are not suitable for routine use.

In the realm of shape, CT scans have not been widely used. Clinically, the volumes of organs and lesions (Henderson et al 1981, Moss et al 1981, 1981, and Breiman et al 1982) have been measured by summing the volumes an organ occupies in each slice, or by stereographic techniques using CT scans (Reid 1982,1983).

As well as those mentioned above, Johnson et al (1983), and Langrana et al (1982) have used CT scans to acquire shape information for modelling purposes. In these modelling applications and the volume studies, the perimeter of the organ in question in each slice was hand digitized.

e) Magnetic Resonance Imaging

Magnetic Resonance Imaging (MRI) relies on the magnetic properties of hydrogen molecules in the body to generate slice images similar to CT scans. In this shape acquisition technique a large magnetic field is applied to the area in question such that all the hydrogen molecules align themselves. When the magnetic field is suddenly removed the hydrogen bounces back to its preferred positions. Energy is produced in the process. Some of the energy is in the form of radio signals of varying frequency depending on molecule properties. The MRI equipment senses the radio signals and reconstructs the shape from them.. The radio signals are very weak, thus some time is necessary to construct each slice.

MRI has the distinct advantage over radiographic techniques in that the cross sections are generated without radiation exposure. That is MRI's great potential.

Doctors Hannam and Wood (1985) of the Department of Dentistry at the University of British Columbia, have been using MRI to gather data for reconstructing the shape of the mandible and associated musculature.

Variability of Bone Geometry

When incorporating scaling procedures it is appropriate to understand how bone geometry varies within and between individuals, and how it changes after amputation.

Some shape characteristics of normal bones are very well understood. There are many excellent references to variability in overall dimensions but very little is understood about the variability of bone shapes and the shapes of abnormal bones. There has been considerable investigation into the atrophy of bone during the aging process but with little reference to bone geometry. Similarly, there have also been a few studies on abnormal bone growth with minor reference to their shapes.

Breakey (1973) reports an average knee breadth (widest part of femur) of 9.76 cm for 206 below knee residuums. The standard deviation is 0.635 cm with a range of 8.26 to 11.77 cm. It should be noted that Breakey's sample ranged from 20 to over 80 years old, it contained 76% males from Manitoba and Ontario. Cause of amputation was 64% vascular disease, 28% trauma and 8% `other'.

Persson and Liedberg (1983) report the average length from the distal end of the stump to the medial femerotibial joint space as 16.19 cm with s = 2.96 cm and a range of 10 to 25 cm. Their sample of 93 below knee residuums were from Sweden. The sample was 58% male. The mean age was 72.5 years ranging from 10 to 94 years old. 82% of the amputations were for vascular disease.

In measurements on the skeletons of 24 individuals, Todd

and Foort, (1960, unpublished), found the skeletal dimension at the knee which exhibited the greatest variance was the distance between the tibial tubercle and the patella. It was considered in the design of the standard shape Winnipeg Below-Knee Sockets, (Foort 1967). Also of considerable variance was the position of the fibular head.

Mysorekar et al (1983) found considerable difference between individuals in soleal line characteristics. They studied 330 tibia and found that it shows mixed characteristics of a line, a wide line, a ridge or a groove. The line is frequently absent in the upper third of the tibia, otherwise it is usually a depression 1 to 2 mm in depth. In the middle third it is seen as a wide line or as a ridge varying from 1 to 2 mm in height or as a depression varying from 1 to 2 mm in depth. In the lower third it usually presents itself as a ridge or as a depression. Also, the line shows a left-limb dominance. Though the soleal line is not a prime concern because it is located on the. posterior surface of the tibia, this study does indicate the type and magnitude of bone geometry variations that can be expected.

The growth of bone tissue is affected by amputation. In a radiographic study of 18 children with below knee amputation due to either traumatic or congenital reasons, Christie et al (1979) found that growth of the cortical bone was reduced when compared to the intact limb. Riseborough et al (1983) examined radiographs of adults who had distal femoral fractures in their youth. They found growth disturbances in 20% of those studied.

It is possible that the growth disturbance alters bone geometry from normal.

A study of skeletal changes of the amputated limb by Sevastikoglou et al (1969) showed that bone atrophy in the femur and tibia was more pronounced on the amputated side than the intact side of unilateral below knee amputees. They were studying cortical thickness and it is not clear where the increased atrophy was occurring. It is likely that it was in the medullary cavity. Left-right differences up to 10 millimeters were reported. It is expected that there would be less bone loss from the tibial tubercle and tibial condyles which retain a high level of function after amputation than the more distal structures which do not. The difference is not reported to have a substantial correlation with age or with time since amputation. Two factors that were not reported and which may be related to shape changes, are the activity level of the amputee and the level of amputation.

Atrophy of cortical bone in the tibia and femur during the aging process has been well documented, (Arnold et al (1966), Garn et al (1969), Van Gerven (1973), Cumming et al (1973), Martin et al (1977), Ericksen (1979) and Plato et al (1982)). All have shown, the loss of cortical bone to be universal after the first 3 or 4 decades of life and that it varies considerably with individuals. The bone loss is from the medullary cavity and not from the exterior of the bone.

OBJECTIVES

The objectives of this thesis were to develop and test procedures for modelling from selected anthropometric measures the size, shape and relative orientations of the bones that are contained within below knee artificial limb sockets. The bones of concern are the tibia, fibula, patella and distal portion of the femur.

There were four specific objectives.

1. To generate reference shapes of the bones that are contained within below knee sockets. To meet this objective it was necessary to develop procedures for generation of bone shapes from CT scans. The reference bone shapes were to be represented as computer images to be used in the CAD procedures.
2. To develop procedures for scaling the reference bone shapes according to anthropometric measures from the amputees' residual limbs.
3. To test the accuracy of the scaling procedures by comparison of the scaled bone shapes to the amputee in vivo bone shapes acquired by CT. The objective was to have the scaled bone radii within 2mm of actual bone radii. This test objective is based on clinical observations. 2mm is approximately the minimum difference that amputees can feel, (Foort, 1985). To meet this objective it was necessary to develop a procedure for comparing the radii of 2 bones.
4. To investigate nonhomogeneous shape differences by comparison of amputee bone shapes to the reference bone shapes.

METHODS

The development of experimental methods involved 4 stages.

a) Acquisition of reference bone shapes. The bone shapes of one "reference" subject was measured by Computerized Tomography (CT) and reconstructed as a three dimensional computer image using hand digitizing techniques.

b) Development of scaling procedures. Three dimensional transformation procedures were developed for each bone. The procedures were required to transform the reference bone shape data acquired in a) to match the proportions of the individual amputees.

c) Testing of the bone shape reconstruction. The bone shapes from a number of amputees were reconstructed from the reference shapes using the transformation procedures developed in b). The actual bone shapes of each subject were also measured directly by CT scanning as in a). The transformed bone shapes were then compared with the directly measured shapes for determination of accuracy of shape replication.

d) Analysis of error. The sources of error arising in the reconstruction of individual bone shapes were evaluated.

Reference Bone Shapes

Reference shapes of the tibia, fibula, patella and condylar portion of the femur were taken from the in vivo bone shapes of an individual who was arbitrarily chosen. The reference shapes were represented in the computer as a series of transverse cross sections, (figure 14). The cross sections were spaced at 4 millimeter intervals proximal of and including the tibial tubercle and at 8 millimeter intervals distal to the tubercle.

Each cross section was represented by a series of points about its perimeter. From 18 to 60 points were used per cross section depending on the complexity and size of the perimeter shape. The spacing between points was variable, dependent on curvature.

Reference Shape Acquisition.

The reference bone shapes were obtained by digitizing Computerized Tomography (CT) scans of the lower limb of one nonamputee of average stature.

The CT scans were produced using the Siemens Somatom DR scan unit at Health Sciences Centre, University of British Columbia. The scan width was 4 millimeters. Each scan produced one transverse cross section of the reference shape. The scans were taken from 2 cm proximal of the femoral condyles to the distal end of the tibia with transverse and sagittal scans to show the general orientation of the limb in the CT scanner. The radiation exposure to the subject was the Siemens Somatom's minimal setting, 96KV and 0.075 MAS per slice. This was

equivalent to a skin dosage of 3 mGray. This provided sufficient definition of the bone while keeping exposure of the subject to a reasonable level. The scanning procedure took approximately 45 minutes to complete.

Each CT scan produced a radiograph film with the particular cross section and scan parameters printed on it, (figure 9).

A calibration and alignment jig was attached to the limb of the reference person. The jig consisted of 4 parallel lexan tubes with one larger diameter tube to maintain the jig's integrity, (figures 9 & 10). The 2 lower tubes served as calibration and alignment references. Separation of the tubes was used to determine the calibration factor in the plane of the scan.

Data Format

The data describing each bone was transformed from digitized coordinates in the reference system of the CT scanner to the reference system of the alignment and calibration jig. The z axis was along the longitudinal axis of the lower left tube of the jig. The x axis was oriented through the centre of the 2 lower tubes. The 3 axes were mutually orthogonal and in accordance with the right hand convention.

Rotations about the x and y axes were determined from the sagittal and frontal view CT scans. These rotations were assumed not to change during the scanning process. An attempt was made to monitor rotations about the X and Y axes by the separation between the 4 parallel tubes. It was not possible due to

insufficient digitizing resolution. Similarly, it was not possible to account for movements along the z axis.

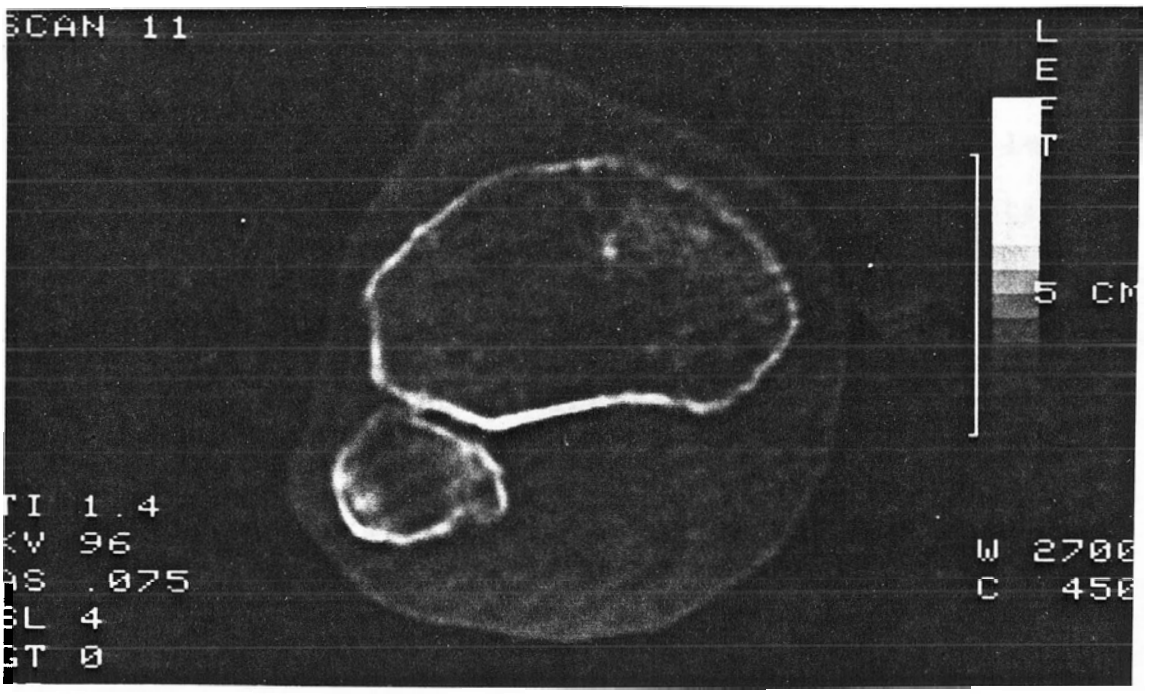

Figure 9: Sample CT scan at the tibial condyle level. Also seen are 4 of the tubes of the calibration and alignment jig.

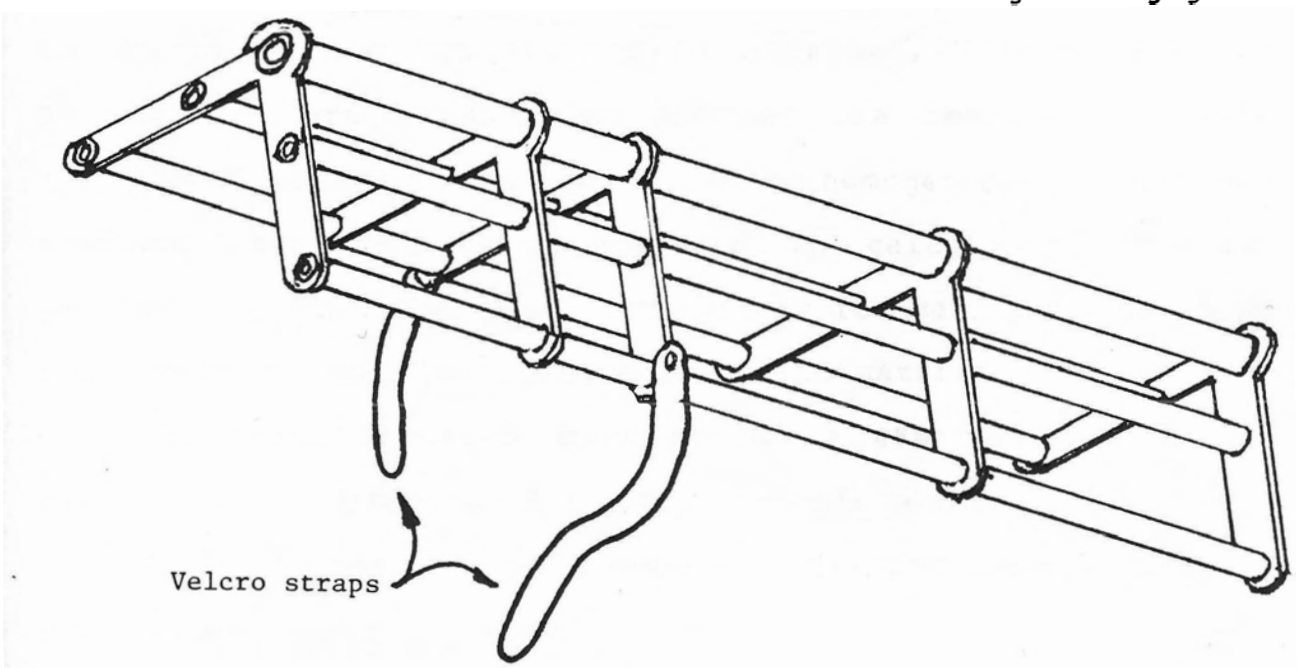

Figure 10: The alignment and calibration jig that attached to the subject's limb.

Scaling Procedures

Anthropometric scaling methods are commonly used during internal force analysis of human locomotion. The objective in these instances is to determine the locations of origins and insertions of muscles and ligaments. Because the exact locations of these origins and insertions are inaccessible, position data from cadaver studies is used. Through scaling procedures this data is transformed to the human subject. Though objectives of this project were slightly different, (i.e. shape data was necessary), the same principles can be applied.

The scaling format includes generation of one or more transformation matrices and then use of these matrices to transform the reference bone shapes to the subject's residual limb bone shapes. Palpable landmarks from the subjects' residual limb and matching points from the reference bone shapes are used to determine the transformation matrices, (figure 11). In instances where homogeneous changes are desired a single transformation matrix is used. When nonhomogeneous changes are required 2 or more matrices are used. The calculated shapes are generated by multiplying the coordinates for each point defining the reference shape by the transformation matrix.

The transformation matrices were 4X4 matrices as is standard for 3-dimensional graphics transformations.

Scaling procedures were necessary for the patella, fibula, tibia and distal portion of the femur.

Reference points were measured using the MERU anthropometer.

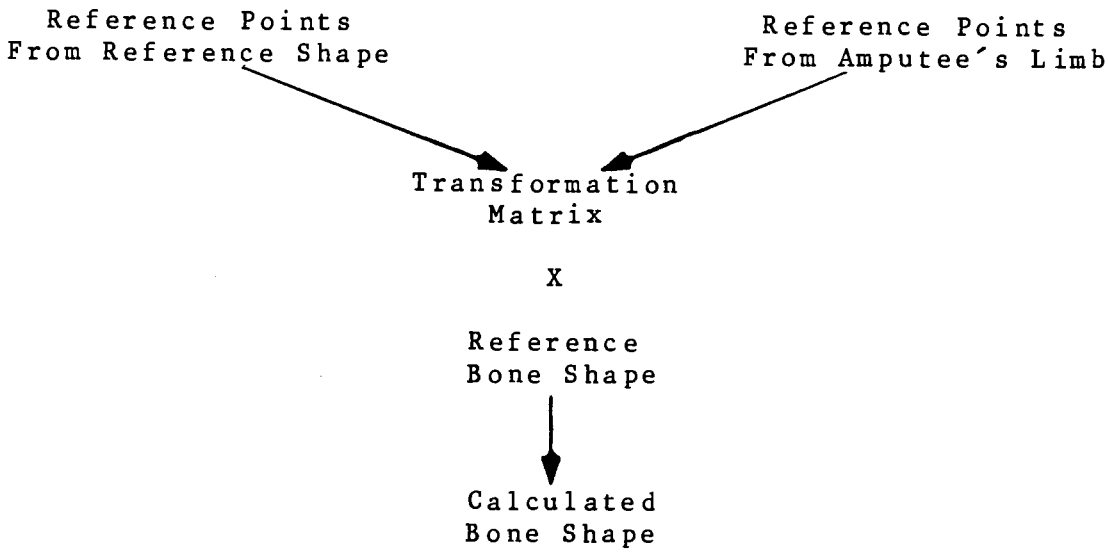

Figure 11: Overview of the scaling procedure used to calculate the bone shapes.

Generation of Transformation Matrices

Four different procedures were used to calculate the transformation matrices:

a) uniform dilation - equal proportion on 3 mutually orthogonal axes;

b) orthogonal - different proportions on 3 mutually orthogonal axes;

c) nonorthogonal - different proportions on 3 nonprescribed axes;

d) nonhomogeneous - a separate transformation for each cross section, specific to the tibia.

a) Uniform Dilation

Uniform dilation involves shrinking or expanding all the dimensions of the reference bone in a proportion derived from 2 points measured on the subject's limb and the complimentary 2 on the reference bone shape. A comparison of various scaling methods by Lew and Lewis (1977) shows the accuracy of this procedure on the tibia and femurs they were measuring to be similar to no scaling at all. However, tibia and femurs exhibit distinct nonhomogeneous shape differences. Uniform dilation could be sufficient for bones with relatively homogeneous shape differences, such as the patella. The advantage of proportional scaling is that only two reference points need be located to calculate the scaling portion of the transformation matrix. A third point was necessary to position and orient the bone shape relative to the reference points measured from the subject's limb.

The steps used to generate the matrix were as follows:

scaling in the 3 mutually orthogonal planes, x, y and z, by the ratio of subject bone reference point separation divided by reference bone reference point separation;

translation of the scaled shape to the origin;

rotation of the scaled shape to match the scaled reference point orientation to the subject's reference points;

translation of the scaled shape to match the scaled reference point location to the subject's reference points.

Accuracy of the software was confirmed by scaling a cube of

known dimensions. The cube was defined as X,Y,Z coordinates of its apices. Reference points were chosen to increase the cube's linear dimensions by factors 1.5 and 2.0. Accuracy was determined by comparing the calculated shapes to what they should be.

b) Orthogonal

Orthogonal scaling involves shrinking or expanding the reference bone in 3 different proportions along 3 axes approximating the critical dimensions of the bone. The scaling proportions were derived from the distances between reference points. This procedure is similar to that used by Morrison in 1970.

The steps used to generate the matrix were as follows:

translation of the reference points to place a designated reference point at the origin;

rotation of the 2 sets of reference points to align the critical axes of the bone with the coordinate axes;

scaling in the 3 mutually orthogonal planes, x, y and z, by the ratio of subject bone reference point separation divided by reference bone reference point separation, specific reference points were used for each critical dimension for each bone;

translation and rotation of the scaled shape to match its scaled reference points with the subject's original reference points.

c) Nonorthogonal

The nonorthogonal scaling technique was at different proportions on 3 nonprescribed axes. The principal directions of deformation are determined by the location of the reference points rather than the bone's principal axes. Each of the three axes has its own uniform scaling parameter. This procedure is described in some detail by Lew and Lewis (1977). Software to implement it, was developed at Simon Fraser University (Pierrynowski 1982). It was used by Pierrynowski and Morrison (1982, 1985) in human locomotion modelling and modified to scale shape data by Cooper (1982). The algorithm developed by Pierrynowski and modified by Cooper was the basis for nonprescribed axes scaling procedure in this project. The algorithm was translated from Fortran to Pascal and run on an IBM PC/XT Computer.

The transformation matrix was generated as follows:

the centroids of the subject's and reference shape's palpable points were calculated;

the subject's and reference shape's palpable pointswere translated to zero their centroids on the origin;

the rotation and scaling components of the transformation were calculated through matrix manipulation of the subject's and reference shape's palpable points. The Crout reduction for factorization (Rice 1981), a variation of Gauss eliminization, was included in this procedure;

the translationcomponent was calculated from the nonzeroed

centroids.

This scaling technique required at least four reference points from the amputee's limb.

In a comparison of various scaling techniques applied to the tibia and femur, Lew and Lewis (1977) found that scaling about 3 nonprescribed axes was the most accurate, followed by scaling about 3 mutually orthogonal axes as used by Morrison (1970), then by uniform dilation. It should be noted that Lew and Lewis used extracted bones where palpation error would be negligible.

A pilot study by Cooper (1982) modified the software developed by Pierrynowski to scale simple geometric shapes. This has shown that for homogeneous shape changes that differ in 3 mutually orthogonal axes the scaling procedure can be 100% accurate but that measurement of the reference point coordinates was critical. Error in the scaled shape was of similar magnitude as the error in reference point measurement.

d) Nonhomogeneous

A scaling procedure was developed to account for any bending of the tibial shaft that may be different than the shaft of the reference tibia. For this procedure a set of 5 reference points were measured along the tibial crest of all the subjects. These reference points were used to determine cross section translations in the x and y directions to maintain the right amount of bending of the tibia. Nonhomogeneous scaling was done after the tibia was scaled nonorthogonally.

The steps used to generate the nonhomogeneous transformation matrices were as follows:

proceeding distally along the tibia, when the first of the 5 reference point was reached, the equation of the line between the first and second reference points was calculated;

the point on the cross section representing the tibial crest was determined;

the translation required to position the tibial crest on the line between the 2 reference points was calculated;

the translation factor was updated for each subsequent cross section until the next reference point was reached;

when the next reference point was reached the equation of the line was updated.

Scaling of the Patella

The patella was scaled by 2 different techniques, uniform dilation and orthogonal.

Four reference points were measured from the patella; its most proximal, distal, medial and lateral aspects. All 4 points were used for orthogonal scaling. The medial-lateral (ML) and proximal-distal (PD) proportions were used. Scaling in the direction of the third axis, anterior-posterior (AP), was by the ML proportion. The patella was scaled by uniform dilation twice. Once using the ML proportion to determine the scaling factor,

and once using the PD proportion.

Scaling of the Fibula

The fibula was scaled by uniform dilation, orthogonal and nonorthogonal techniques.

The reference points used for uniform dilation were the most distal lateral aspect of the fibular head and the distal lateral aspect of the amputated end of the fibula. To obtain a reference point representative of the fibular length, the distal end of the fibula was compared to a point on the reference fibula shape at a proportion of its length equal to the proportional lengths of the amputated fibula to the contralateral intact fibula. A third reference point, the medial tibial-femoral joint space was added to help orient the fibula.

Orthogonal and nonorthogonal scaling requires at least four reference points from the amputee's limb. There are not 4 suitable reference points on the amputated fibula that are accessible. Therefore, for these techniques, the fibula was scaled according to tibial parameters. Reference points from the tibia were used to generate the transformation matrix for scaling the fibula. These were the same reference points that were used to scale the tibia.

Scaling of the Tibia

The tibia was scaled by 4 techniques; uniform dilation, orthogonal, nonorthogonal and nonhomogeneous.

The following reference points were used:

- tibial tubercle, superior anterior aspect
- posterio-lateral joint space
- posterio-medial joint space
- distal end of the tibia. The distal end of the tibia was compared to a point on the reference tibia shape at a proportion of its length equal to the proportional lengths of the amputated tibia to the contralateral intact tibia.

Uniform dilation scaling used the tubercle and distal end of the residual limb as scaling reference points.

For orthogonal scaling the distance between the tibial plateau, (average of the 2 joint space reference points), and the distal end of the residual limb was used to determine the PD scaling factor. The distance between the 2 joint space reference points was used to determine the ML scaling factor. The perpendicular distance from the tubercle to the plane defined by the 2 joint space points and the distal end point was used to determine the AP scaling factor.

All 4 reference points were used for nonorthogonal scaling. Five tibial crest reference points were used for nonhomogeneous scaling of the tibial shaft.

Scaling of the Femur

The condylar portion of the femur was scaled by uniform dilation, orthogonal and nonorthogonal techniques.

Six palpable landmarks were located on the femur. These were:

- tip of adductor tubercle
- lateral epicondyle
- medial epicondyle
- medial ridge of patellar surface
- posterio-medial joint space
- posterio-lateral joint space

Uniform dilation used the medial and lateral epicondyle reference points to determine the scaling factor.

For orthogonal scaling the distance between the adductor tubercle and an average of the 2 joint space reference points was used to determine the PD scaling factor. The distance between the epicondyles was used to determine the ML and AP scaling factors.

The patellar ridge, adductor tubercle, and 2 joint space reference points were used for nonorthogonal scaling. Of the available points, these encompased the critical dimensions of the bone to the greatest extent.

Testing of the Scaling Procedure

To meet the stated objective of testing the scaling procedure described above, the bone shapes and sizes of 6 below knee amputees were calculated by scaling the reference shapes. The actual bone shapes of each amputee were obtained by digitizing CT scans of the residual limb of each amputee. The procedures followed were identical to those previously described for obtaining the reference bone shapes. The scaled shapes were then compared to their in vivo bone shapes and sizes as measured by CT scanning.

Selection of Subjects

Six amputees were selected from the patient population seen at the Medical Engineering Resource Unit of the University of British Columbia located at Shaughnessy Hospital. To reduce the effect of nonhomogeneous growth due to amputation at an early age, subjects were chosen whose amputation occured at an age greater than 18 years. When possible, unilateral amputees were selected to enable attainment of a length representative reference point for the tibia and fibula by comparison to the intact limb. For bilateral amputees an estimated intact leg length was used.

The subjects were selected to represent the range of knee breadth and residuum length characteristic of the below knee amputee population.

Shape Comparisons

The CT acquired and scaled bone shapes were compared. As a result of the scaling procedure scaled shapes were positioned and oriented according to the reference points measured from the subject. The CT shapes were positioned according to the alignment and calibration jig used during the scanning process. Before comparison could be possible, the 2 sets of data had to be brought into alignment. A program was written that cycled through alignment and comparison of the 2 shapes. The alignment was done interactively. After each alignment the 2 shapes were compared. This cycle was broken when the operator was satisfied that the alignment was the best possible. The algorithm flow chart is provided in appendix III.

Cylindrical coordinates were generated from the X,Y,Z coordinate data to enable direct comparison of radii magnitudes. Both the scaled and CT data were fitted into a cylindrical coordinate system of known increment. This was necessary to put the 2 sets of data in phase. In the new data format, cross sections were generated every 7 millimeters. Each cross section was represented by a series of radii extending from the central axis, (Z axis), in 5 degree increments about the axis, (figure 12).

Fitting to the new data format required x,y,z coordinate interpolation. Point interpolation was in 2 steps. First the points describing the perimeter of each cross section were fitted to a 5 degree increment about the central axis. Interpolation was linear. After this step every cross section

was described by 72 points. In some instances, the central axis could not pass through all the cross sections describing the bone. This occurred when small cross sections were at the ends of a bone. The algorithm for comparing radii could not process these cross sections, therefore they were omitted from the data describing the bone.

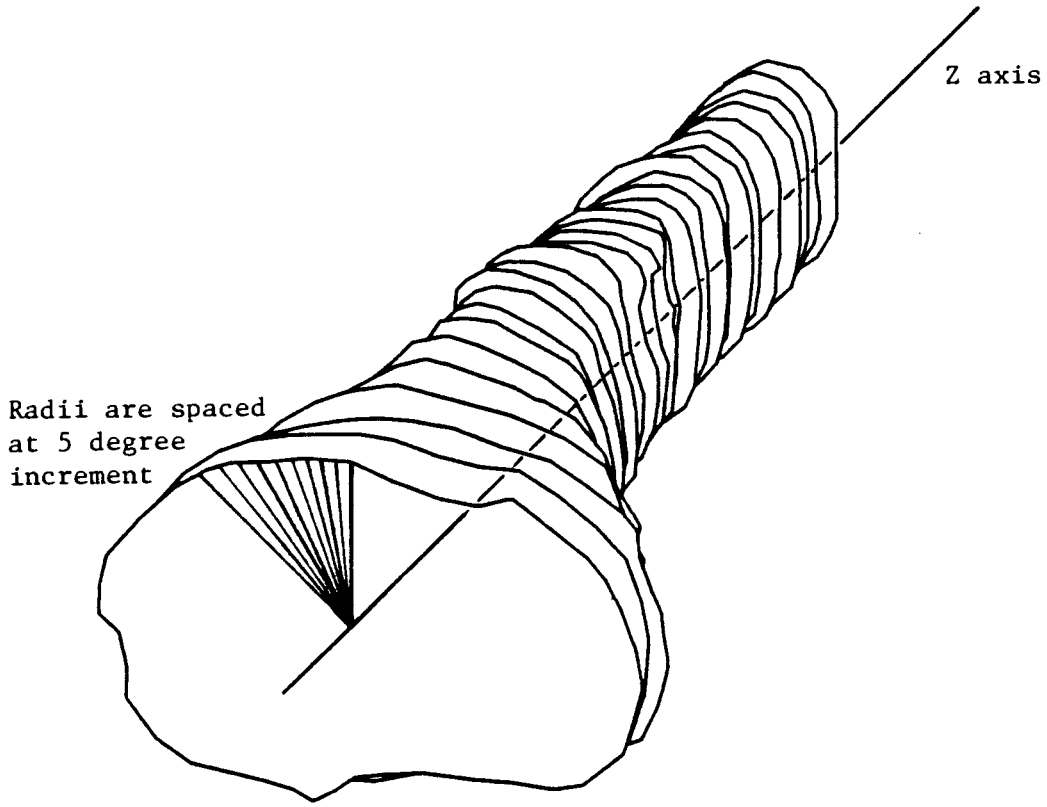

Figure 12: The cylindrical coordinate system used when comparing bone shapes.

The second interpolation step was along the z axis which typically was the longitudinal axis of the bone. This fitting process was also linear.

Longitudinal interpolation was followed by smoothing about each cross section's perimeter. This was by a least squares parabola fit over 5 consecutive points (Scheid, 1968). Each point being smoothed was bracketted by the 2 points on each side.

When solving the equation of the parabola

$$p(t) = a_0 + a_1 t + a_2 t^2 \qquad 1$$

where $t = (x-x_k)/h$

k = index of point being smoothed

h = x interval between points

over the 5 equally spaced points k-2, k-1, k, k+1, k+2,

at the centre argument t=0 and

$$p(t) = a_0 = y_k - 3/35(y_{k-2} - 4y_{k-1} + 6y_k - 4y_{k+1} + y_{k+2}) \qquad 2$$

Estimation of size and shape differences.

After interpolation of the CT and scaled shape the data describing both were in phase. Comparison was then a matter of examining the differences between the magnitude of their radii for each data point location.

Each comparison generated 3 numbers. The first was the mean difference between the radii of the 2 shapes being compared. The second number was the root mean square (RMS) of the differences between radii. The third number was the standard deviation from the mean. For each comparison between 2 bones, the mean difference and standard deviation was calculated for each cross section and for each bone. The RMS differences were calculated for each bone. Combined mean and RMS differences were calculated

over all the bones scaled by each procedure.

These 3 measures were chosen in order to provide insight into different aspects of bone geometry. The mean differences were considered to be representive of size differences between 2 bones. The standard deviations were considered to be representive of shape differences. RMS differences were representive of size and shape differences.

All three difference parameters were dependent on the positioning of one bone relative to the other. For example, in figure 13, two cylinders of 100 mm diameter were moved opposite directions from a central axis in 5 mm increments. Each time they were moved the mean difference did not change but the standard deviation did. The shapes were not changing but there was a perceived shape change. With one cylinder kept at the origin and the other moved in 10 mm increments there was a change in the mean as well as the standard deviation. Indicating a size and a shape change.

When comparing 2 bones, optimum alignment was critical. In the comparison process, one bone was interactively translated and rotated relative to the other an average of 8 times. With each move the standard deviation was observed to indicate the quality of the fit. The objective was to minimize the the standard deviation.

Radii differences were displayed graphically as three dimensional difference maps and as cross sections overlayed. The means difference and standard deviation of each the cross section for each bone were plotted.

Both cylinders moving simultaneously in opposite directions.

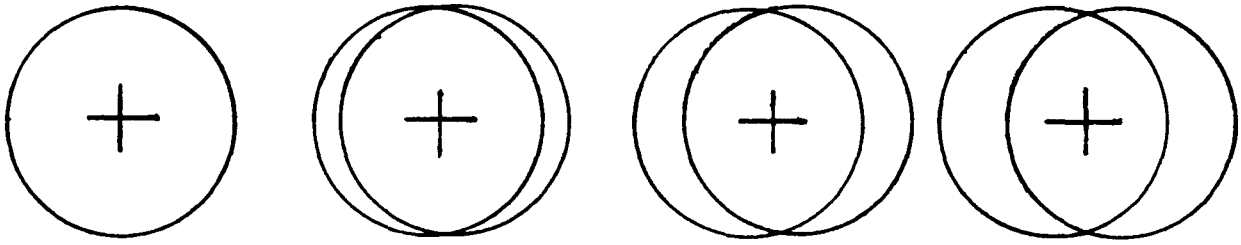

Mean	0.0	0.0	0.0	0.0
SD	0.0	7.1	14.1	21.2

Only one cylinder moving.

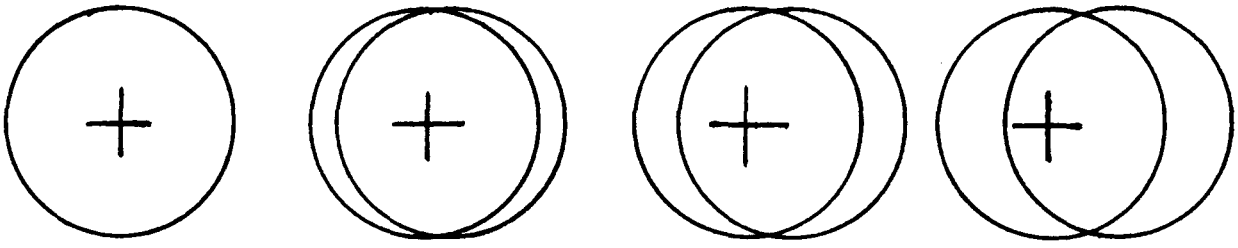

Mean	0.0	0.5	2.1	4.9
SD	0.0	7.1	14.1	21.2

Figure 13: The dependence of mean differences and standard deviation (SD) values on positioning of cross sections relative to each other.

Nonhomogenity of Bone Shapes

In order to obtain an estimate of the nonhomogenity of bone shapes existing between the reference shapes and the actual bone shapes of the individual amputees, comparisons of the shapes obtained by CT scans were made. This was done in the same manner as comparing the CT and scaled shapes described above.

Positioning Error Calculation

The accuracy of the scaling procedure in orienting the bones relative to each other in space was checked through scaling the reference shapes' reference points. If scaled correctly the calculated reference points matched the reference points measured from the amputee.

Data Acquisition Error Analysis

To determine digitizing variability, two CT cross sections of the tibia were selected for repeated digitizing. One cross section contained compact bone the other was a tracing of a cross section. CT scans that were not sufficiently bright were traced onto paper before digitizing. These cross sections were primarily of cancellous bone at the knee joint. Six points were identified on each slice which could be easily found for repeated digitizing. These points were identified by obvious changes in the perimeter shape. Both cross sections were digitized ten times at half hour intervals.

To determine the accuracy and reproducability of shape definition by CT scans and hand digitizing, a cylinder of known diameter was scanned and digitized. Four points were digitized ten times at half hour intervals. The four points formed two perpendicular lines each bisecting the cylinder. Cylinder diameters were calculated from the digitized data then compared to their known values.

Palpation variability was indicated by a comparison of the distances between reference points. The reference points of 5 subjects were measured 3 times each. The distance of each point from the tibial tubercle was calculated. The tubercle was chosen as the origin because there is a high degree of confidence in correct palpation and it is centrally located. The standard deviation for these distances for each reference point for all the subjects and for all the reference points was calculated.

RESULTS

The results are in four sections.

a) The amputee and reference subjects are described by demographics, body dimensions and three dimensional reconstructions of the bones of their limbs from the Computerized Tomography (CT) scans.

b) The data acquisition errors are reported. This includes digitizing variability, CT scanning error, and reference point measurement variability.

c) Bone shape variability is presented as comparisons between the reference bone shapes and the amputees' CT bone shapes.

d) Finally, the scaling accuracy is presented as comparisons between the scaled bone shapes and the amputees' CT bone shapes. Positioning and length accuracy is reported as differences between scaled reference points from the reference shapes and the reference points from the amputees.

Subject Description

Subject demographics are presented in table 1. All the subjects were male. The youngest at the time of amputation was 26 years old. The least mature residual limb was 7.9 years old.

The subject who provided the reference shape was not an amputee, both limbs were intact. The subject was male, the reference shapes were from his right limb, and he was 25.8 years old.

Table 1. Subject demographics.

Subject	Reason for amputation	Side	Contralateral limb	Age	Age at Amputation	Years since Amputation
JD	infection	left	intact	58.4	47.1	11.3
EH	trauma	right	intact	39.5	27.5	12.0
BW	infection	right	intact	68.9	61.0	7.9
GS	trauma	right	intact	64.0	41.0	23.0
FD	trauma	left	above-knee	54.6	30.9	23.7
DL	trauma	left	intact	60.5	26.0	34.5
mean				57.7	38.9	18.7
standard deviation				10.1	13.6	10.1
range				39.5-68.9	26.0-61.0	7.9-34.5

Subject residual limb and body dimensions are presented in table 2. The femoral biepicondular breadth and amputated tibial length means and ranges were less than reported in the literature. Biepicondular breadth range was 35% of that reported by Breakey, (1973). Tibial length range was 70% of that reported by Persson and Liedberg, (1983).

Table 2. Subject residual limb and body dimensions, and body weight. Tibia length is from the medial joint space to the distal end on the tibial crest of the amputated tibia.

Subject	Femoral Biepicondular Breadth mm	Amputated Tibia Length mm	Body Height mm	Body Weight kg
JD	98.0	155.6	1790	102.3
EH	88.5	222.7	1727	68.2
BW	85.7	137.7	1778	81.8
GS	89.2	135.6	1728	77.3
FD	97.3	122.3	1854	90.9
DL	91.0	117.8	1778	79.5
mean	91.6	148.6	1775	83.3
std dev	5.0	38.6	46	11.8
range	85.7-98.0	117.8-222.7	1727-1854	68.2-102.3

As reported in the literature:
biepicondular breadth, Breakey (1973),
tibial length, Persson and Liedberg (1983).

mean	97.6	161.9
std dev	6.4	29.6
range	82.6-117.7	100-250

Dimensions of the subject who provided the reference shapes are listed in table 3. All his dimensions were within the range of the amputee subjects. His biepicondular breadth was 5.9% greater than the subject average, height was 1.4% greater, and weight was 10% less.

Table3. Dimensions of the reference subject.

Femoral Biepicondular Breadth mm	Body Height mm	Body Weight kg
97.0	1800	74.0

Three dimensional representation of the reference shapes are in figure 14. The cross sections of the distal end of the tibia and fibula are malaligned. The calibration and alignment jig did not extend to the end of the bone. When digitizing these distal cross sections their relative positions were estimated. This portion of the bone was not required in the scaling routines.

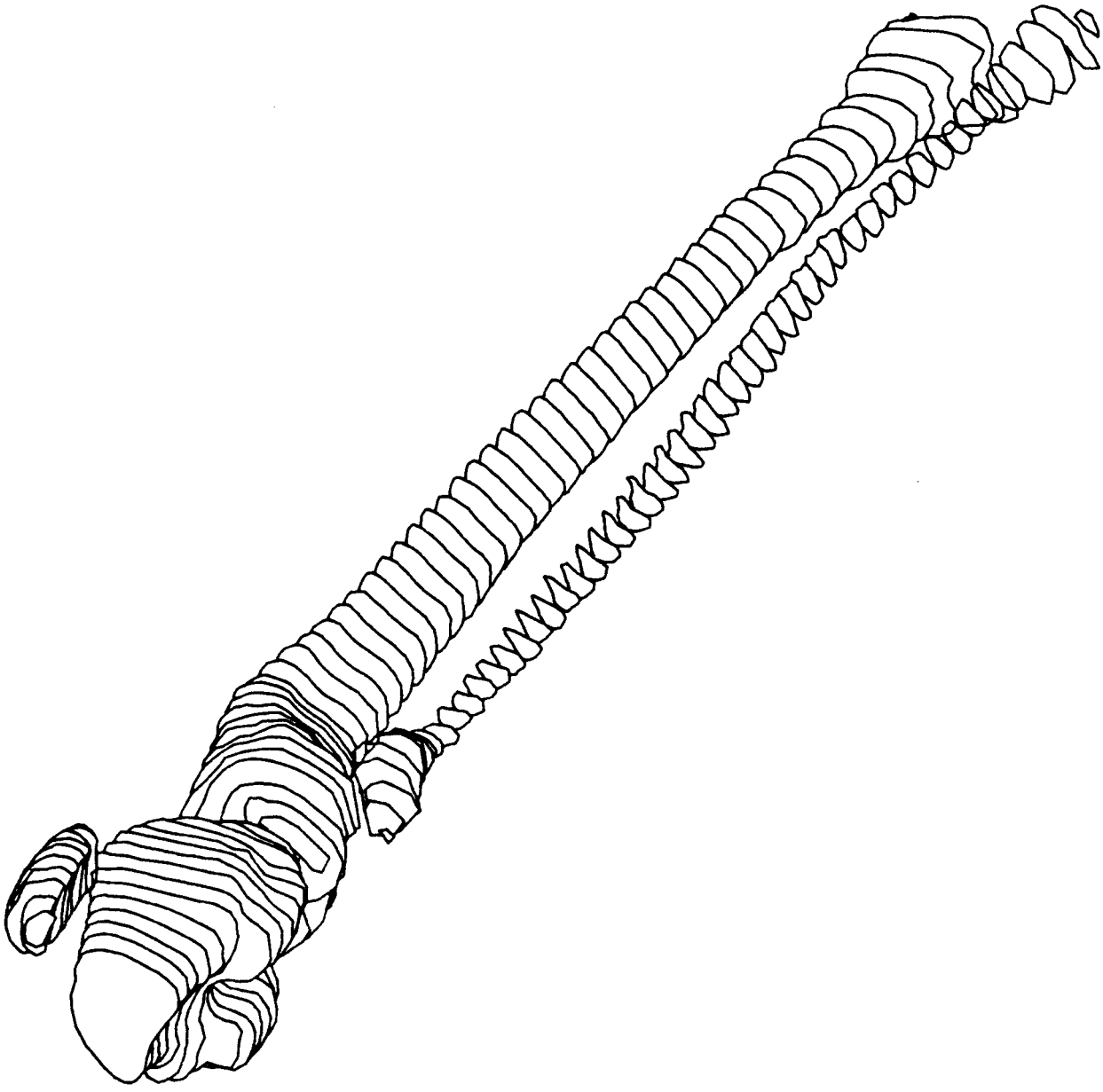

Figure 14: The femur, patella, tibia and fibula reference shapes.

Graphic representations of the bones of the residual limbs are presented in figures 15 to 20. This shape information was acquired by Computerized Tomography, as described in the Methods section. Four bones of the residual limb are depicted; the tibia, fibula, patella and distal portion of the femur.

Subject DF does not have a fibula, it was removed at the time of amputation. The limb of subject DL was crushed. It was suspected that the injury changed the shapes of the bones in his residual limb. DL's fibula was deformed to the extent that a reasonable comparison to other bone shapes was not possible. As a consequence, it was not included in the results. The remaining three bones of DL were included.

A total of six tibia, four fibula, six patella and six femurs were used in the study.

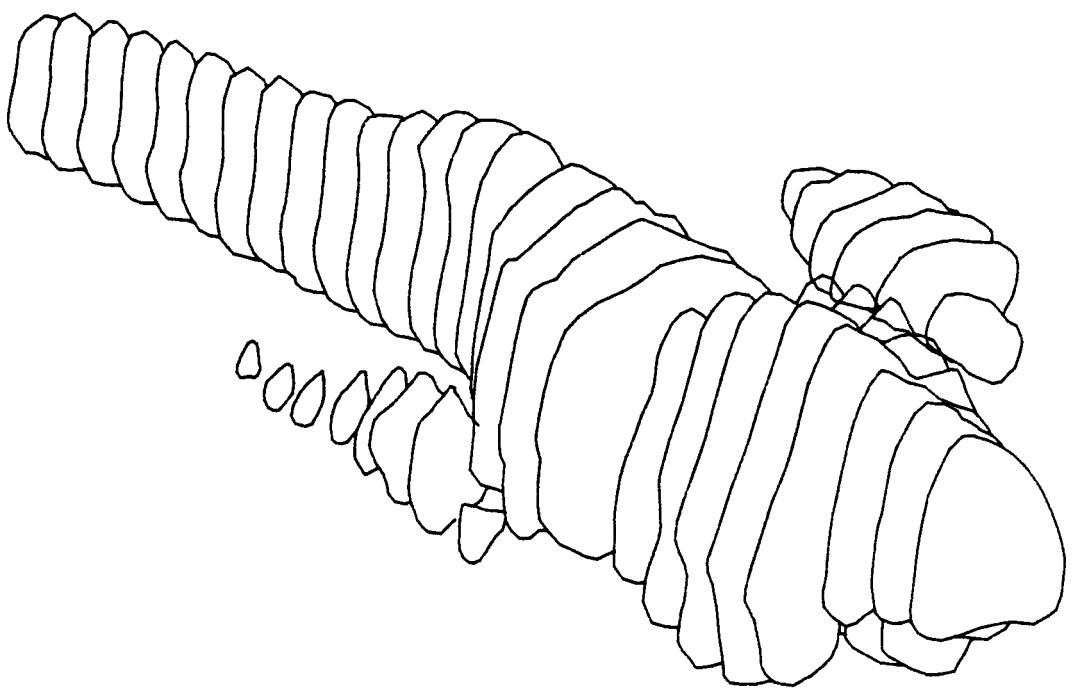

Figure 15: The bone shapes of subject JD, reconstructed from CT data. The tibia, fibula, patella and distal portion of the femur are shown. The view is from the lateral side, proximal of the left knee.

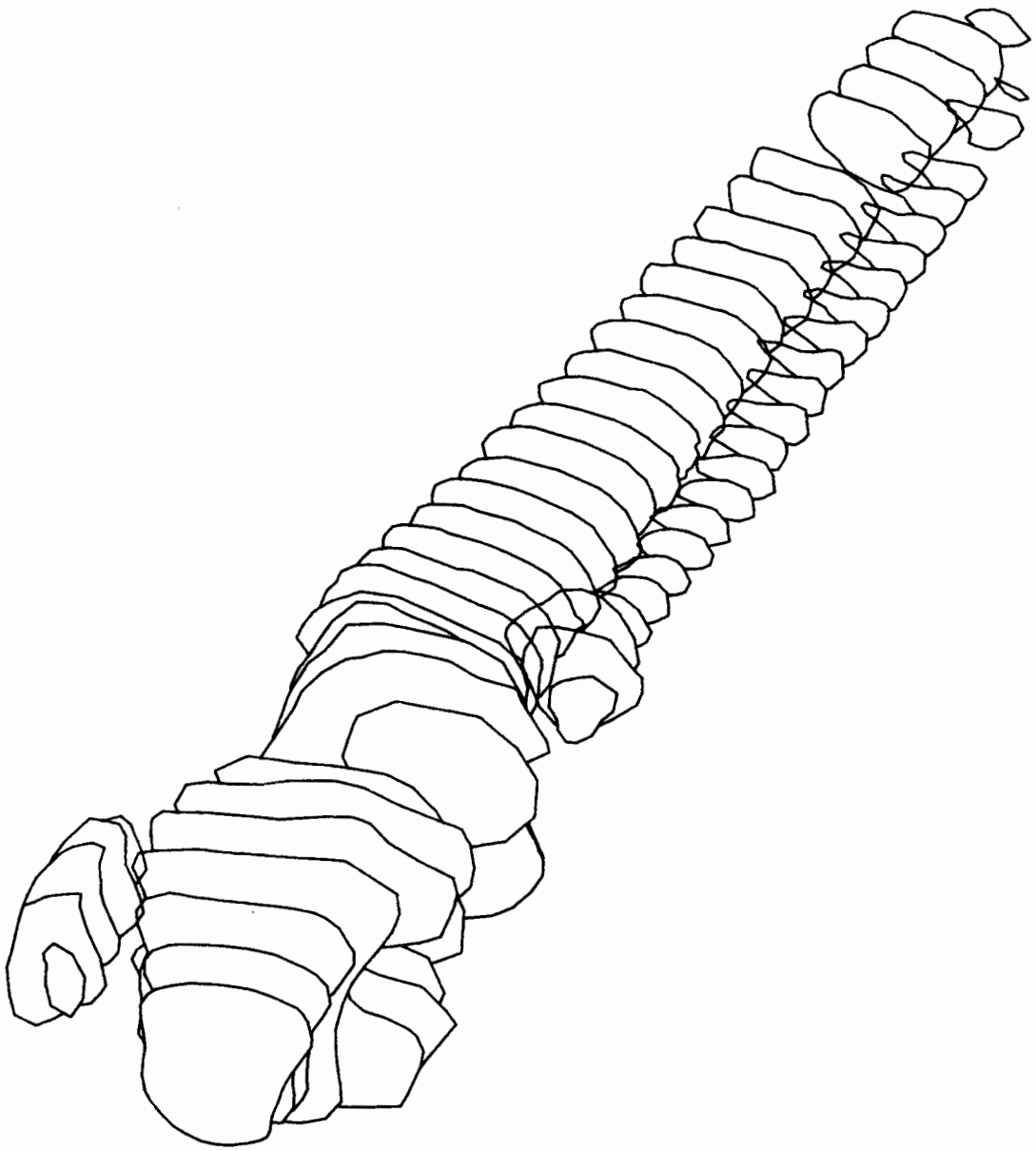

Figure 16: The bone shapes of subject EH, reconstructed from CT data. One CT slice at the distal end of the tibia was missed. Note the rounded distal end of the tibia and fibula. This is a right limb.

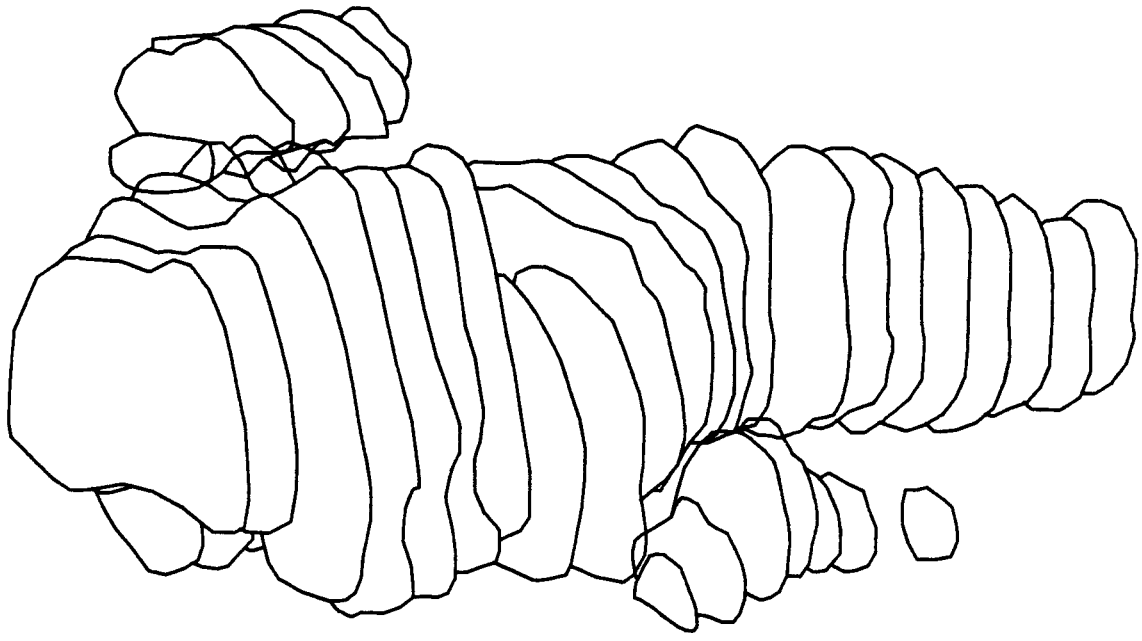

Figure 17: The bone shapes of subject BW, reconstructed from CT data. One slice of the tibia and fibula was missed. The most distal cross section appears to be out of alignment. This is a right limb.

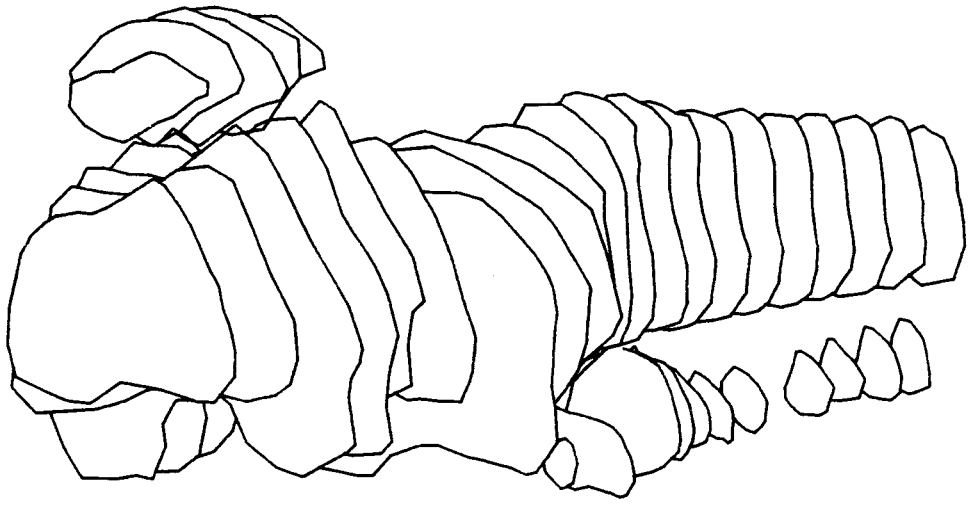

Figure 18: The bone shapes of subject GS, reconstructed from CT data. One fibula scan was missed. This is a right limb.

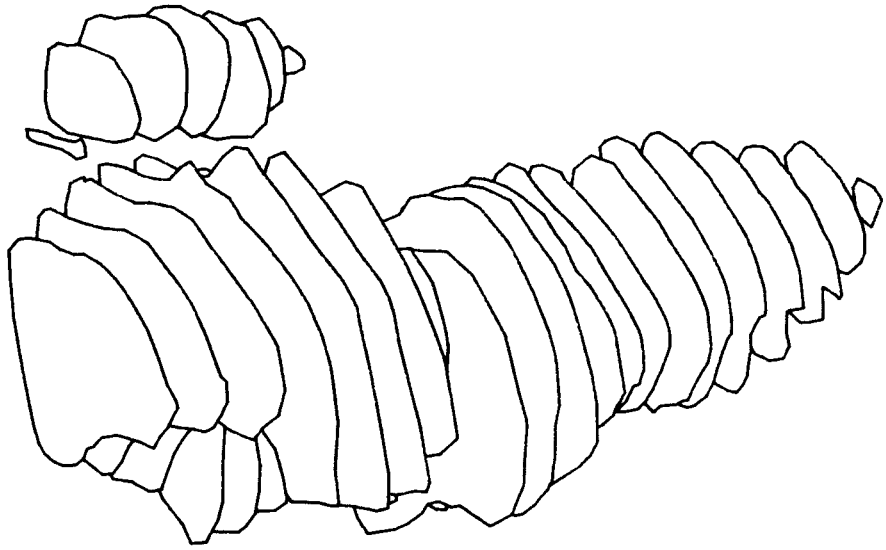

Figure 19: The bone shapes of subject FD, reconstructed from CT data. This is the left limb viewed from the medial side. FD did not have a fibula. The tibia of FD had an unusual shape. There was a large bulge on the posterior of the shaft and a distinct taper at the distal end.

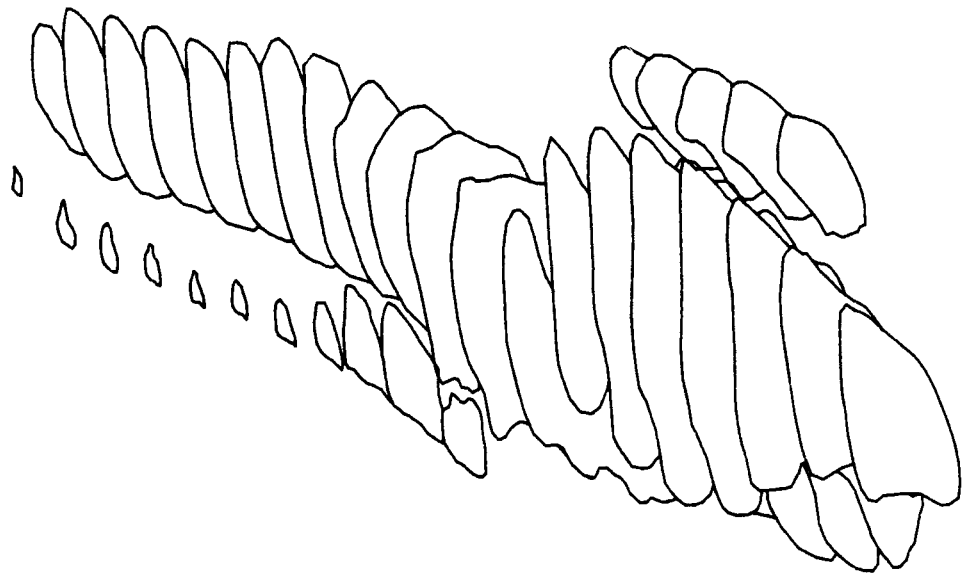

Figure 20: The bone shapes of subject DL, reconstructed from CT data. The longitudinal axis of the bone was not perpendicular to the CT plane. The limb of DL was crushed prior to amputation. The fibula has unusual bends in it. The tibia appears rotated about its long axis relative to the femur. This is a left limb.

Data Acquisition Errors

Digitizing variability.

The digitizing variability was represented by standard deviations of 0.30 mm in the x coordinate and 0.34 in the y coordinate.

Within a 95% confidence limit, digitizing variability could result in an error of ± 0.68 mm in x and ± 0.77 mm in y. A deviation of this much would not be noticed in the bone plots, (figures 14 to 20). Bone radius varied from about 5 mm to 55 mm. The error range due to digitizing variability could be as high as 15 percent of the radii of small bones.

Digitizing variability of the traced perimeters was analysed in the same manner as for the CT scans. The standard deviations were 0.25 mm for x, 0.22 mm for y and 0.04 mm for z. Although digitizing was less variable than for direct measurement from the scans themselves, it was not possible to establish the amount of error introduced due to the difficulty determining te exact bone perimeter from the CT scan.

Computerized Tomography error.

The diameters of the acrylic cylinder measured from from the digitized data were 4.9 persent less than the actual diameter.

Reference point measurement variability.

Only one set of measurements were taken from the first subject. The reference points of the remaining 5 subjects were measured three times each. The variability in the distance of 13 measured points from the tibial tubercle was calculated. Results are shown in table 4 and plotted in figure 21 in the order that

they were measured. They indicate stabilization of the measurement error for the last 4 subjects.

Table 4. Reference point measurement variability. The standard deviation of the measured distances of reference points from the tibial tubercle for 3 sets of measurements on each subject. This includes 13 reference points except subject FD for whom 11 points were used due to absense of fibula. Subjects are arranged in order of measurement. Units are in millimeters.

Subject	GS	FD	BW	EH	DL
Order of Measurement	2nd	3rd	4th	5th	6th
Standard Deviation	5.17	2.41	2.06	2.45	2.03

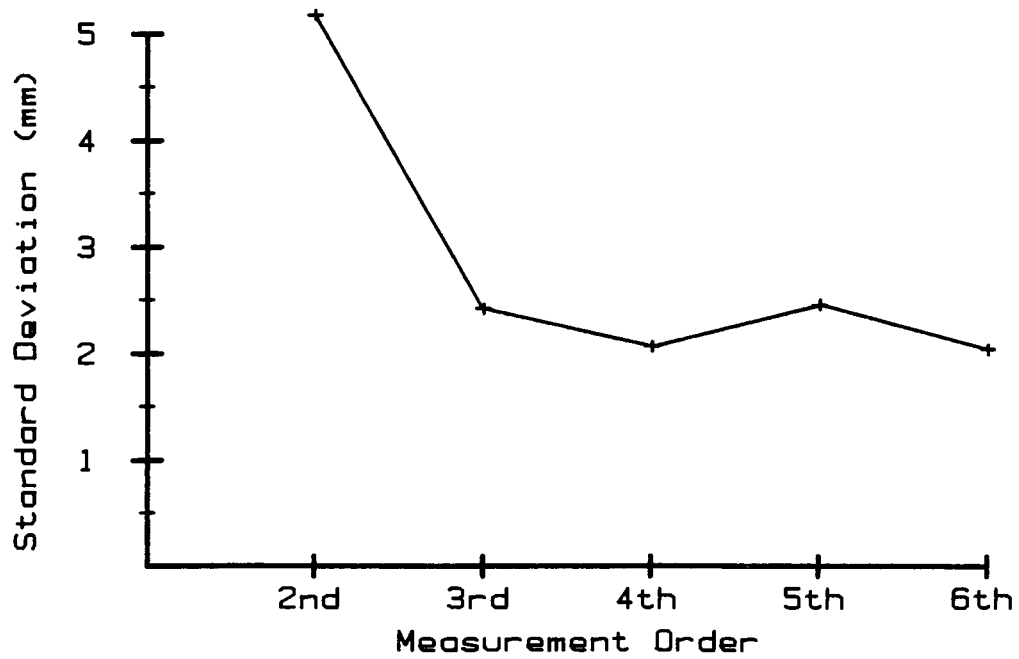

Figure 21: Reference point measurement variability verses order of measurement.

Comparison of Amputees to Reference Shapes

Each bone shape acquired by CT was compared to the corresponding (unscaled) reference bone shape. The techniques for alignment, interpolation and comparison are explained in the methods section. Three graphic outputs were generated from each comparison. In view of the extent of this material, two of the graphical outputs are presented in appendix I. These consist of radial difference maps and cross section overlays which illustrate exactly where shape and size differences occur. Numerical output of mean differences and standard deviations are also presented in appendix I. The third graphic output illustrating the mean differences and standard deviation for each cross section are presented in figures 22 to 25. These graphs show trends in size and shape differences between cross sections.

Table 5 summarizes the bone differences for all 6 subjects. The differences are absolute rather than relative to bone radius. This is because absolute information is the most relevant in the application of this data to Computer Aided Socket Design.

The mean difference is indicative of size difference. A negative value indicates that the reference bone is smaller than the amputee's bone. The RMS difference indicates shape variability. A greater RMS values indicates less shape congruence. For example, a bone having a mean difference of zero but a large RMS error, would indicate that the bone was the same overall size as the reference bone, but exhibited substantial shape, (or nonhomogeneous size), differences. A bone having a

large mean difference, and a RMS difference approximately the same magnitude would indicate a substantial size difference but small shape difference. The combined mean and RMS difference calculated over all the subjects is also presented.

Table 5. Comparison of amputee to reference bone shapes. A negative mean indicates the reference shape was smaller than the amputee shape. Larger RMS differences indicate less shape congruency. Units are millimeters.

	Tibia		Fibula		Patella		Femur	
Subject	mean	RMS	mean	RMS	mean	RMS	mean	RMS
JD	0.01	1.99	0.90	1.52	-1.57	1.91	-0.02	4.97
EH	0.82	2.09	-0.76	1.54	-0.27	1.64	1.73	3.96
BW	-1.08	2.29	-1.78	2.77	-1.41	2.17	-1.09	2.72
GS	-0.62	2.16	-0.38	1.32	-1.58	2.10	0.13	3.57
FD	-2.12	4.83	no fibula		-2.84	3.38	-2.69	4.45
DL	0.53	4.50	no fibula		-0.62	2.90	2.26	8.07
total	-0.20	3.21	-0.59	1.88	-1.42	2.42	0.04	4.92
n	8424	6480	4176	2304	2088	1728	3096	2592

Figure 22 demonstrates that the reference tibia was remarkably close to 4 of the amputees' tibia in size and shape. For 5 of the amputees, the cross sections that correspond to the shaft of the tibia were consistantly within 1 or 2 mm. The cross section overlays in appendix I, show consistant differences in the crest area of the tibia while the rest of the shaft was quite regular between bones. Subject FD had greater differences in size and shape (mean and standard deviation) than the other subjects. This can be confirmed by figure 19 where an enlargement on the posterior portion of his tibia can be seen. The condylar portion of the tibia showed greater size and shape differences than the remainder of the tibia.

In figure 23, the fibula have similar differences as the tibia. Again the mean differences were very small. Though the differences were small, they are not reported as relative to the magnitude of the radius. If they were, the fibula being smaller in diameter would have relatively larger differences between bones. In the cross section overlays in appendix I, the fibular heads and the shafts have considerable shape differences.

In figure 24, the patellae do have definite size and shape differences, but the standard deviation which relates to shape, is fairly constant within and between bones.

The femurs, (figure 25), exhibited the greatest shape variability while the size differences were similar to the other bones.

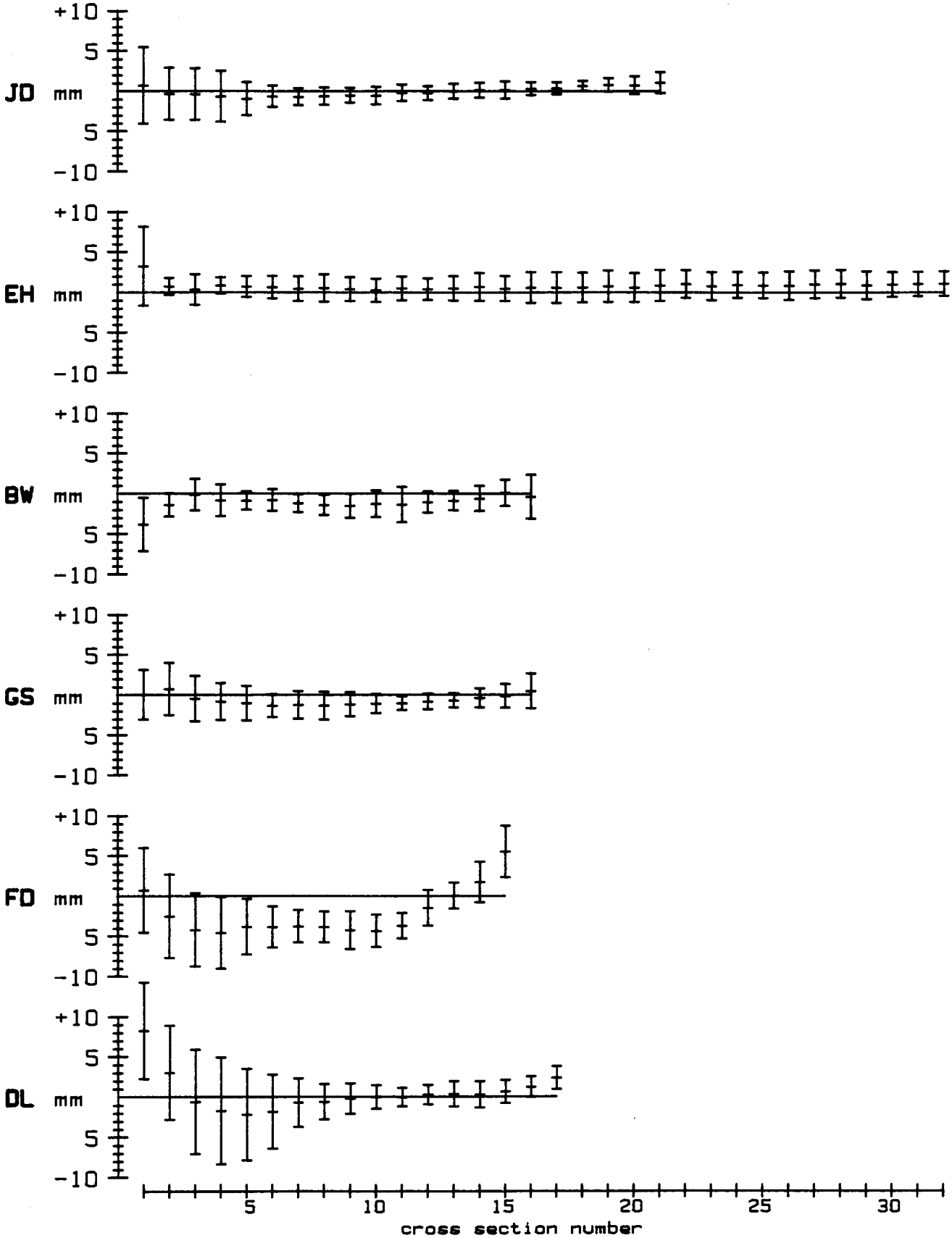

Figure 22: Amputee tibia minus reference tibia.
Mean difference with SD for each cross section.

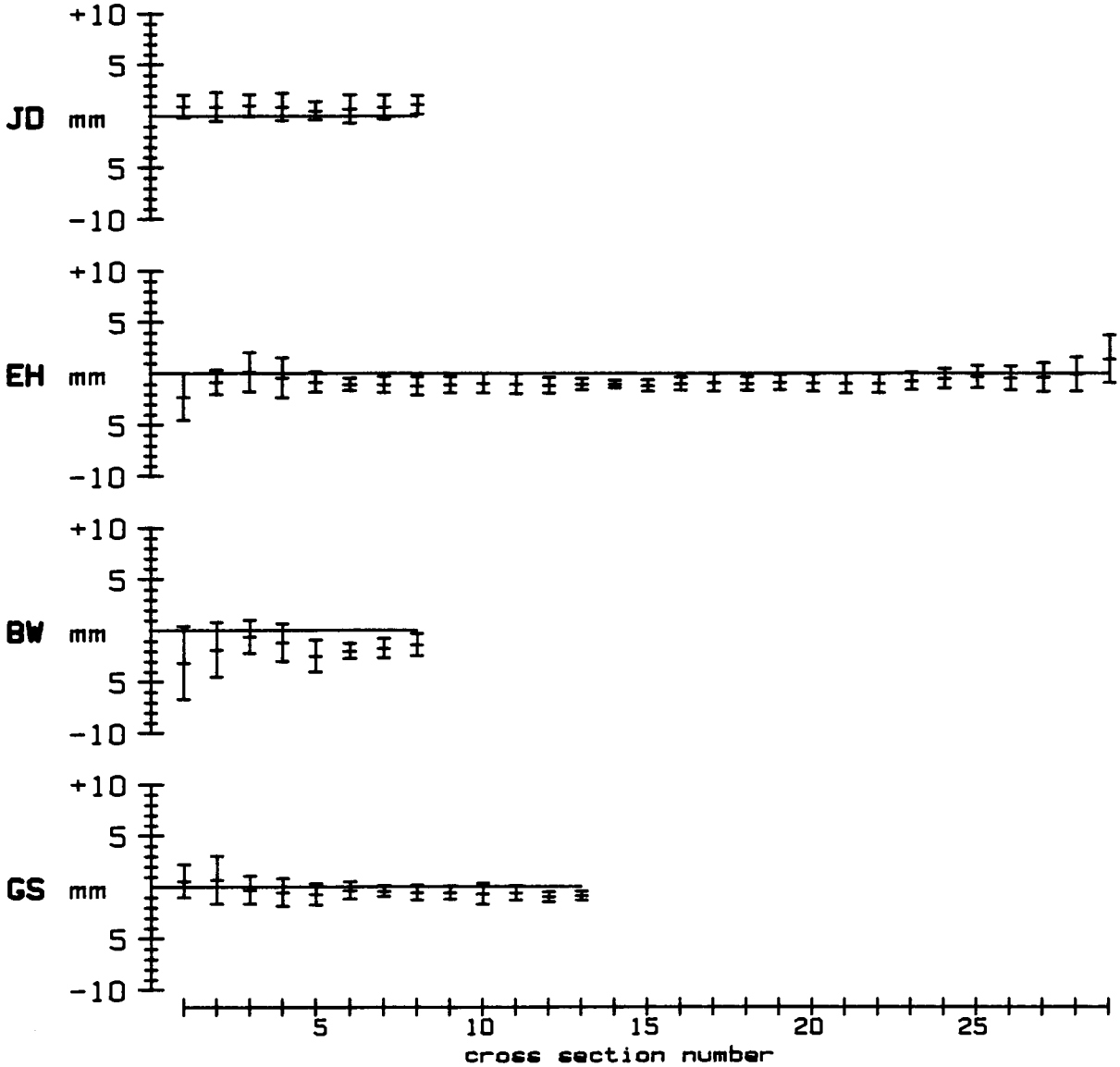

Figure 23: Amputee fibula minus reference fibula. Mean difference with SD for each cross section.

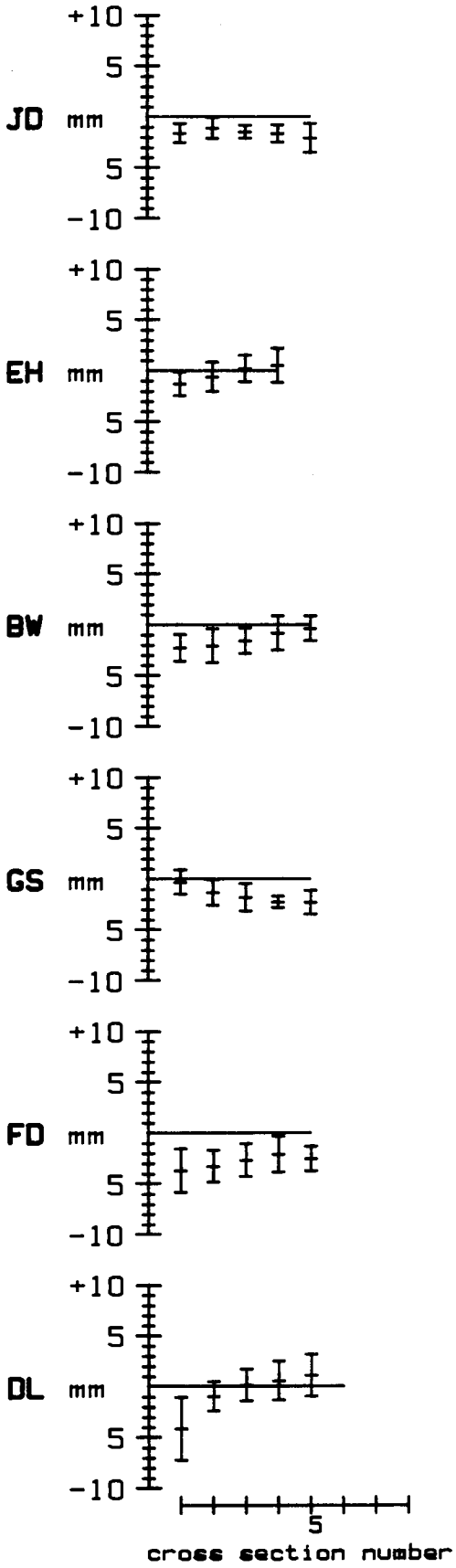

Figure 24: Amputee patella minus reference patella. Mean difference with SD for each cross section.

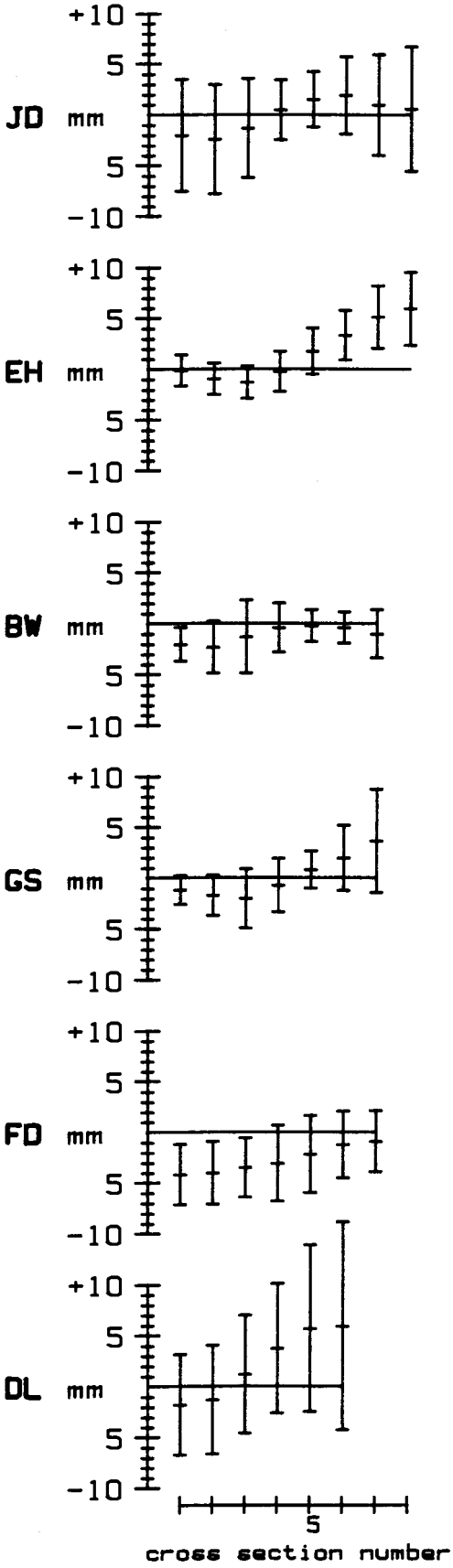

Figure 25: Amputee femur minus reference femur. Mean difference with SD for each cross section.

Comparison of Scaled Reference Bone shapes to Amputee Bone Shapes

Each scaled bone shape was compared to the corresponding amputees' bone shapes acquired by CT scan. Shape alignment, interpolation between elements and calculation of differences is described in the methods section.

Tables 6 to 9 summarize the bone differences for all the scaling techniques for each of the bones.

The means and RMS differences for each scaling technique were ranked relative to the other scaling techniques and to no scaling. For each subject, the scaling technique with the lowest mean value scored one point. The next lowest scored two points. This continued until every scaling technique for the amputee had a score. This was repeated for all the amputees and for the RMS differences. The totals for each scaling technique are given in tables 6 to 9. The lower scores indicate more accurate shape replication.

The best technique for each of the tibia, fibula, patella and femur were selected for further illustration. Selection was based on the mean and RMS totals and the ranking for each scaling procedure.

The scaling procedures determined to be the best were:

Tibia - uniform dilation;

Fibula - nonorthogonal by tibial parameters;

Patella - uniform dilation to ML proportion;

Femur - uniform dilation.

The mean and RMS for these procedures were comparable or better and their rankings were better than the other scaling techniques for their respective bones.

Table 6. Comparison of scaled tibia to amputee bone shape as acquired by Computerized Tomography. The comparisons between the reference and amputee are included to facilitate comparison. A negative mean indicates that the scaled shape was smaller. A larger RMS difference indicates less shape congruence. Units are in millimeters.

	Reference Shape		Uniform Dilation Prox-Dist		Orthogonal		Non-Orthogonal		Non-Homogeneous	
Subject	mean	RMS	mean	RMS	mean	RMS	mean	RMS	mean	RMS
JD	0.01	1.99	-0.10	1.64	2.78	4.28	1.02	3.78	1.22	4.57
EH	0.82	2.09	-1.75	2.11	0.13	1.95	-0.04	2.15	0.03	2.23
BW	-1.08	2.29	0.11	1.70	-0.60	2.92	-0.72	3.42	0.07	2.84
GS	-0.62	2.16	-0.60	2.24	-3.10	3.78	-3.17	4.79	-2.53	3.76
FD	-2.12	4.83	1.12	3.43	-2.44	4.10	-0.01	4.79	-1.94	4.35
DL	0.53	4.50	5.20	6.64	3.45	5.10	2.76	5.31	2.73	5.65
total	-0.20	3.21	0.23	3.44	0.10	3.82	-0.07	4.17	-0.05	4.06
n	8424	6480	7776	5616	7632	5616	7488	5184	7632	6048
order rank	17	13	17	12	25	17	17	24	14	24

For the tibia, the combined mean differences for all subjects were all less than 0.23 mm. Likewise, the total RMS differences are all within a range of 0.85 mm. DL is the subject whose limb was crushed. His differences were the largest.

Table 7. Comparison of scaled fibula to amputee bone shapes as acquired by Computerized Tomography. The comparisons between the reference and amputee are included to facilitate comparison. A negative mean indicates that the scaled shape was smaller. A larger RMS differnce indicates less shape congruence. Units are in millimeters.

	Reference Shape		Uniform Dilation Prox-Dist		Orthogonal by Tibia		Non-Orthogonal by Tibia	
Subject	mean	RMS	mean	RMS	mean	RMS	mean	RMS
JD	0.90	1.52	0.46	1.77	1.62	2.47	1.27	2.12
EH	-0.76	1.54	-1.98	2.30	-1.11	1.75	-1.11	1.73
BW	-1.78	2.77	-1.75	2.80	-1.40	2.63	-1.12	2.39
GS	-0.38	1.32	-1.48	1.91	-1.11	1.59	-1.14	1.18
total	-0.59	1.88	-1.46	2.23	-0.74	2.16	-0.80	2.03
n	4176	2304	3816	1728	3744	2016	3888	2016
order rank	8	8	12	13	10	13	9	8

By all of the indicators, none of the scaling procedures for the fibula were more accurate than no scaling. This reflects how closely the reference fibula matched the amputees' fibula before scaling. The most accurate of the scaling procedures was nonorthogonal scaling by tibial parameters.

Table 8. Comparison of scaled patella to amputee bone shapes as acquired by Computerized Tomography. The comparisons between the reference and amputee are included to facilitate comparison. A negative mean indicates that the scaled shape was smaller. A larger RMS differences indicate less shape congruence. Units are in millimeters.

	Reference Shape		Uniform Dil. Med-Lat		Uniform Dil. Prox-Dist		Orthogonal	
Subject	mean	RMS	mean	RMS	mean	RMS	mean	RMS
JD	-1.57	1.09	-1.21	1.75	0.18	1.11	-0.19	0.98
EH	-0.27	1.64	0.08	1.27	0.44	1.73	1.36	1.76
BW	-1.41	2.17	-0.29	1.27	0.43	1.79	0.25	1.31
GS	-1.58	2.10	-0.25	1.42	-0.63	1.56	0.25	1.26
FD	-2.84	3.38	-0.12	1.78	0.33	1.45	0.05	1.37
DL	-0.62	2.90	0.18	2.19	0.54	2.21	0.51	1.94
total	-1.42	2.42	-0.30	1.64	0.20	1.67	0.38	1.47
n	2088	1728	2016	1728	2160	1296	2088	1728
rank order	22	20	10	11	16	15	14	10

All of the patella scaling procedures resulted in an improvement in combined mean and RMS differences. The results are less random than for the other bones.

Table 9. Comparison of scaled femurs to amputee bone shapes as acquired by Computerized Tomography. The comparisons between the reference and amputee are included to facilitate comparison. A negative mean indicates that the scaled shape was smaller. A larger RMS differences indicates less shape congruence. Units are in millimeters.

	Reference Shape		Uniform Dilation Med-Lat		Orthogonal		Non-Orthogonal	
Subject	mean	RMS	mean	RMS	mean	RMS	mean	RMS
JD	-0.02	4.97	0.32	4.36	0.36	4.92	2.87	7.58
EH	1.73	3.96	-1.89	3.43	0.07	2.62	1.74	6.19
BW	-1.09	2.72	2.71	3.91	-3.95	4.95	-1.43	4.60
GS	0.13	3.57	-0.14	2.77	-2.71	3.52	-0.04	4.74
FD	-2.69	4.45	1.11	2.73	-3.40	4.74	-7.07	8.71
DL	2.26	8.07	0.40	6.23	1.74	7.60	-1.13	8.27
total	0.04	4.92	-0.42	4.08	-1.38	4.96	-0.81	6.87
n	3096	2591	2088	1728	2592	2160	2664	1728
rank order	12	15	14	9	18	14	16	23

The combined mean differences for the femur indicate no scaling to be best, while the RMS differences indicate uniform dilation to be best. The rankings suggest uniform dilation is most often the most accurate.

Graphs of the mean difference and standard deviations are presented in figures 26 to 29. Difference maps and cross section overlays of the selected scaling techniques are in appendix II along with numerical output of mean differences and standard deviations.

For the tibia, a comparison of figure 22 to 26 indicates a general reduction in the standard deviations. There are exceptions to this, notably the shaft portion for FD and DL. The means for each bone have shifted, some better, some worse. The pattern of mean and standard deviation is usually maintained. Subject FD is again an exception, his curve has straigtened.

The same trends can be seen in the fibula, patella and femur as existed in the tibia.

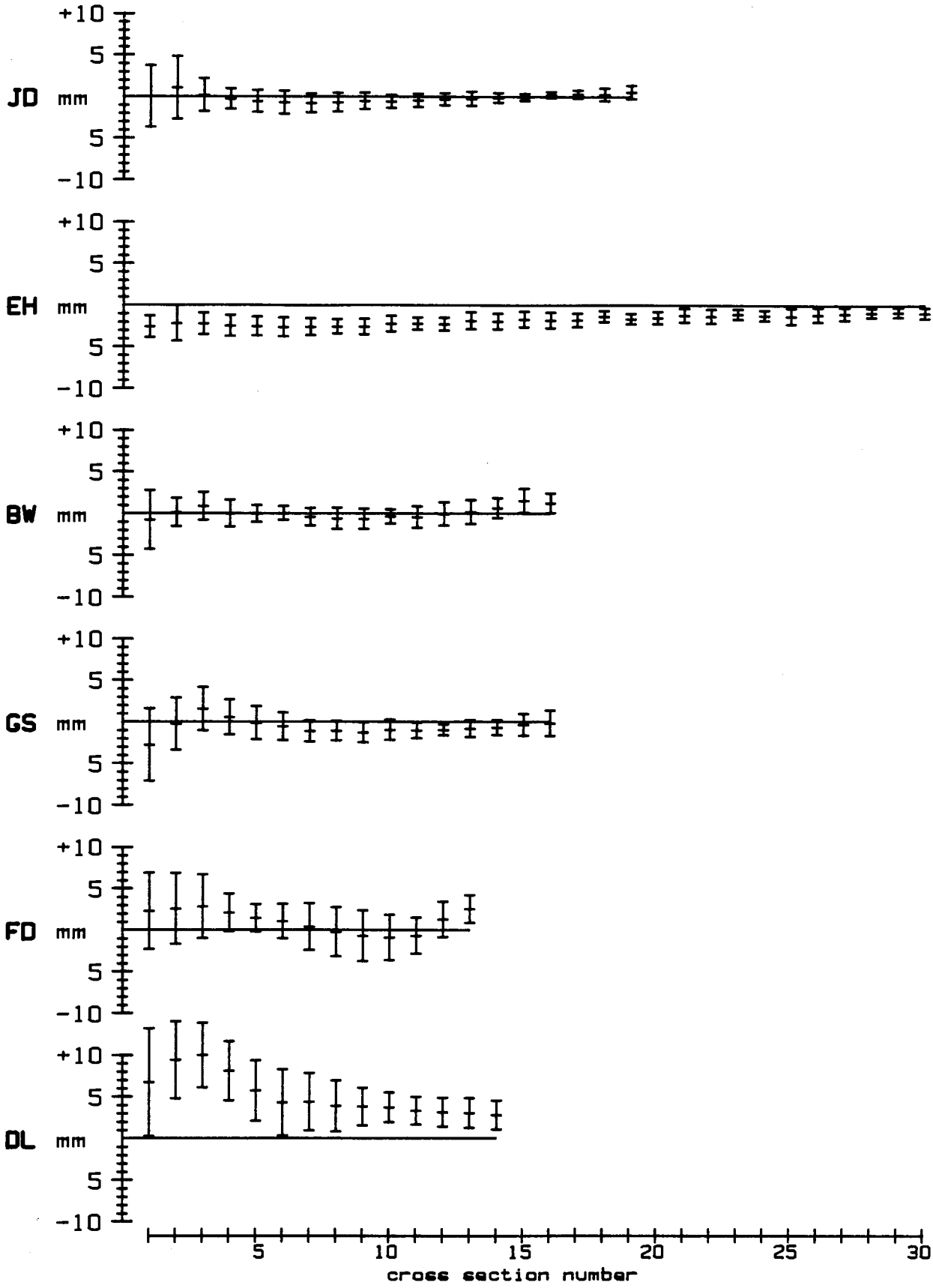

Figure 26: Amputee minus uniform dilation tibia.
Mean difference with SD for each cross section.

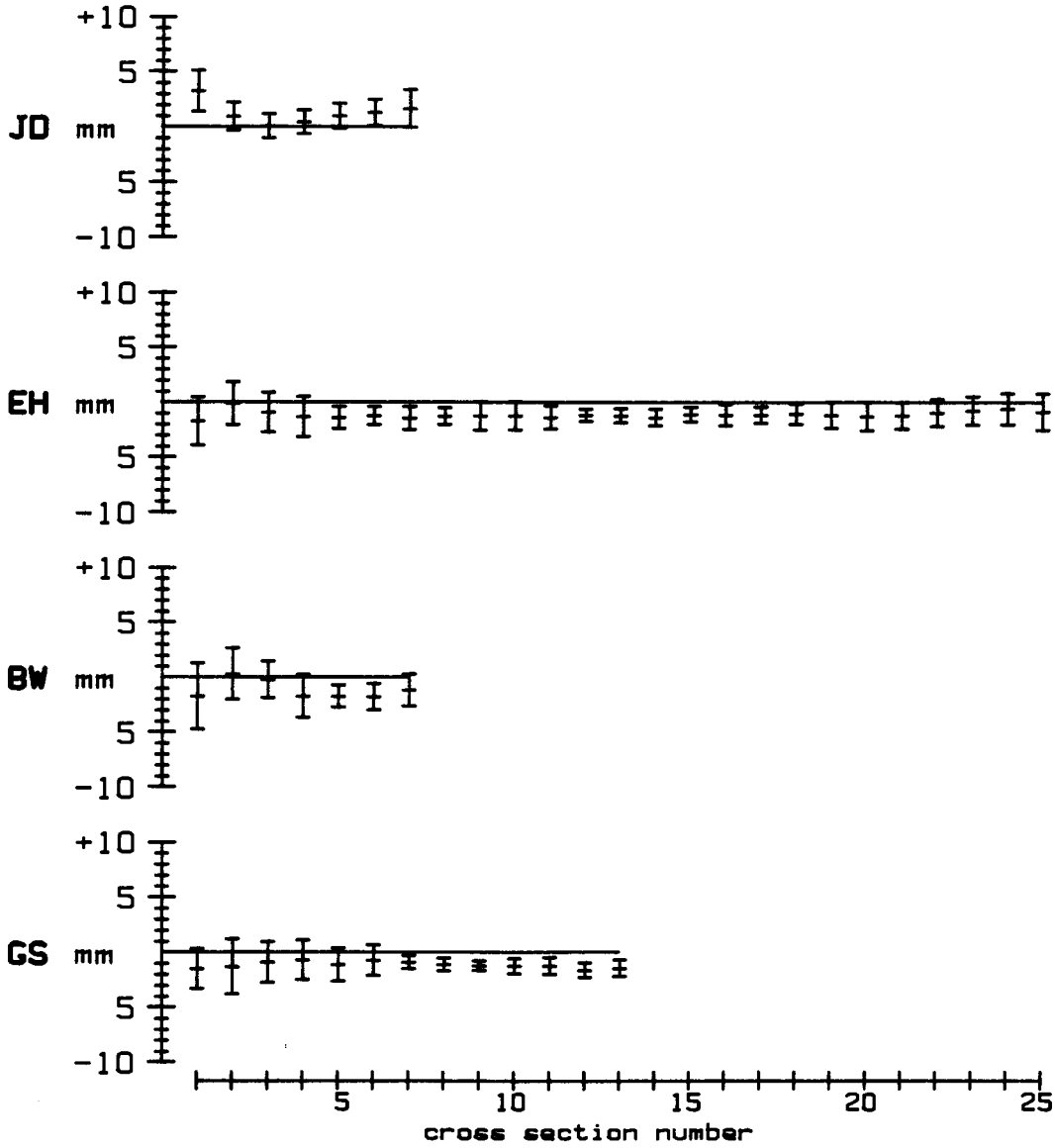

Figure 27: Amputee minus non-orthogonal fibula. Mean difference with SD for each cross section.

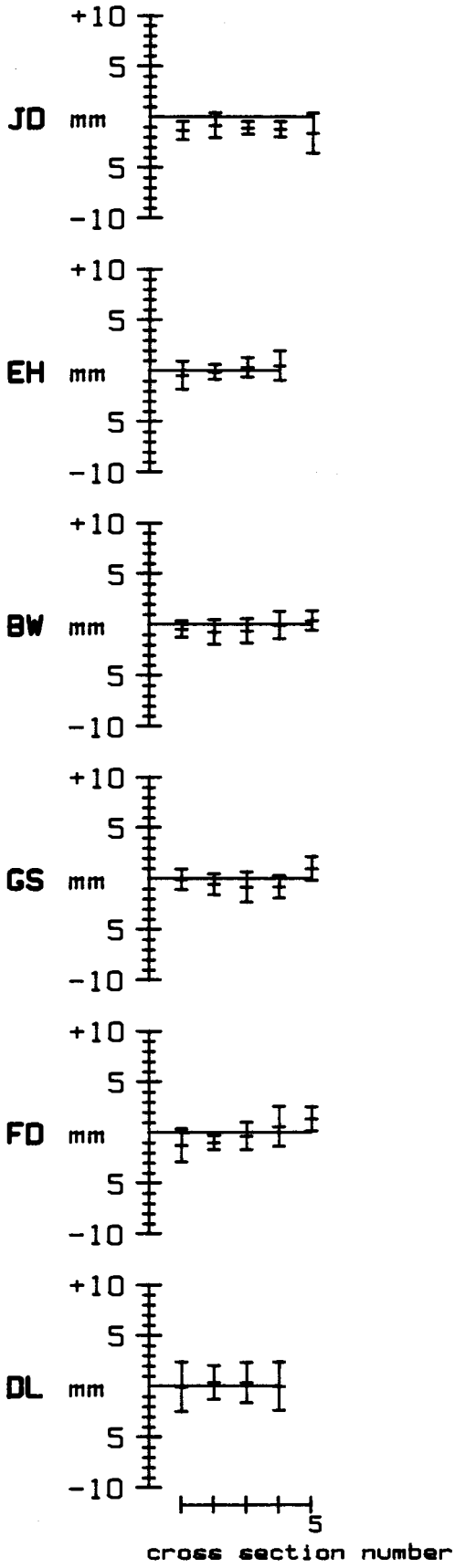

Figure 28: Amputee minus ML uniform dilation patella. Mean difference with SD for each cross section.

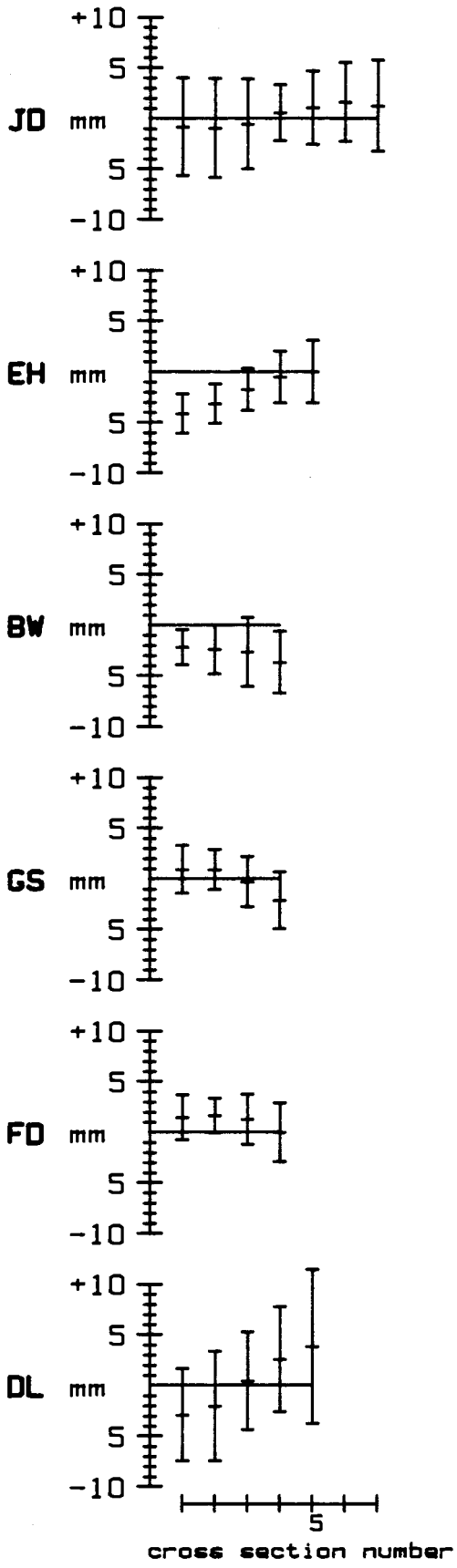

Figure 29: Amputee minus uniform dilation femur.
Mean difference with SD for each cross section.

Bone positioning.

Upon scaling, the new bone shapes were positioned such that the scaled reference shape reference points matched the amputees' reference points. Any error in the match indicates that the new shape was not positioned correctly. Also, the reference points spanned the critical dimensions of the bone, therefore longitudinal scaling accuracy can be approximated by the accuracy of the match between the 2 sets of reference points. Reference point measurement errors contribute to the errors in this technique.

Table 10 shows the RMS error in reference point scaling. It can be seen that uniform dilation of the fibula and nonorthogonal scaling always positioned the reference points accurately. The fibula has only 2 reference points. Uniform dilation will always scale the points used to derive the proportion correctly. This was true for all the uniform dilation scaling techniques, the 2 reference points used to calculate the scaling proportion were always positioned correctly. With 4 reference points the scaling axes of nonorthogonal scaling will always be placed such that after scaling the 4 points from the reference shape match the subject's reference points.

The fibula was scaled orthogonally and nonorthogonally using tibial scaling and transformation parameters. In orthogonal scaling only one fibular reference point was used to translate the fibular head to the correct position.

Table 10. Positioning error. The discrepancy between the scaled reference points from the reference shape and the reference points from the subject was calculated as a RMS error. Table 10 contains the mean and standard deviation of the RMS error for each bone and for each scaling technique. Units are millimeters.

	Uniform Dilation			Orthogonal			Non-orthogonal		
	mean	SD	n	mean	SD	n	mean	SD	n
Tibia	0.30	0.24	4	0.35	0.09	5	0.00	0.00	4
Fibula	0.00	0.00	2	0.00	0.00	1	5.08	1.55	2
Patella ML	0.52	0.06	4	0.52	0.05	4	----	----	0
PD	0.52	0.08	4						
Femur	0.18	0.09	6	0.60	0.22	6	0.00	0.00	4

DISCUSSION

One of the results of this project has been graphic depiction of the extent of bone shape and size variability. The degree of nonhomogenity is well defined for the limited number of subjects observed. It is unfortunate that more subjects could not be included in the study. However, the number of subjects investigated was constrained by the labour intensive nature of the data collection procedures. Each subject required serial CT scans of four discrete bone shapes, followed by manual digitization of each bone segment. A total of 25,000 digitizations were necessary to construct the 26 bone shapes acquired. Because of the small number of subjects, caution is urged in interpretation of the results.

In general, the results did not show an improvement in the differences from before scaling to after scaling. These results were not expected. There are three factors that contributed to these results.

1. Four of the amputees met the 2mm objective for the tibia, fibula and patella before scaling.
2. The variability of reference point measurement was greater than 2mm.
3. In some individuals a large degree of nonhomogenity was identified in the analysis. This could not be accounted for by homogeneous scaling.

Details of these findings will be discussed in the following

paragraphs.

Three separate measures of accuracy were calculated from bone shape comparisons. These were mean difference, standard deviation of the mean, and RMS difference. None of these measures can be considered to describe precisely the difference in size and shape of the bones. However, in general the mean error is considered to be indicative of the difference in overall size between two bones, while the standard deviation is indicative of difference in shape. The RMS difference is indicative of overall accuracy of the comparison, and hence includes both size and shape differences. The RMS difference will also detect nonhomogeneous size differences between different sections of the bone which would not be detected by composite mean difference and standard deviation calculated for the entire bone. To appreciate the nature of nonhomogeneous size and shape differences it is necessary to study the serial comparisons generated in figures 22 to 29 and appendices I and II.

It should be noted that the calculated differences were primarily due to size and shape differences of the bones and not due to alignment of the bones during the comparison process. Alignment errors were minimized by an iterative alignment process as described in the methods section.

The reference bone shapes were arbitrary shapes. By coincidence, they were not much different than the amputee bone

shapes. This had a profound effect on the accuracy of the scaling procedures in comparison to the initial differences between the reference bone shapes and the amputee bone shapes. The size of the reference shape has no effect on the outcome of the scaling process as long as the reference points are appropriate. For example, if the tibia reference shape was twice the size it actually was, and separation between the reference points expanded by the same proportion, then the scaling procedures would generate the same tibia shapes as were produced in this project. Improvement from the reference shapes would be substantially better than as observed.

With respect to the measured differences between the reference and amputee bone shapes, scaling by uniform dilation was expected to reduce the mean and RMS radial differences by similar amounts. Of the 28 uniform dilation scalings there were 19 improvements in the mean difference. Scaling of the patella to its medial-lateral (ML) proportions was the most successful; the mean radial difference was reduced in all 6 subjects. The femur was the least effective with only 2 improvements in the mean difference.

These results reflect the relative nonhomogenity of the bones. The shape differences found between patellae are less than the differences found between femurs. Therefore, one dimension is a better indicator of size for the patella than for the femur. The total RMS difference of the reference to amputee bone comparisons reflect this with RMS differences of 2.42 mm

and 4.92 mm respectively for the patella and femur.

The ML reference points on the patella were more accessible than the proximal-distal (PD) reference points. It was expected that palpation error would be less for the ML reference points and therefore, ML scaling would be more accurate. This proved to be true for 5 of the 6 amputees.

The proportions for uniform dilation of the tibia and fibula were derived from reference points positioned along the longitudinal axis of the bone. Only 50 percent of the scalings resulted in size improvements. This is to be expected when considering that bone diameter is not dependent on length. It could be hypothesised that reference points in the transverse plane would give better results for comparisons made in the transverse plane. This is probably true for any one section, but differences in bone lengths at a different proportion than transverse proportions would not be reflected in the scaling procedure. Hence, substantial length scaling errors could occur.

The RMS values were reduced in 17 of the 28 uniform dilation scalings. Shape changes do not occur with uniform dilation. But, the mean and RMS difference values are dependent on how well bones are aligned during the comparison process, (see figure 13). The changes in RMS differences are attributed to size changes with the exception of alignment error. The remaining RMS error will then tend to reflect the actual shape difference between the bones.

Length comparisons were not made using the cross sectional data. It was attempted, but the results were extremely variable.

This was due to the cross section data format. The gap between CT slices was 4 mm. With a gap at each end the CT bone could appear to be up to 8 mm short of actual size. When interpolating cross sections additional length could be lost depending on the interval of the cross sections being interpolated.

Orthogonal scaling was in different proportions in either 2 or three orthogonal axes depending on the bone type. Since each axis was scaled independently this should have given an improvement in fit over uniform dilation. This occurred in 8 mean differences and 10 RMS differences, of the 22 orthogonal scalings. Size was only better than the unscaled reference shape in 10 cases (as measured by mean difference), and overall accuracy (RMS difference) in 12 cases.

In general, there is an increase in differences as a result of orthogonal scaling for all the bones except the patella. Examination of figures 22 to 25 reveals that the tibia, fibula and femur have nonhomogeneous shape and size differences other than along their critical dimensions. Examining the tibia first, figure 23 shows differences in the mean and standard deviation between cross sections along their lengths. These differences can not be accounted for by orthogonal scaling. Generally, there was greater variability in the proximal end rather than the distal end. This observation is confirmed by the plots in appendix I. The shaft portion of the tibia did not vary substantially from the standard tibia. On some the crest was exaggerated more than others, but with the exception of subject

FD who had a calcification on the posterior portion of the shaft, the majority of the shafts were quite similar. On the other hand the tibial condyles varied considerably in size and shape. There were also variations in rotation of the tibia about its long axis where the condyles were at a different orientation than the shaft, (subject EH in particular).

Similar nonhomogenities existed for the fibula and femur as did for the tibia, (figures 24, 26 and appendix I). Because of the lack of sufficient palpable points on the amputated fibula, it was scaled orthogonally and nonorthogonlly by tibial scaling parameters. When comparing the fibulas scaled by tibial parameters to fibular uniform dilation the mean differences were less by close to 50%, while the RMS differences were increased only slightly. The fundamental differences between these techniques is that the procedures using tibial parameters scale in the transverse plane according to proportions derived in the transverse plane while uniform dilation uses longitudinal proportion. It is possible that the tibia and fibula cross sectional areas are related but the directions of greatest diameter increase differ. This would give the observed result of a decreased mean difference but not an accompanying decrease in RMS difference.

Nonorthogonal scaling is also at different proportions in 3 directions, but the direction of scaling is defined by the reference points which are not necessarily located orthogonally. When the axes of the reference points from the reference shape

and the amputee do not match, shearing of the bone occurs. At first approximation this should have been a more accurate scaling technique than either uniform dilation or orthogonal. But, this was only true in 6 out of 18 cases for the mean difference and only in 3 cases for RMS differences.

Because of its shearing action, nonorthogonal scaling is more sensitive to reference point measurement error than uniform dilation or orthogonal scaling. Table 3 indicates a reference point measurement variability in the order of $\pm$ 4 mm with 95 percent confidence. Palpation and instrumentation variability, and movement of the subject during the measurement sequence all contribute to this error.

The reference points used to derive the scaling factor for the anterior-posterior (AP) direction of the tibia and femur did not span the total depth of the bones. The most posterior points that were available were the posterior aspect of the medial and lateral joint spaces. As a result, size differences in the posterior portion of the bone were not represented. The reference points found to yield the best results by Lew and Lewis, (1977), were those which spanned the critical dimensions of the bone. This poses some problems in the intact limb where tissues other than bone can interfere with the palpation of landmarks. The selection of reference points was based on accessibilty and the presence of characteristics that could be identified with confidence on different individuals. In retrospect it may be more appropriate to measure less reliable but more posterior points.

Any procedure that accounts for the nonhomogenity of bones should reduce the differences in shape and size. This was the objective of the nonhomogeneous scaling procedure for the tibia. Nonhomogeneous scaling always followed nonorthogonal scaling. It did improve the mean difference from nonorthogonal scaling in 4 of the 6 subjects and the RMS difference in 3.

The objective of this scaling technique was to account for bends in the tibia through keeping track of the curve of the tibial crest. Unfortunately, it perceived tapering tibia to be bending and increased their bend. An improved technique would track both the anterior and posterio-medial crests.

Examination of the data acquisition errors indicate a 4.9 percent reduction of size in the data derived from the CT scans. The cause of this reduction is unknown. One possible source is an incorrect calibration factor during digitizing of the CT scans. Checking the calibration and alignment jig eliminated this as a major contributer. The greatest variance of the tubes that serve as calibration endpoints would account for, at most, a 1 percent error. Other possibilites were software problems in the digitizing program or an inappropriate contrast on the CT scanning film generation equipment. With changes in the contrast in the CT image, under operator control, the diameter of objects change.

If the CT size reduction was homogeneous, it would not have an effect on the results of this study. All the shapes would be

reduced by the same proportion. If the absolute dimensions of the reconstructed shape were important, as would be the case in application of the developed technique in Computer Aided Socket Design, then this error would have to be defined and compensation made for it.

An objective of this project was to achieve a scaling accuracy better than plus or minus 2 mm in bone radius. Mean differences were within 2 mm for 57 of the 72 scaled bone shapes. Thus the size of the majority of bones was within 2 mm. But, even though the mean difference for two bones may be the same, their shapes may vary to such an extent that their radii are vastly different. Since RMS differences include size and shape characteristics of the bones they are better indicators of scaling accuracy. The combined RMS errors of the most accurate scaling techniques for each bone were:

tibia	- 3.44 mm	fibula	- 1.91 mm
patella	- 1.47 mm	femur	- 4.08 mm

These represent an error range greater than plus or minus 2 mm.

These results differ from those reported by Lew and Lewis, (1977). They found that nonorthogonal scaling was the most accurate followed by orthogonal then uniform dilation. In a later study, Lewis et al (1980) used more than one nonorthogonal transformation for different portions of the bone and found scaling to be enhanced slightly.

Lew and Lewis used extracted femurs and hence palpation and subject movement errors would not be present. Both these error

sources are factors to which nonorthogonal scaling accuracy is extremely succeptable. Lewis et al were also able to choose reference points that would normally be hidden in vivo by soft tissues. Thus, they were able to use points which encompassed the critical dimensions of the bone and approximate a tetrahedron; a configuration they describe as optimal.

The bones showing the greatest size differences from the unscaled reference shapes also tended to have the greatest nonhomogeneous shape and size differences along the axis of the bone, (for example see figure 22, subjects FD and DL). Thus, although scaling procedures improved the accuracy in the part of the bone from which the scaling measures were taken (for example the tibial condyles), scaling might result in greater errors occurring in different sections of the bone.

The absence of improvement of scaled shapes over unscaled shapes derives from three sources:

a) The study showed nonhomogeneous shape differences to be greater than expected, particularly for the tibia and femur. It is not possible for homogeneous scaling techniques to accommodate these nonhomogeneous differences. The nonhomogeneous technique that was tried for the tibia reduced the scaling error slightly. Additional nonhomogeneous scaling techniques that address other inconsistencies in bone shape would likely reduce scaling error further.

b) The reference shape provided a much better size comparison

than was expected. There was little room for improvement in size by scaling. The biepicondular knee breadth of the reference femur was midrange of that of the amputees. Also the range of amputee biepicondular breadths was only 35% of the range found by Breackey (1973). They only represented a small segment of the possible range of limb sizes.

c) Reference point measurement variability was greater than 2mm, (figure 21). A pilot study, (Cooper 1982), showed that scaling errors are of the same magnitude as reference point measurement errors. The variability of reference points reduces the probability of meeting the scaling accuracy objective of 2mm.

Both measurement error and reference point selection play an important role in the accuracy of the scaling procedures used in this project. But, the bones that were studied do exhibit considerable nonhomogenity in shape. If those shape differences are calculated, then the reference points and scaling algorithm can target those areas and account for the shape discrepancies. Hopefully, this thesis has shed some light on the nonhomogeneous characteristics of bone shapes.

The areas of the bone that are most critical in terms of socket design, are those areas that are near the surface of the limb. In areas where the bone is covered by soft tissues the shape is not critical. If the scaling procedures focussed on the critical areas of the bone surface, then it is likely that these areas would be reproduced with a greater accuracy than the bone shapes as a whole.

CONCLUSIONS

This project had a substantial development component. A technique for 3 dimensional reconstructions utilizing Computerized Tomography was developed, as well as 4 major computer programs:

3-D reconstruction from CT scans;

shape scaling;

3-D shape comparison procedures with graphical representation;

three dimensional graphics plotting routines including view manipulation and hidden line procedures.

The standard reference shape met the stated objective of less than 2mm difference when compared to 4 of the amputees' tibiae, fibulae and patellae.

The scaling procedures developed and tested in this project did not consistently generate bone shapes that were more accurate than the unscaled reference shape. This is believed to be due to 3 factors: considerable nonhomogeneous shape differences between bones of the same type; difficulty in measuring bone reference points in vivo; and relatively small differences of size between the reference and amputee bones.

The most consistent improvement in accuracy achieved by scaling procedures was for the patella which also demonstrated the least degree of nonhomogenity between bones.

Some of the nonhomogeneous features of the bones were identified. It is probable that scaling algorithms of a modular nature that scale individual portions of the bone could account for these shape discrepencies to a greater extent than the techniques that were used.

The fibula and patella scaling procedures met the stated objective of 2mm. The tibia and femur procedures resulted in errors of 2 to 5mm. Whether this accuracy is sufficient cannot be judged until the scaling procedures are incorporated into the CAD system and tested in clinical trials.

APPENDIX I

Bone shape variability comparison plots.

The comparison plots for 22 bones compared to the reference bone shapes follow. They are in the order of tibia, fibula, patella then femur.

Each plot has 3 sections. On the left are the means and standard deviations for each cross section. Proximal cross sections start at the bottom of the page going to distal cross sections at the top of the page.

The centre section contains a map of the differences between radii. The map starts at 355 degrees on the left and goes to 0 degrees on the right. The displacement on the map is relative to the difference between the radii of the 2 bone shapes being compared. The baseline, or zero level is indicated by the straight blue line. The mean difference and its standard deviation are given at the bottom of the page.

The cross sections of the two bones are superimposed in the right hand section. The xy origin is indicated by an '+', with the radian at 0 degrees indicated.

Appendix I

List of Figures

Amputee bone CT scans verses reference bone shapes

Subject		Page
Tibia		
	JD	103
	EH	104
	BW	105
	GS	106
	FD	107
	DL	108
Fibula		
	JD	109
	EH	110
	BW	111
	GS	112
Patella		
	JD	113
	EH	114
	BW	115
	GS	116
	FD	117
	DL	118
Femur		
	JD	119
	EH	120
	BW	121
	GS	122
	FD	123
	DL	124

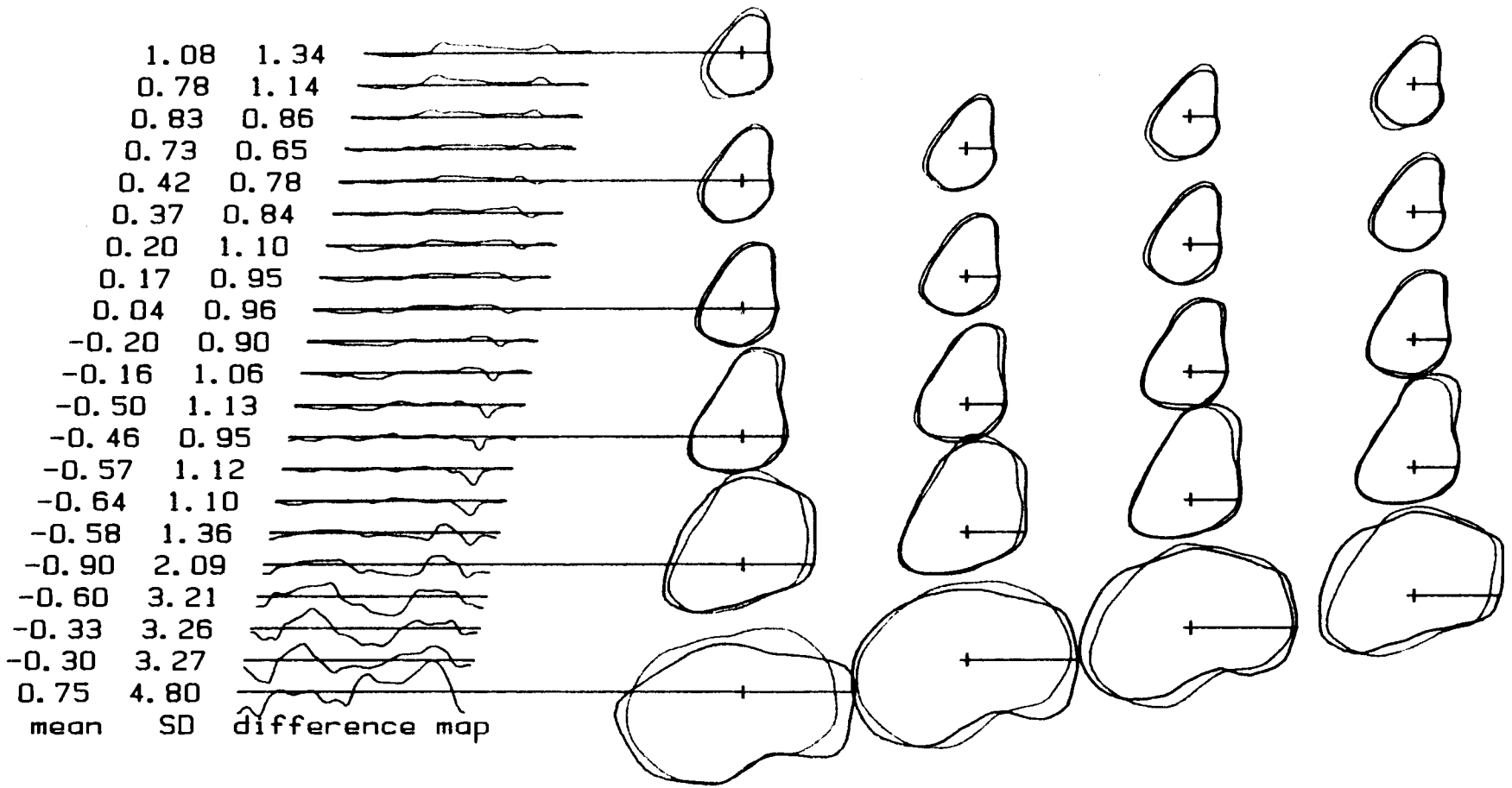

JD tibial CT scan verses reference tibia

Mean difference 0.01 mm
Standard Deviation 1.99 mm

Amputee CT cross sections are in blue
Z increment 7.00 mm

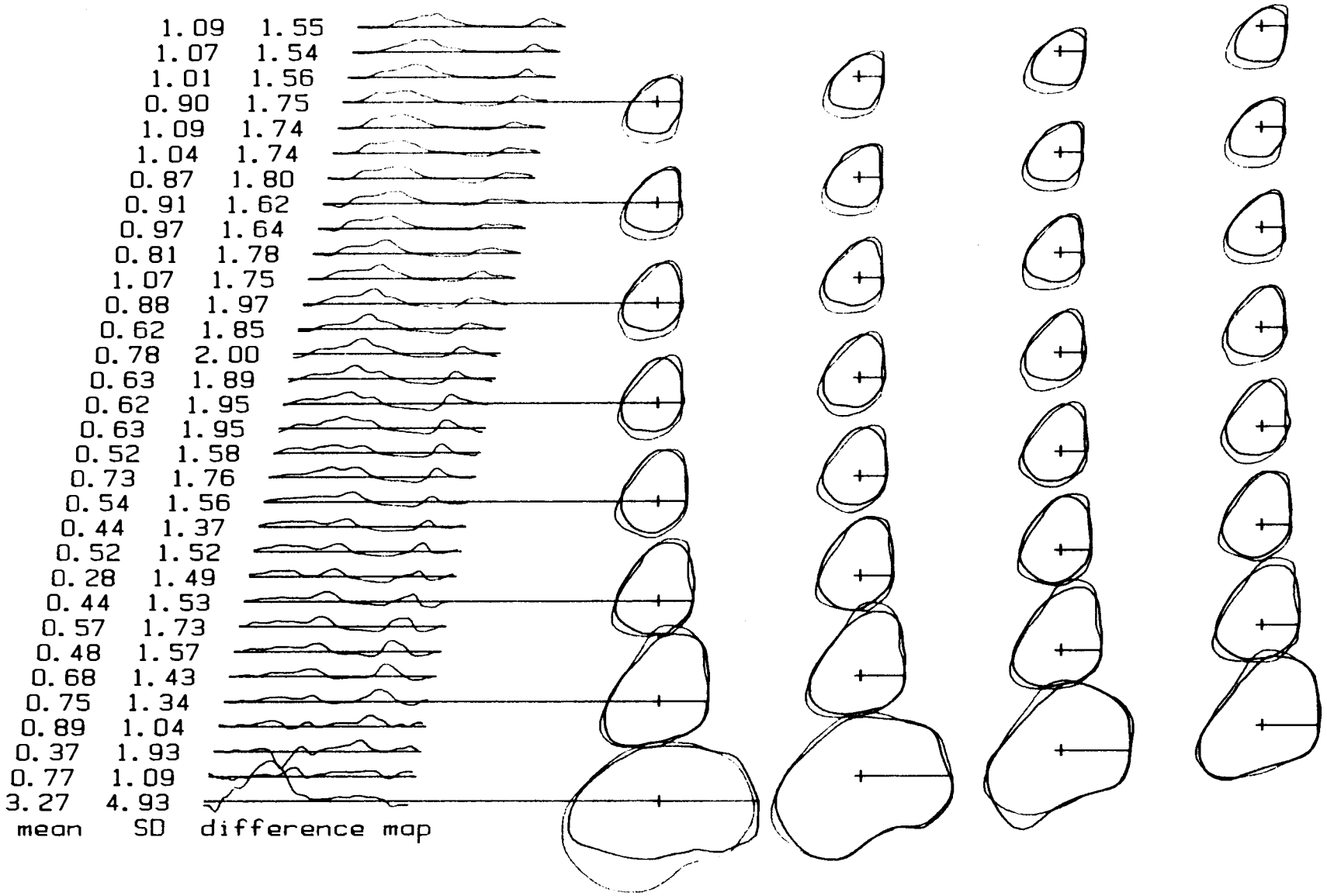

EH tibial CT scan verses reference tibia

Mean difference 0.82 mm
Standard Deviation 1.92 mm

Amputee CT cross sections are in blue
Z increment 7.00 mm

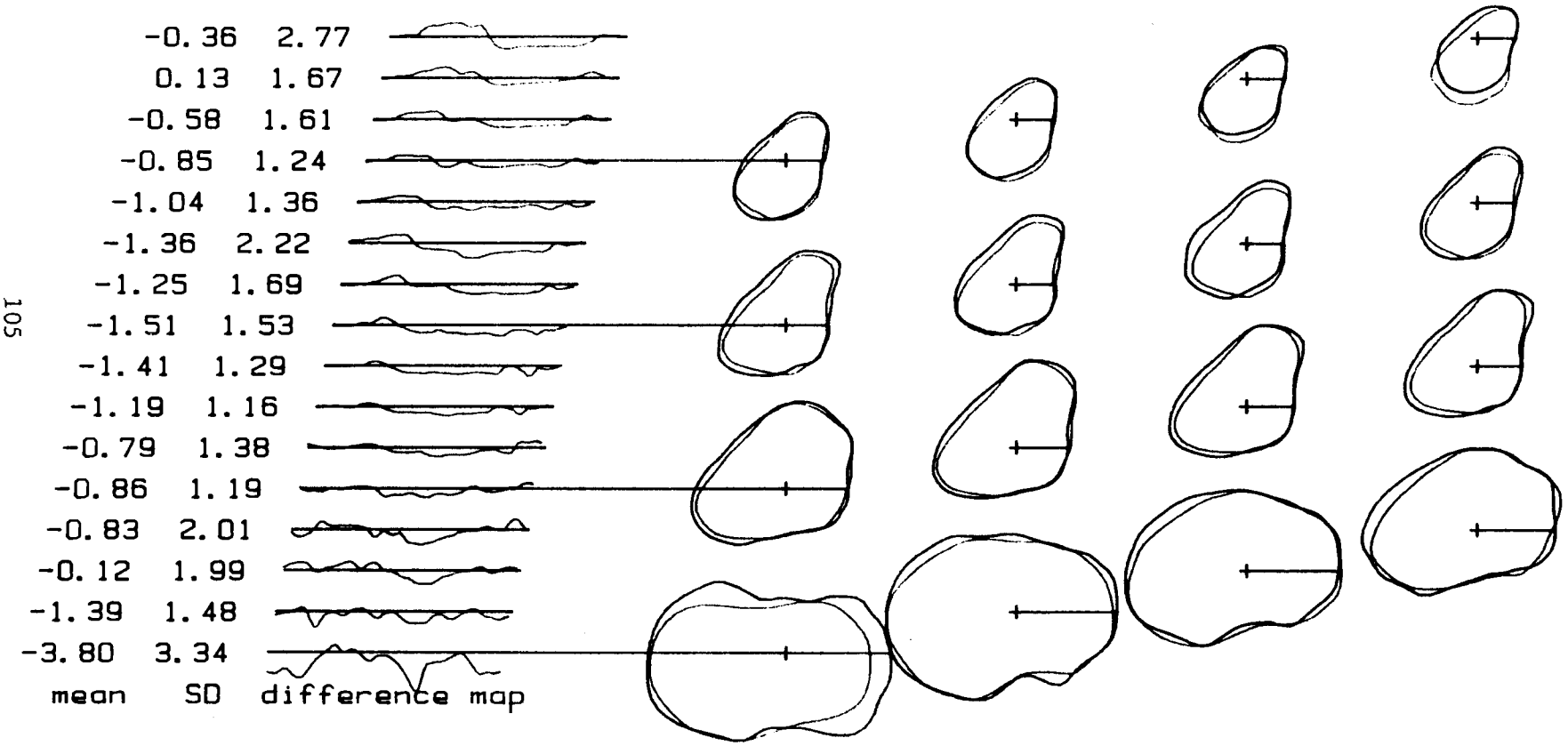

BW tibial CT scan verses reference tibia

Mean difference -1.08 mm
Standard Deviation 2.02 mm

Amputee CT cross sections are in blue
Z increment 7.00 mm

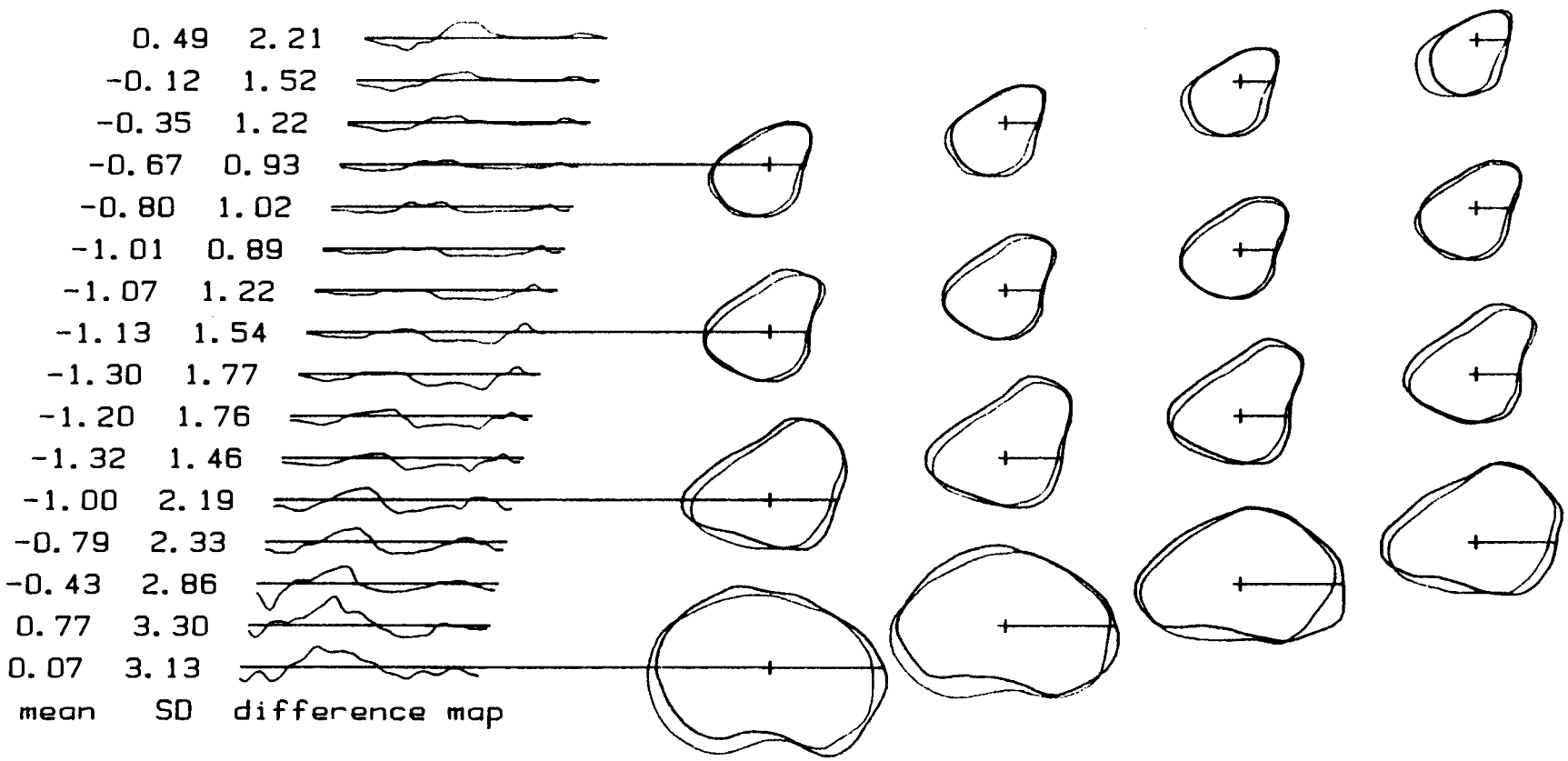

GS tibial CT scan verses reference tibia

Mean difference -0.62 mm
Standard Deviation 2.07 mm

Amputee CT cross sections are in blue
Z increment 7.00 mm

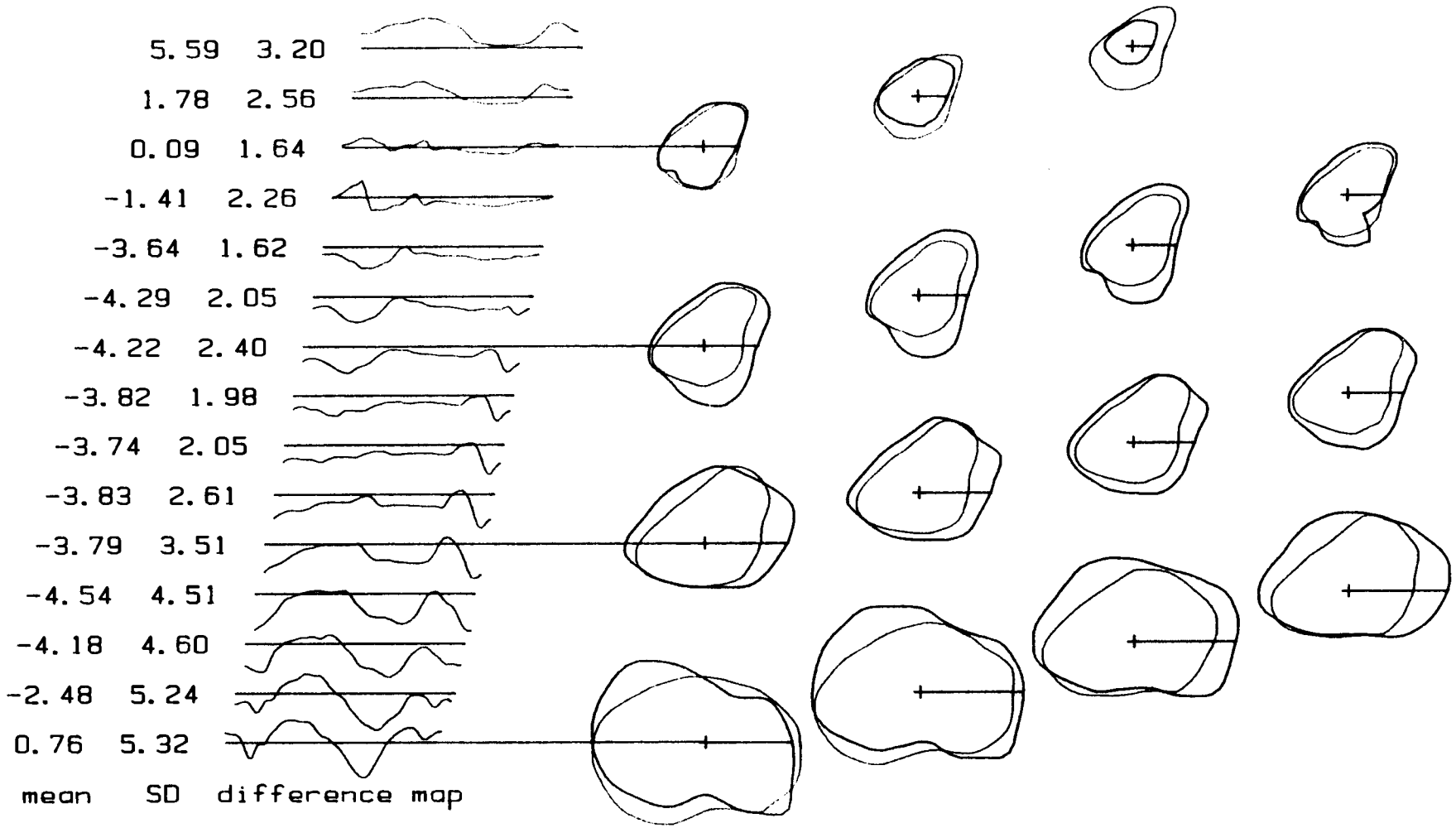

FD tibial CT scan verses reference tibia

Mean difference -2.12 mm
Standard Deviation 4.34 mm

Amputee CT cross sections are in blue
Z increment 7.00 mm

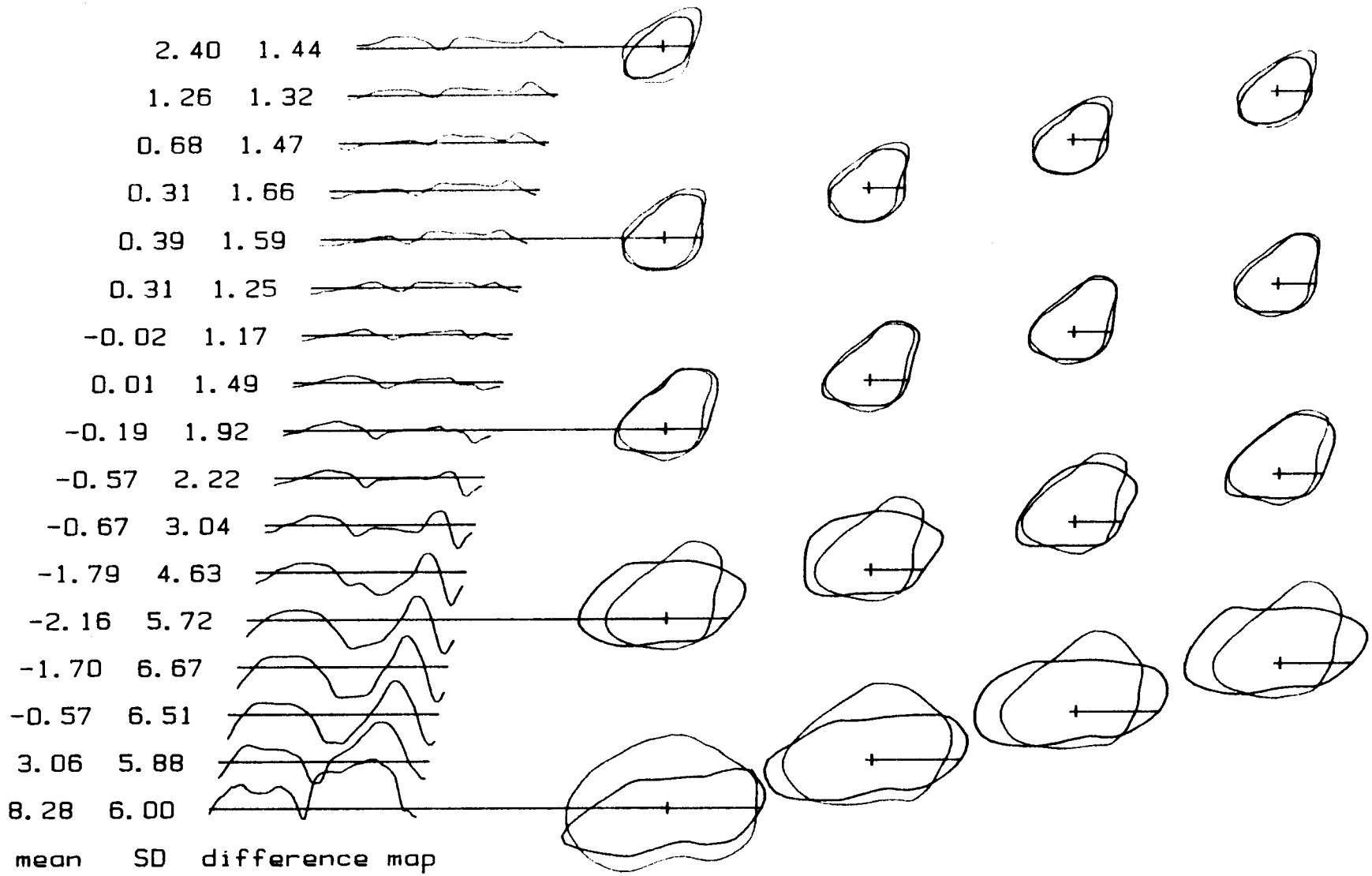

DL tibial CT scan verses reference tibia

Mean difference 0.53 mm
Standard Deviation 4.47 mm

Amputee CT cross sections are in blue
Z increment 7.00 mm

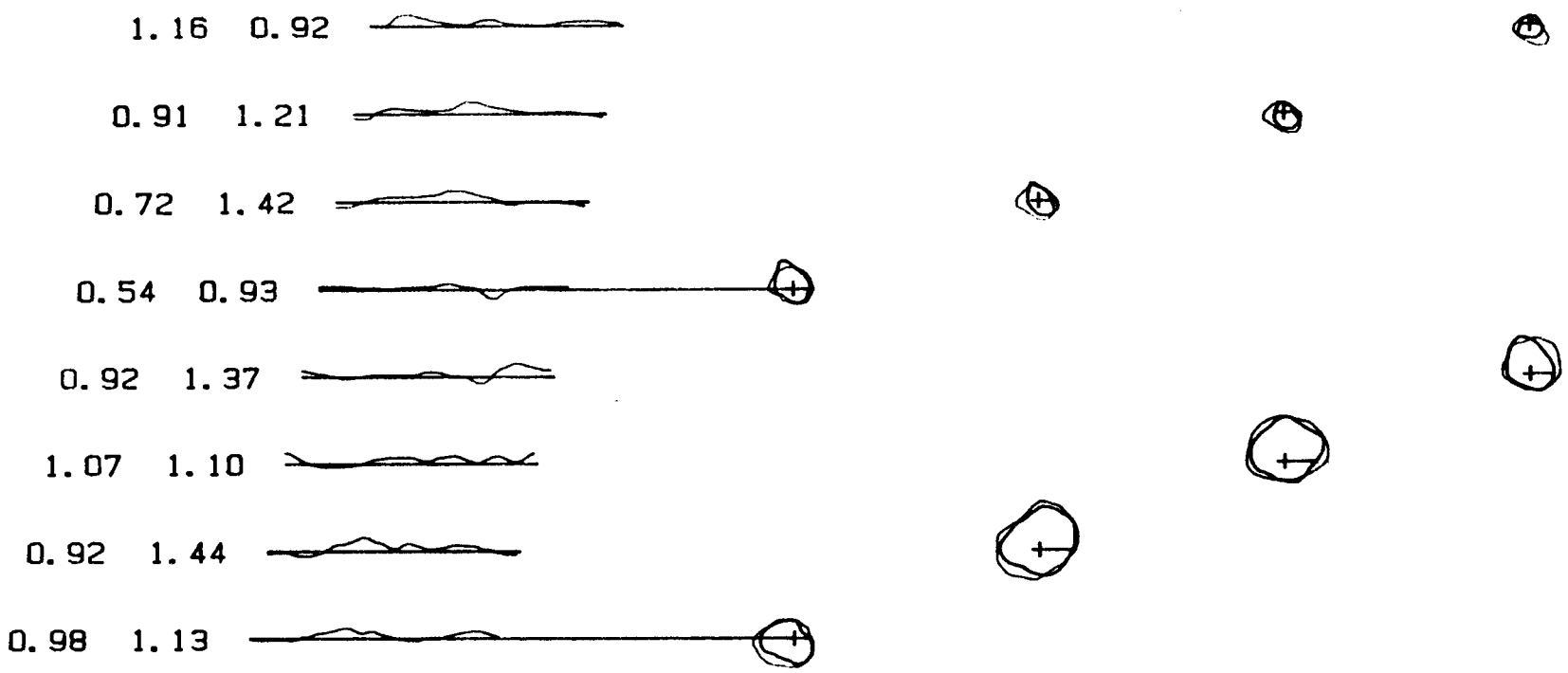

JD fibular CT shape verses reference fibula

Mean difference 0.90 mm
Standard Deviation 1.22 mm

Amputee CT cross sections are in blue
Z increment 7.00 mm

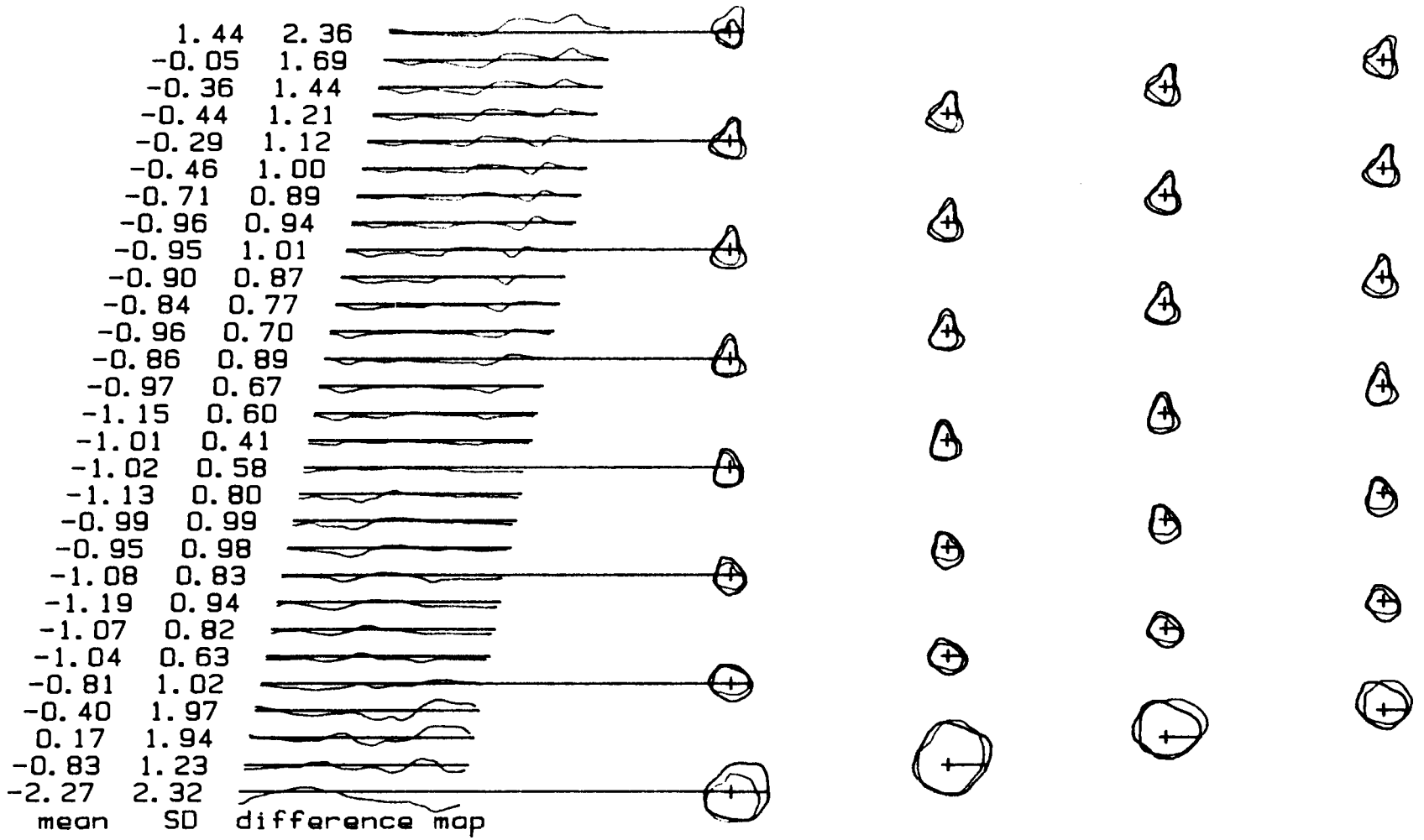

EH fibular CT shape verses reference fibula

Mean difference -0.76 mm
Standard Deviation 1.34 mm

Amputee CT cross sections are in blue
Z increment 7.00 mm

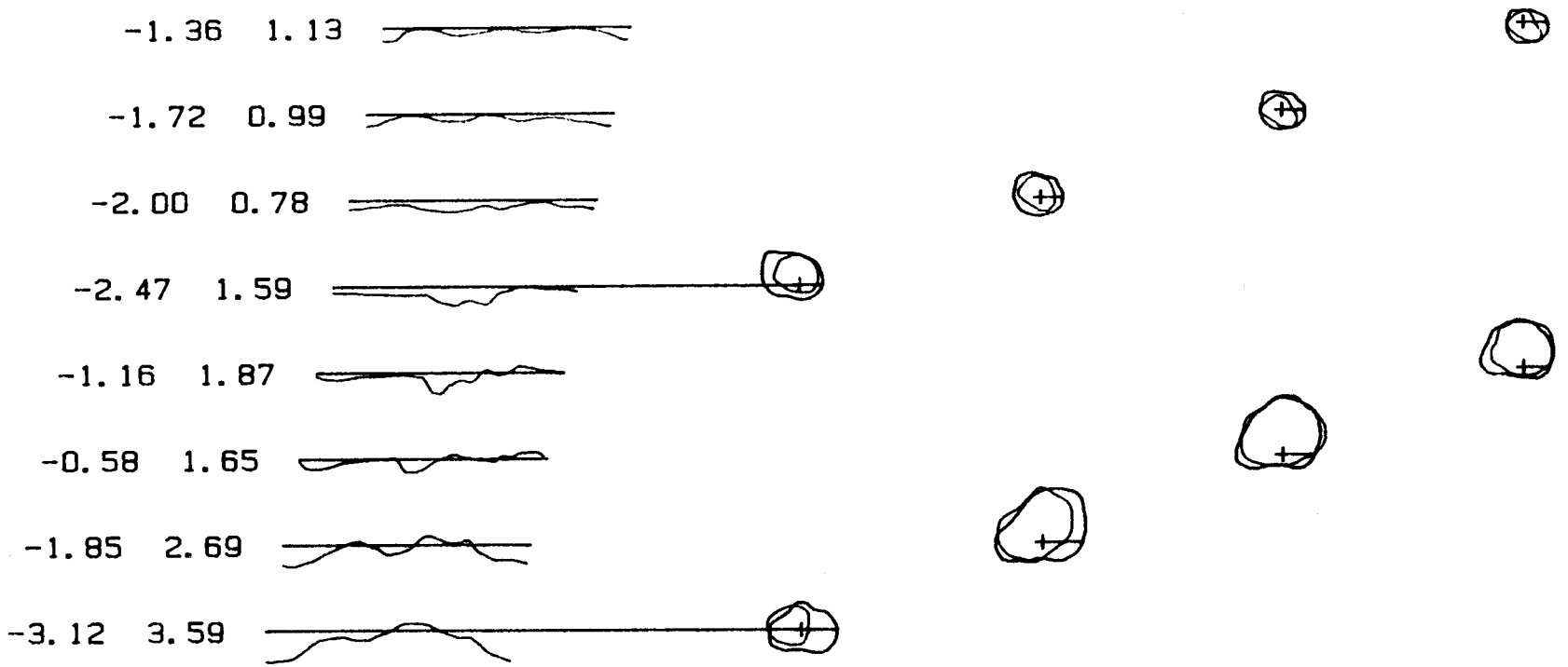

BW fibular CT shape verses reference fibula

Mean difference -1.78 mm
Standard Deviation 2.12 mm

Amputee CT cross sections are in blue
Z increment 7.00 mm

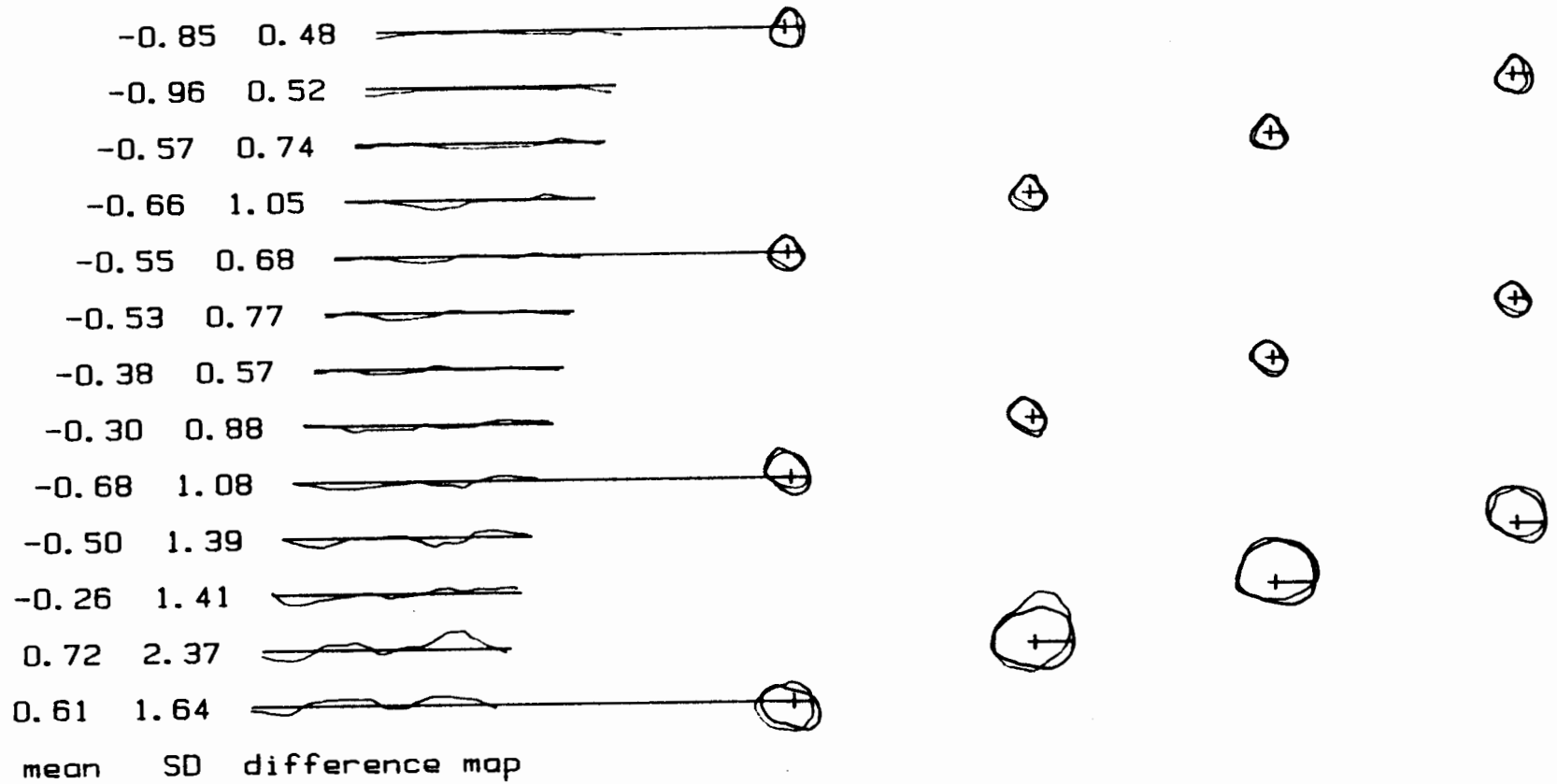

GS fibular CT shape verses reference fibula

Mean difference -0.38 mm
Standard Deviation 1.26 mm

Amputee CT cross sections are in blue
Z increment 7.00 mm

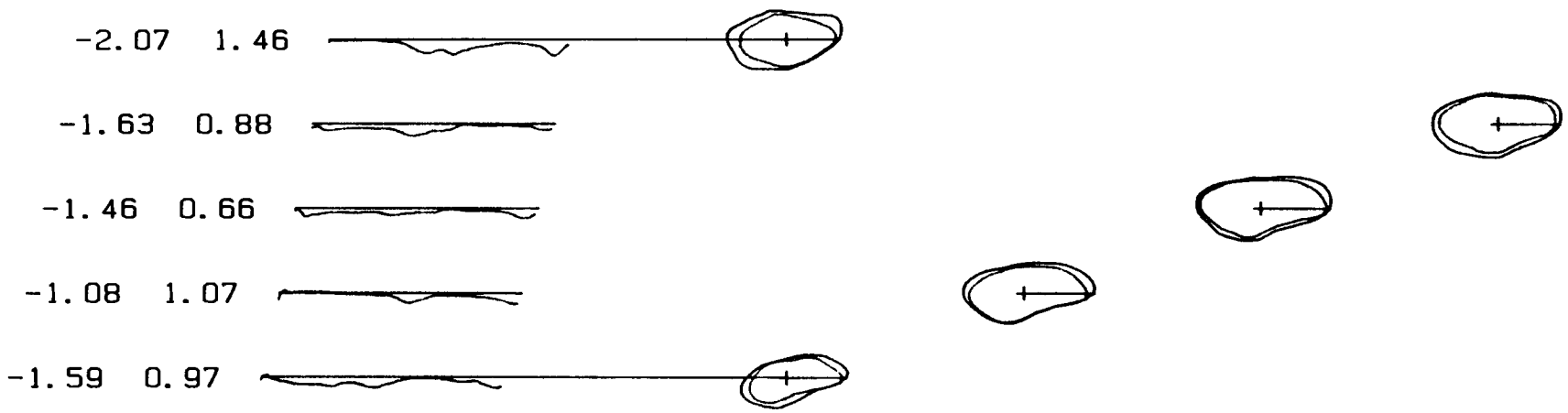

JO patellar CT shape verses reference shape

Mean difference -1.57 mm
Standard Deviation 1.09 mm

Amputee CT cross sections are in blue
Z increment 7.00 mm

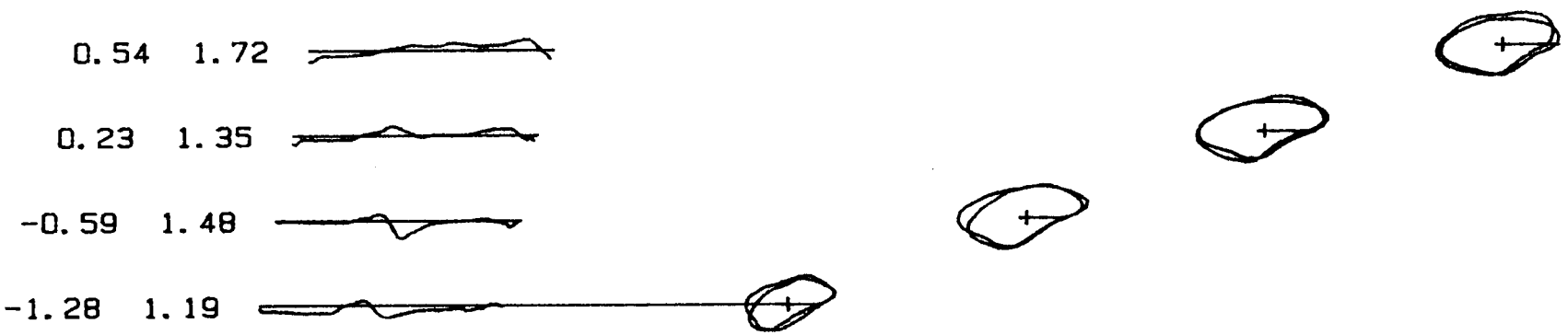

EH patellar CT shape verses reference shape

Mean difference -0.27 mm
Standard Deviation 1.61 mm

Amputee CT cross sections are in blue
Z increment 7.00 mm

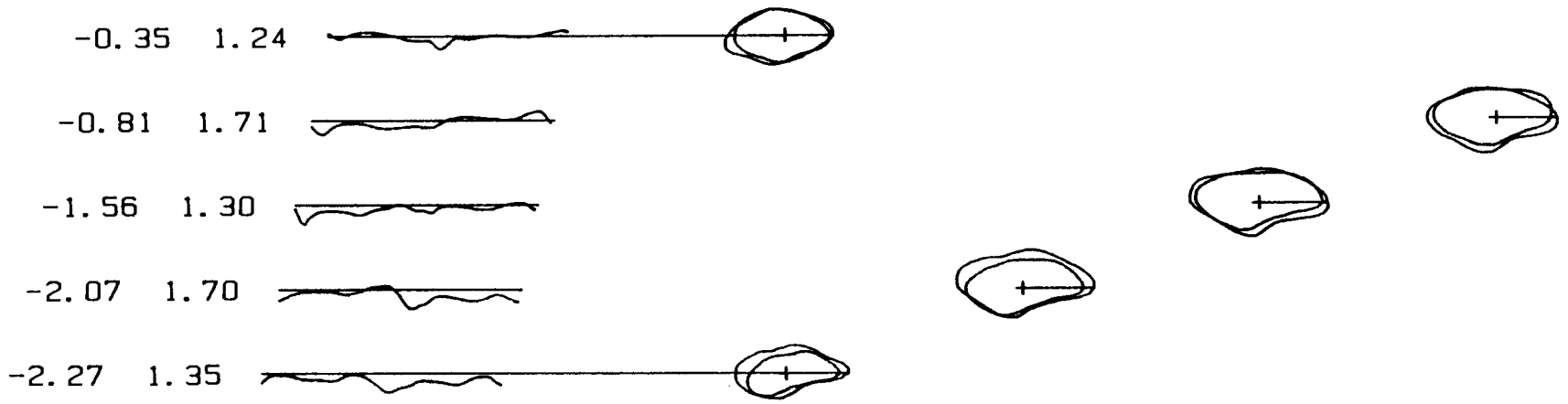

BW patellar CT shape verses reference shape

Mean difference -1.41 mm
Standard Deviation 1.65 mm

Amputee CT cross sections are in blue
Z increment 7.00 mm

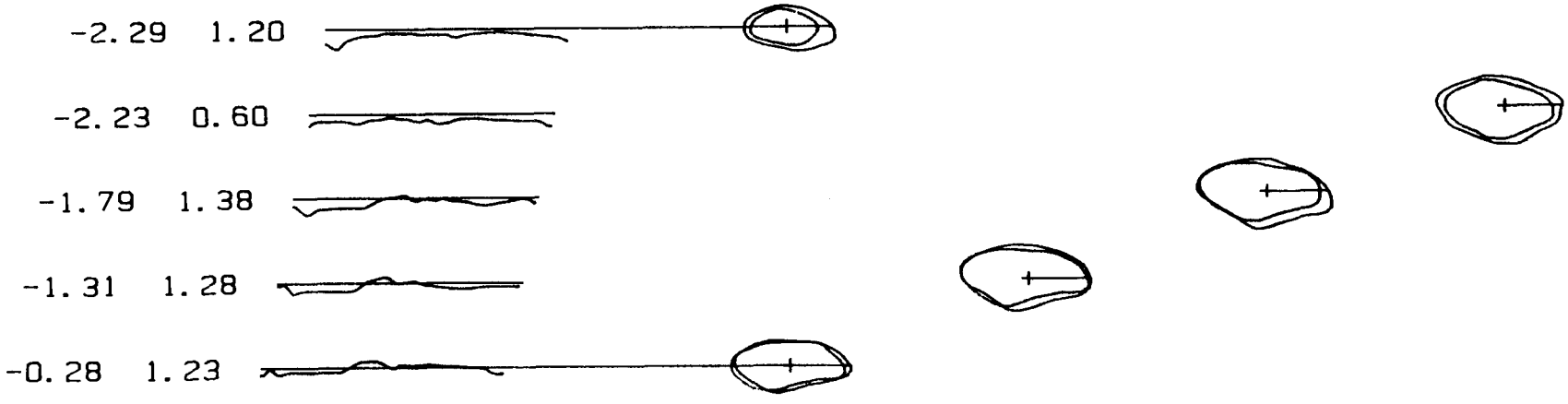

GS patellar CT shape verses reference patella

Mean difference -1.58 mm
Standard Deviation 1.38 mm

Amputee CT cross sections are in blue
Z increment 7.00 mm

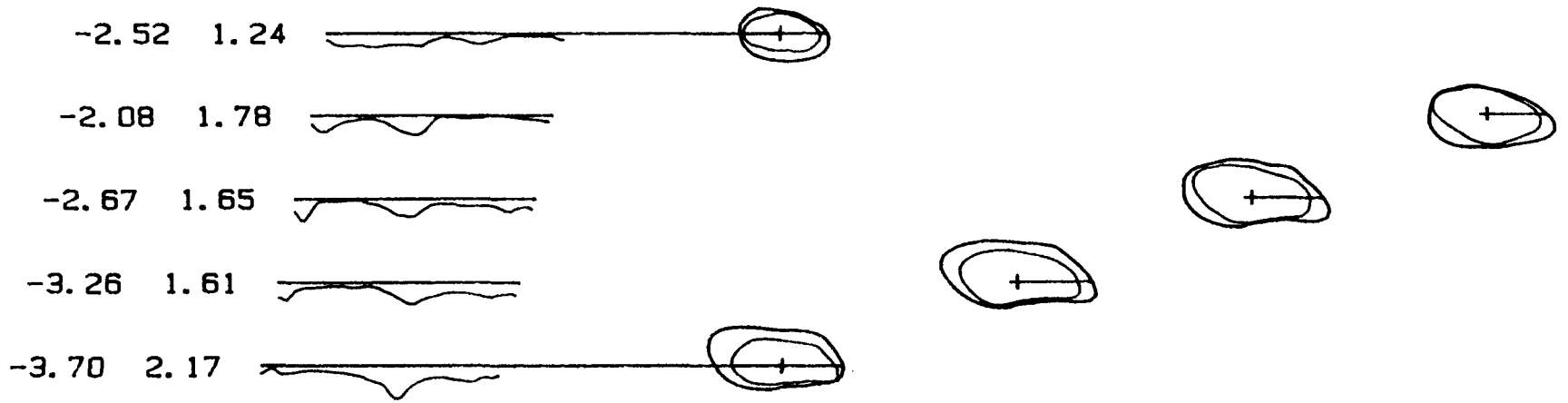

FD patellar CT shape verses reference patella

Mean difference -2.84 mm
Standard Deviation 1.81 mm

Amputee CT cross sections are in blue
Z increment 7.00 mm

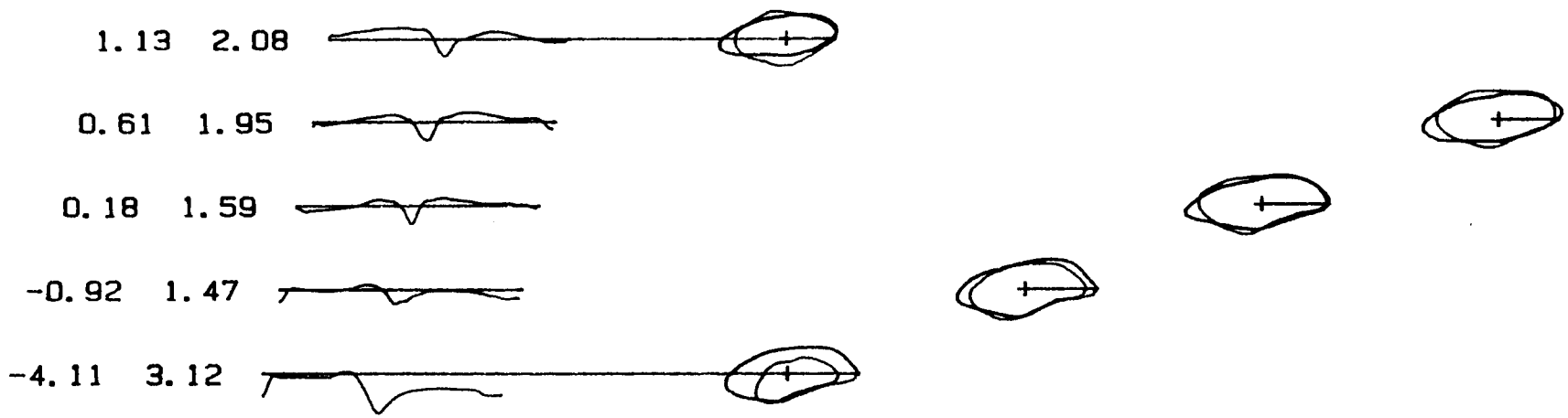

DL patellar CT shape verses reference patella

Mean difference -0.62 mm
Standard Deviation 2.83 mm

Amputee CT cross sections are in blue
Z increment 7.00 mm

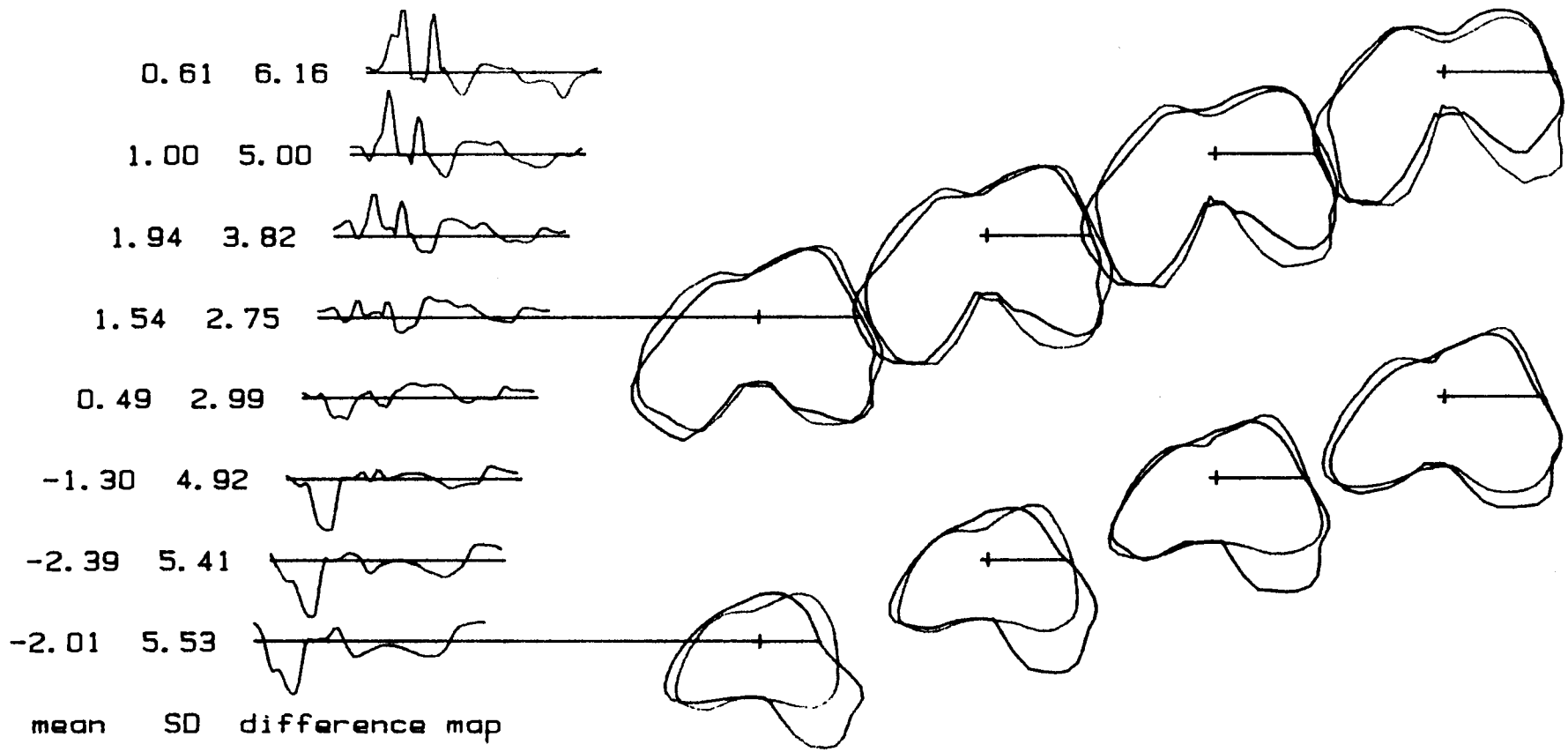

JD femoral CT shape verses reference shape

Mean difference -0.02 mm
Standard Deviation 4.97 mm

Amputee CT cross sections are in blue
Z increment 5.00 mm

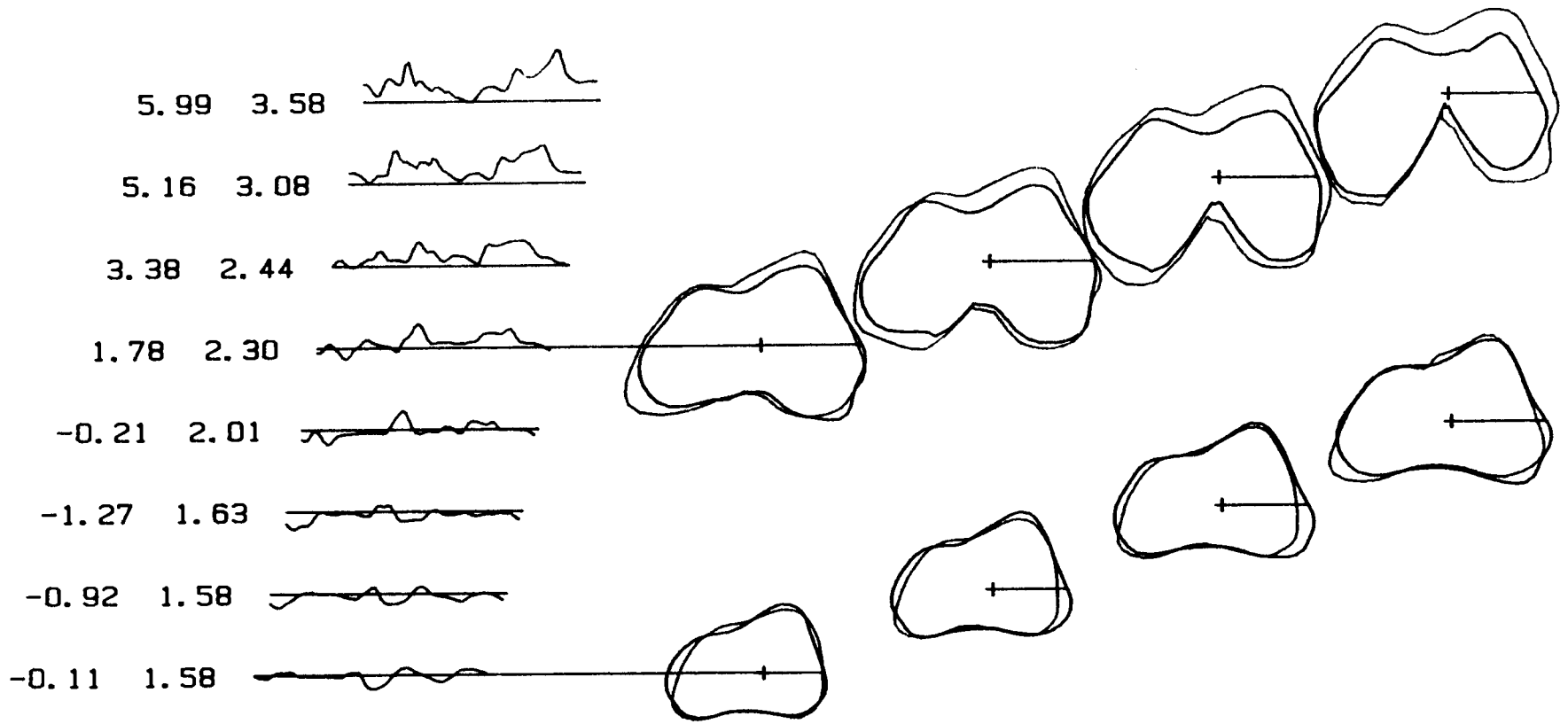

EH femoral CT shape verses reference shape

Mean difference 1.73 mm
Standard Deviation 3.56 mm

Amputee CT cross sections are in blue
Z increment 5.00 mm

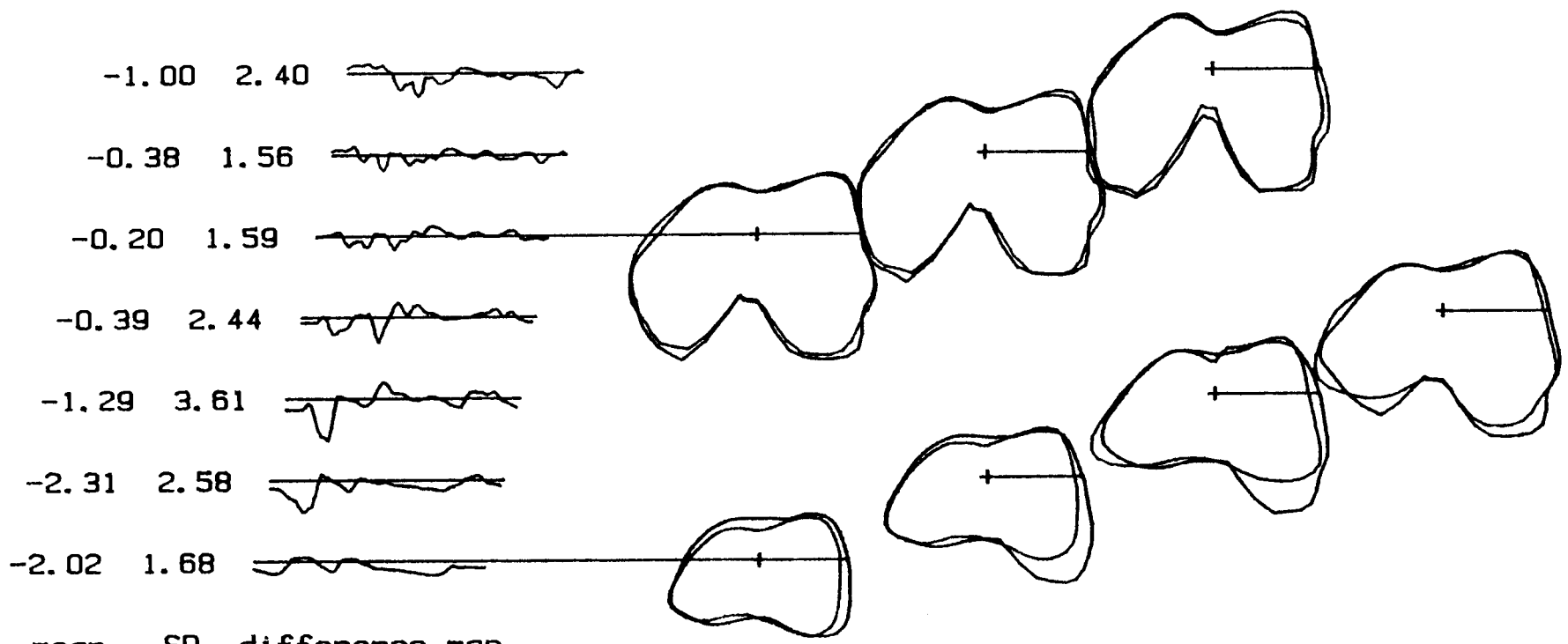

BW femoral CT shape verses reference shape

Mean difference -1.09 mm
Standard Deviation 2.49 mm

Amputee CT cross sections are in blue
Z increment 5.00 mm

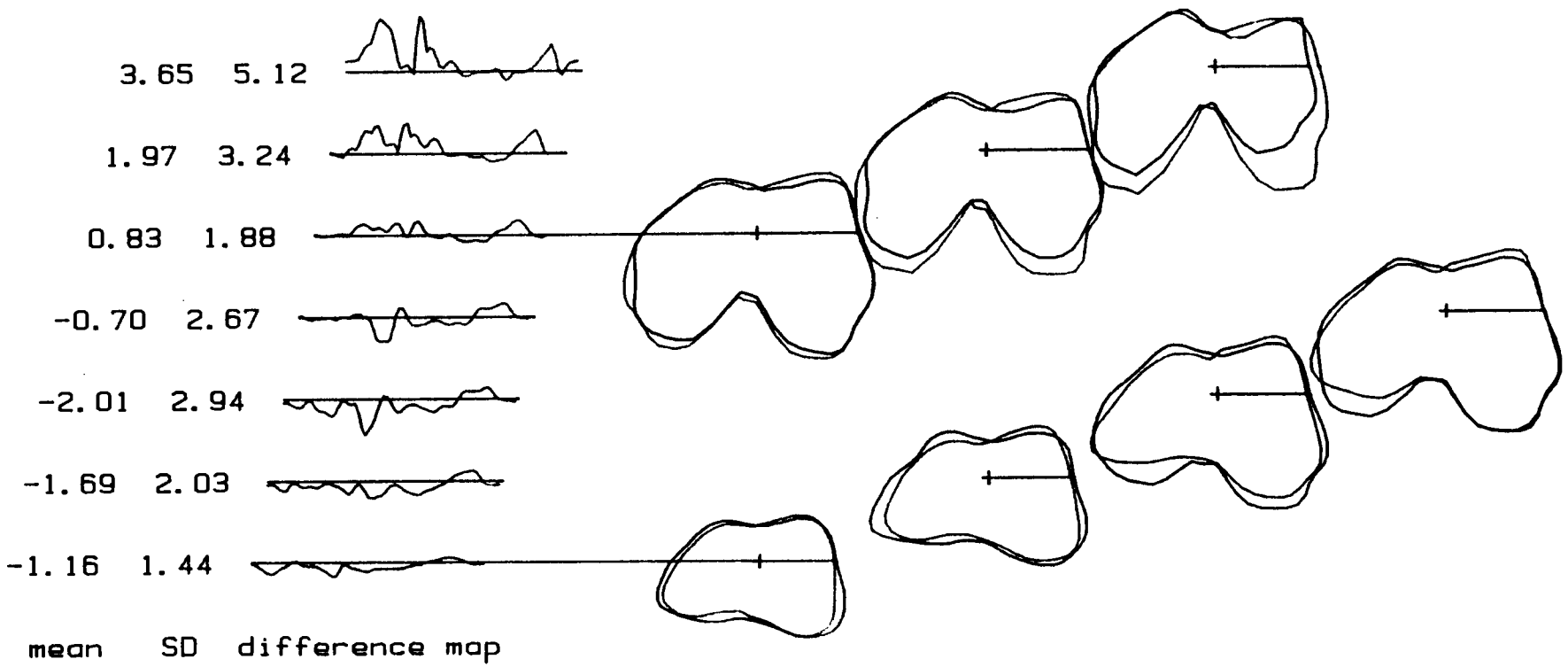

GS femoral CT shape verses reference shape

Mean difference 0.13 mm
Standard Deviation 3.56 mm

Amputee CT cross sections are in blue
Z increment 5.00 mm

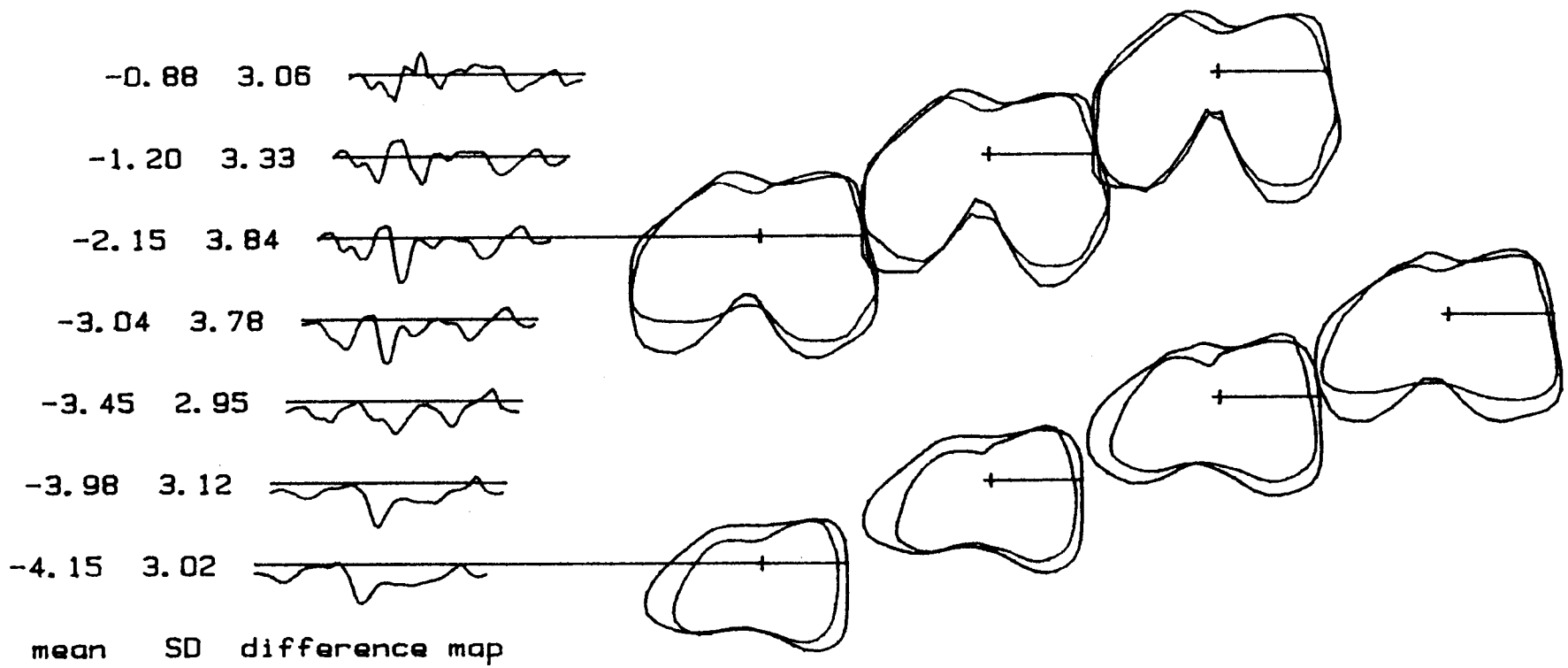

FD femoral CT shape verses reference shape

Mean difference -2.69 mm
Standard Deviation 3.53 mm

Amputee CT cross sections are in blue
Z increment 5.00 mm

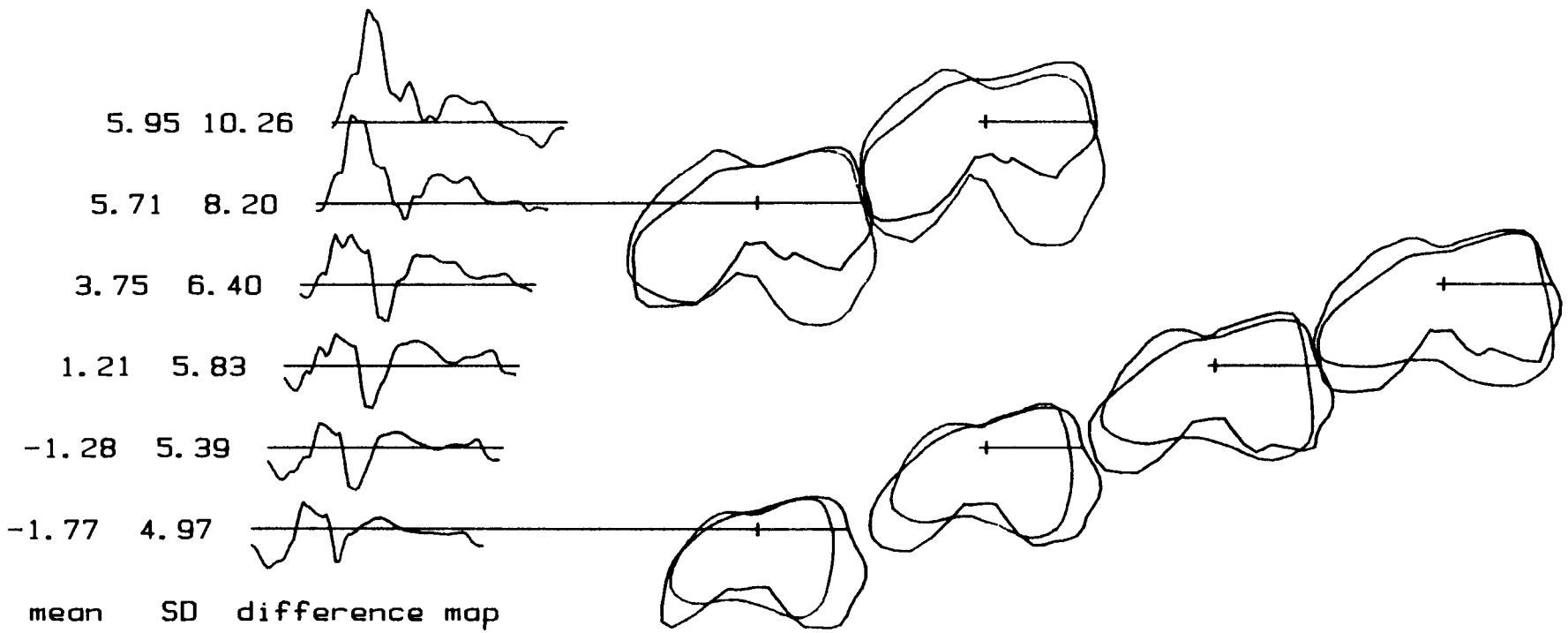

DL femoral CT shape verses reference shape

Mean difference 2.26 mm
Standard Deviation 7.73 mm

Amputee CT cross sections are in blue
Z increment 6.00 mm

APPENDIX II

Comparison plots for the scaling procedures giving the best results for each bone.

The comparison plots for 22 scaled bones compared to the Computerized Tomography bone shapes follow. They are in the order of tibia, fibula, patella then femur.

Each plot has 3 sections. On the left are the means and standard deviations for each cross section. Proximal cross sections start at the bottom of the page going to distal cross sections at the top of the page.

The centre section contains a map of the differences between radii. The map starts at 355 degrees on the left and goes to 0 degrees on the right. The displacement on the map is relative to the difference between the radii of the 2 bone shapes being compared. The baseline, or zero level is indicated by the straight blue line. The mean difference and its standard deviation are given at the bottom of the page.

The cross sections of the two bones are superimposed in the right hand section. The xy origin is indicated by an '+', with the radian at 0 degrees indicated.

Appendix II

List of Figures

Amputee bone CT scans verses scaled bone shapes

Subject		Page
Tibia		
	JD	127
	EH	128
	BW	129
	GS	130
	FD	131
	DL	132
Fibula		
	JD	133
	EH	134
	BW	135
	GS	136
Patella		
	JD	137
	EH	138
	BW	139
	GS	140
	FD	141
	DL	142
Femur		
	JD	143
	EH	144
	BW	145
	GS	146
	FD	147
	DL	148

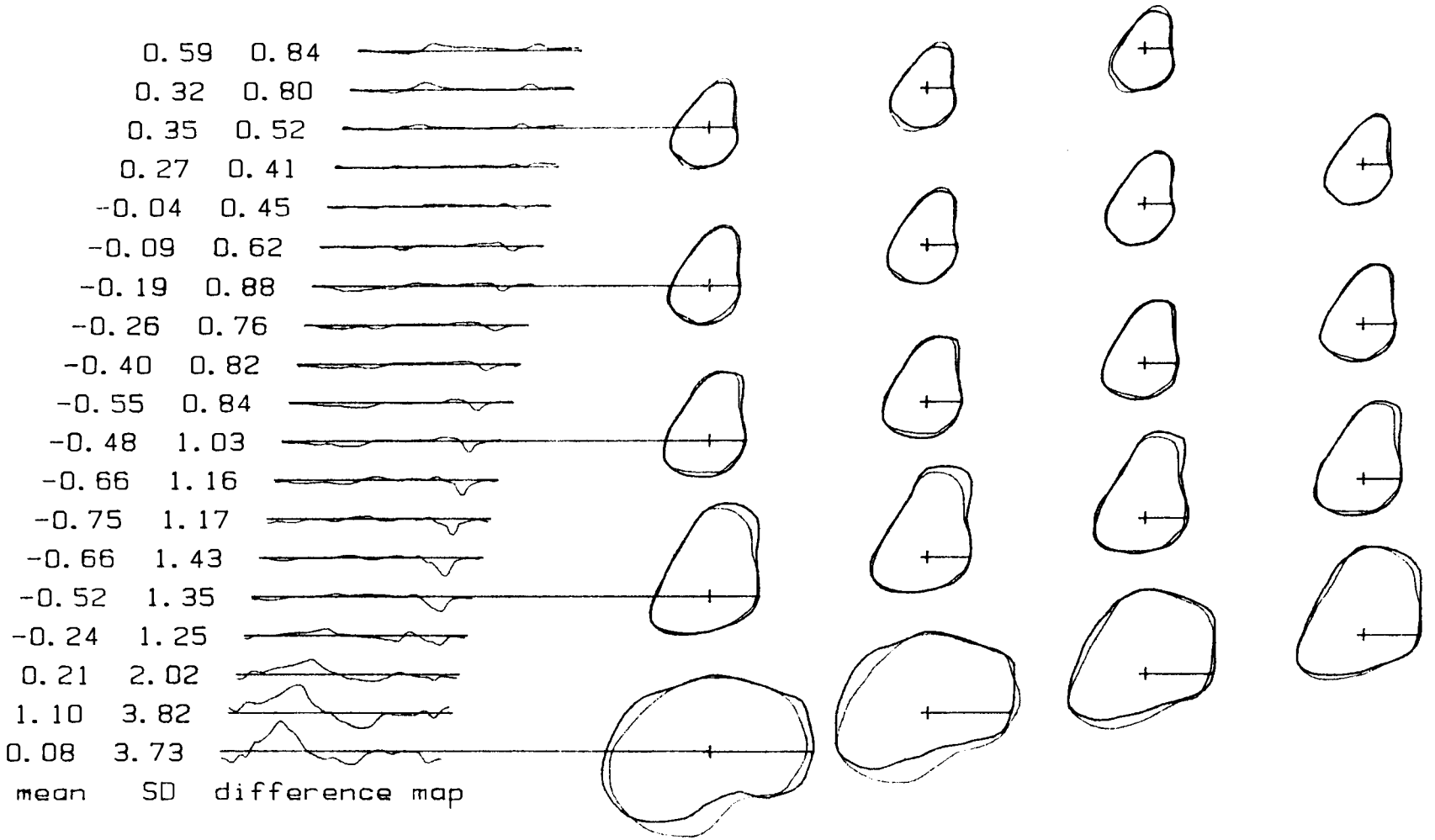

JD tibial CT shape verses uniform dilation tibia

Mean difference -0.10 mm
Standard Deviation 1.64 mm

Amputee CT cross sections are in blue
Z increment 7.00 mm

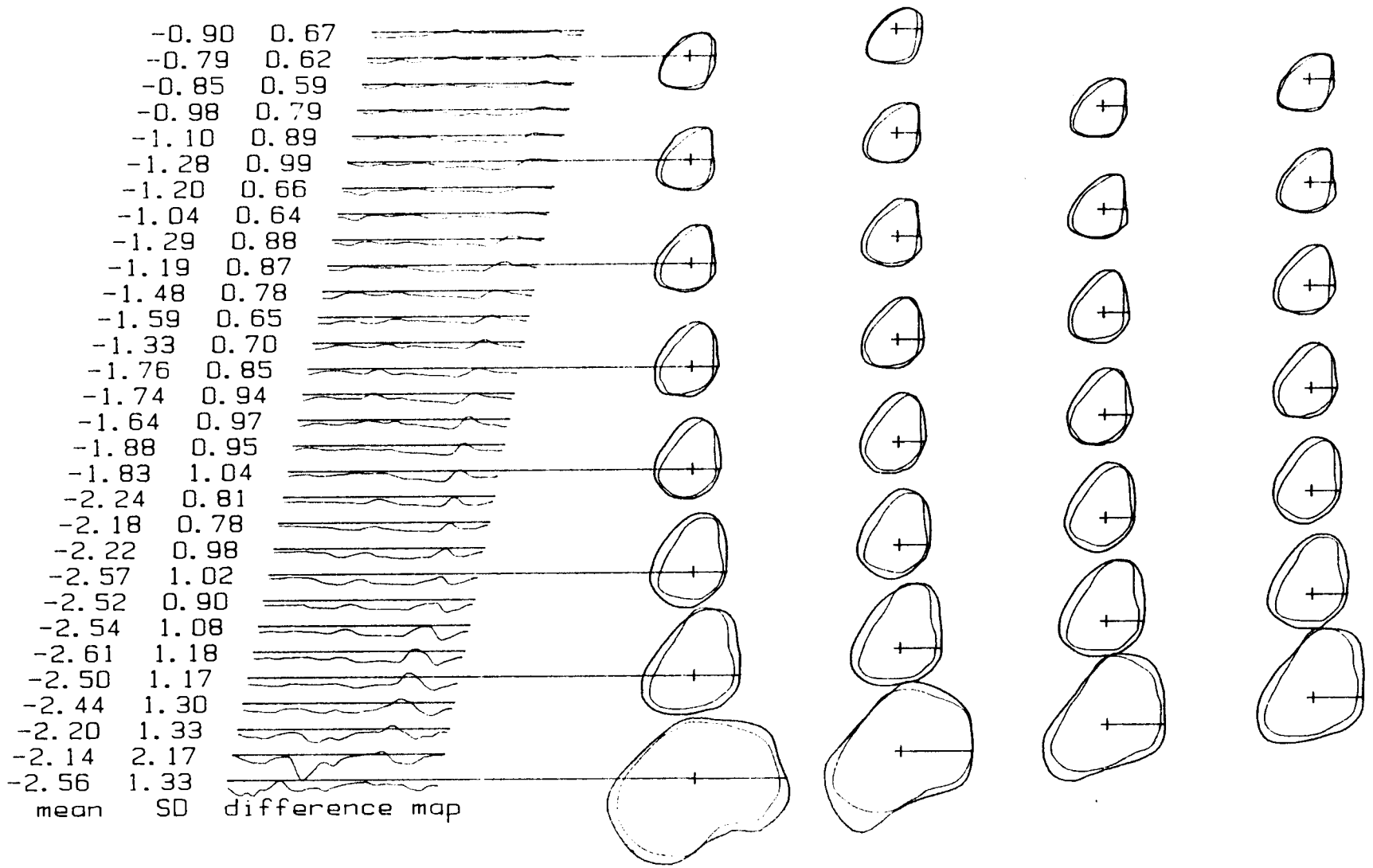

EH tibial CT shape verses uniform dilation tibia

Mean difference -1.75 mm
Standard Deviation 1.16 mm

Amputee CT cross sections are in blue
Z increment 7.00 mm

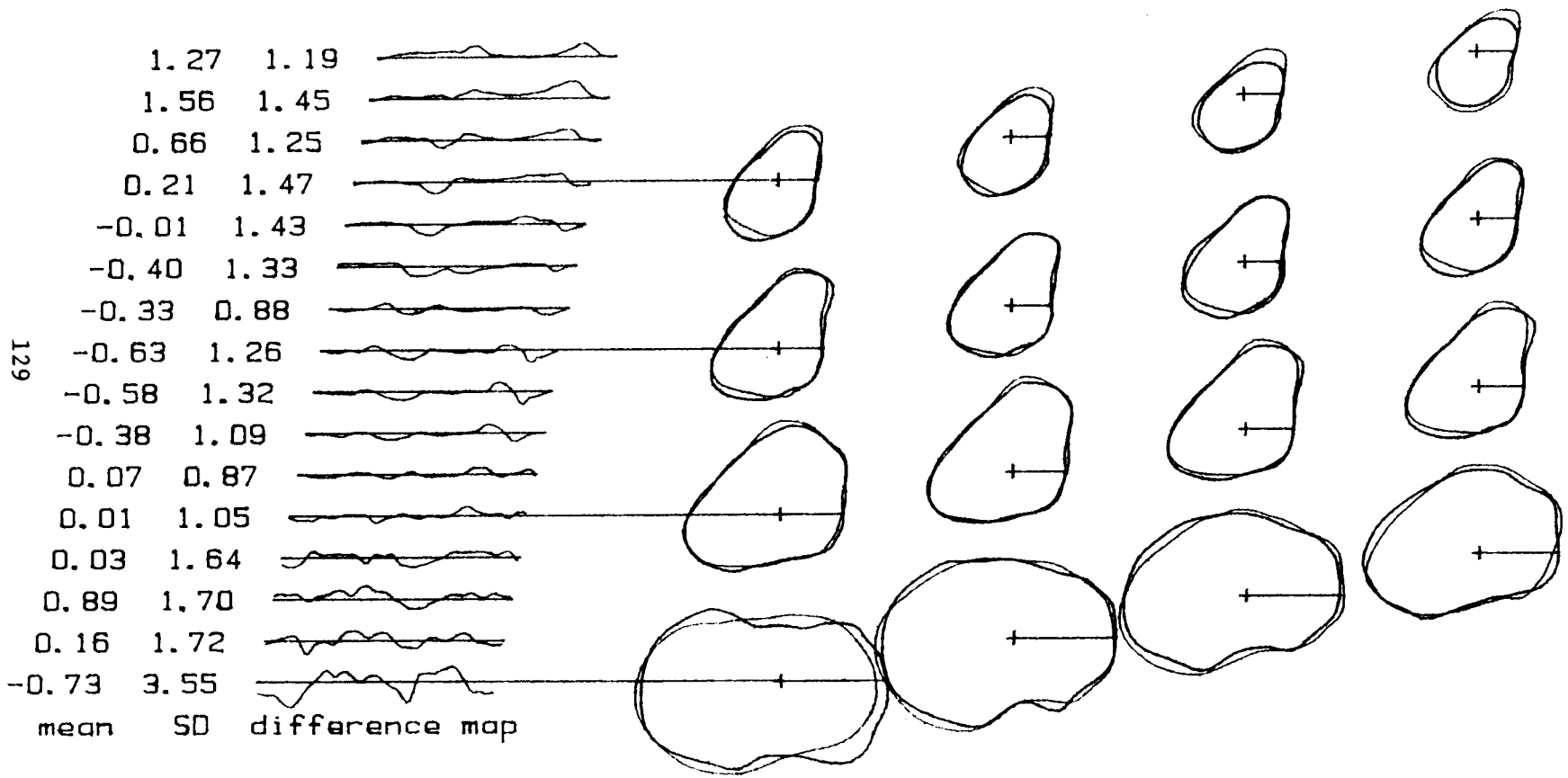

BW tibial CT shape verses uniform dilation tibia

Mean difference 0.11 mm
Standard Deviation 1.70 mm

Amputee CT cross sections are in blue
Z increment 7.00 mm

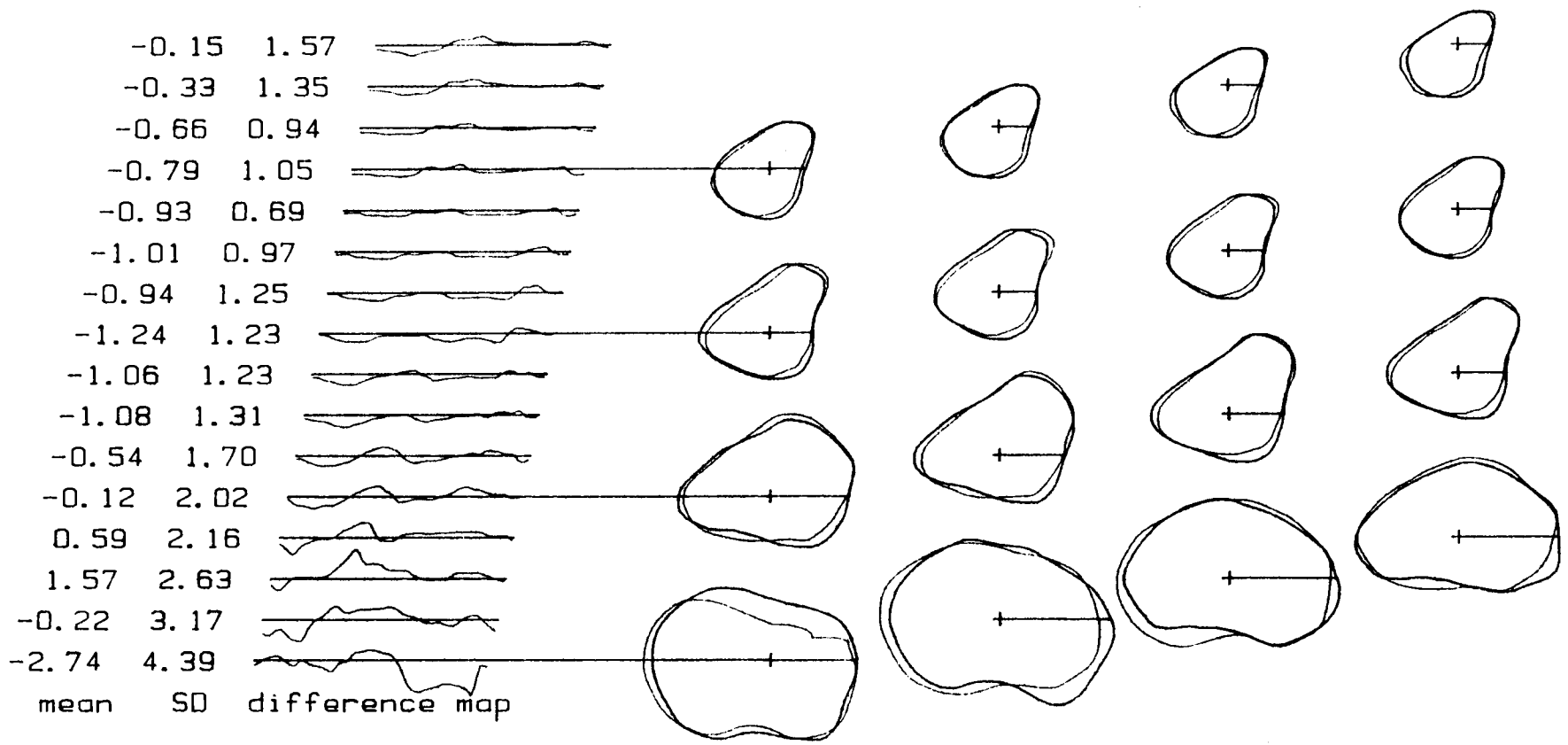

GS tibial CT shape verses uniform dilation tibia

Mean difference -0.60 mm
Standard Deviation 2.16 mm

Amputee CT cross sections are in blue
Z increment 7.00 mm

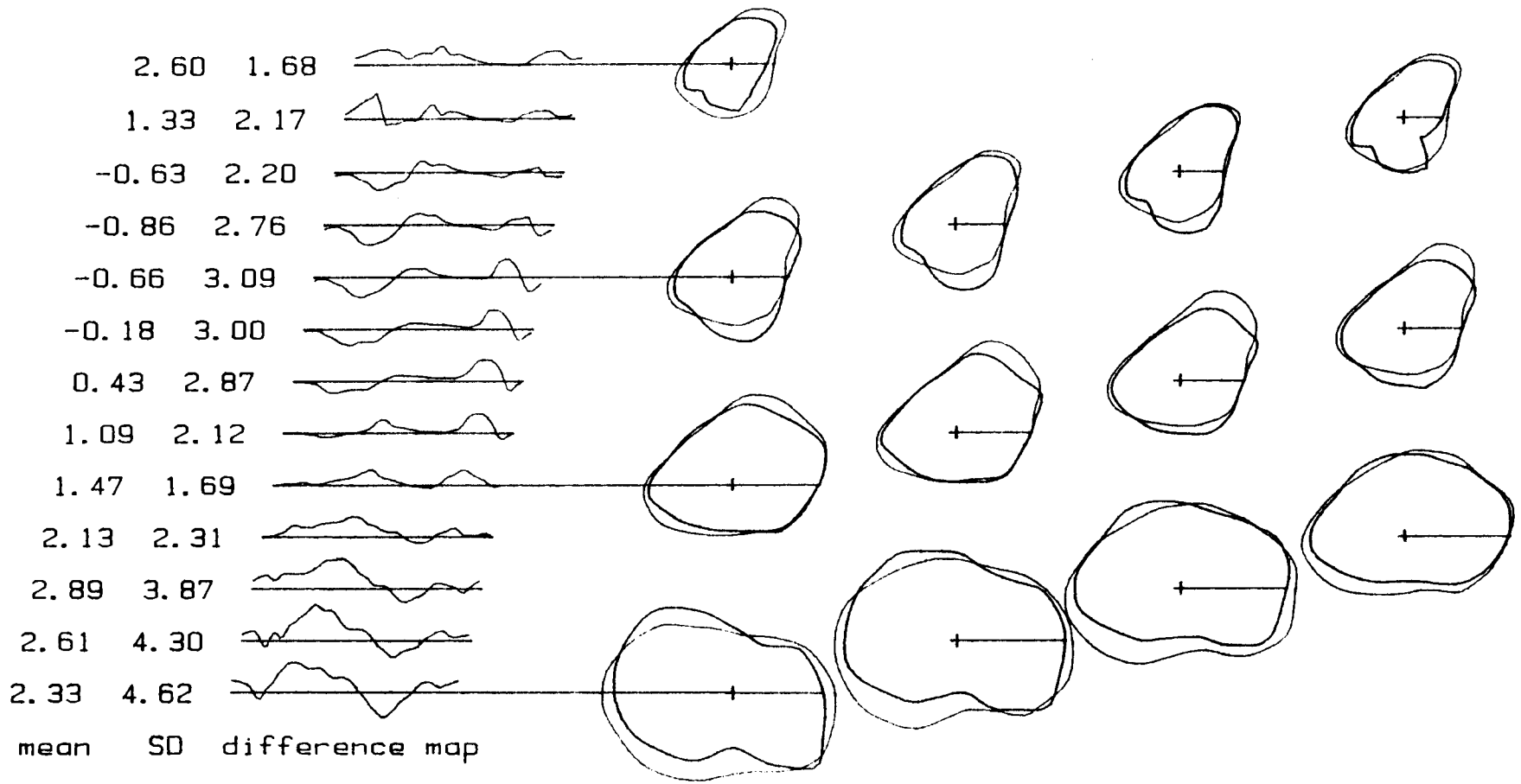

FD tibial CT shape verses uniform dilation tibia

Mean difference 1.12 mm
Standard Deviation 3.24 mm

Amputee CT cross sections are in blue
Z increment 7.00 mm

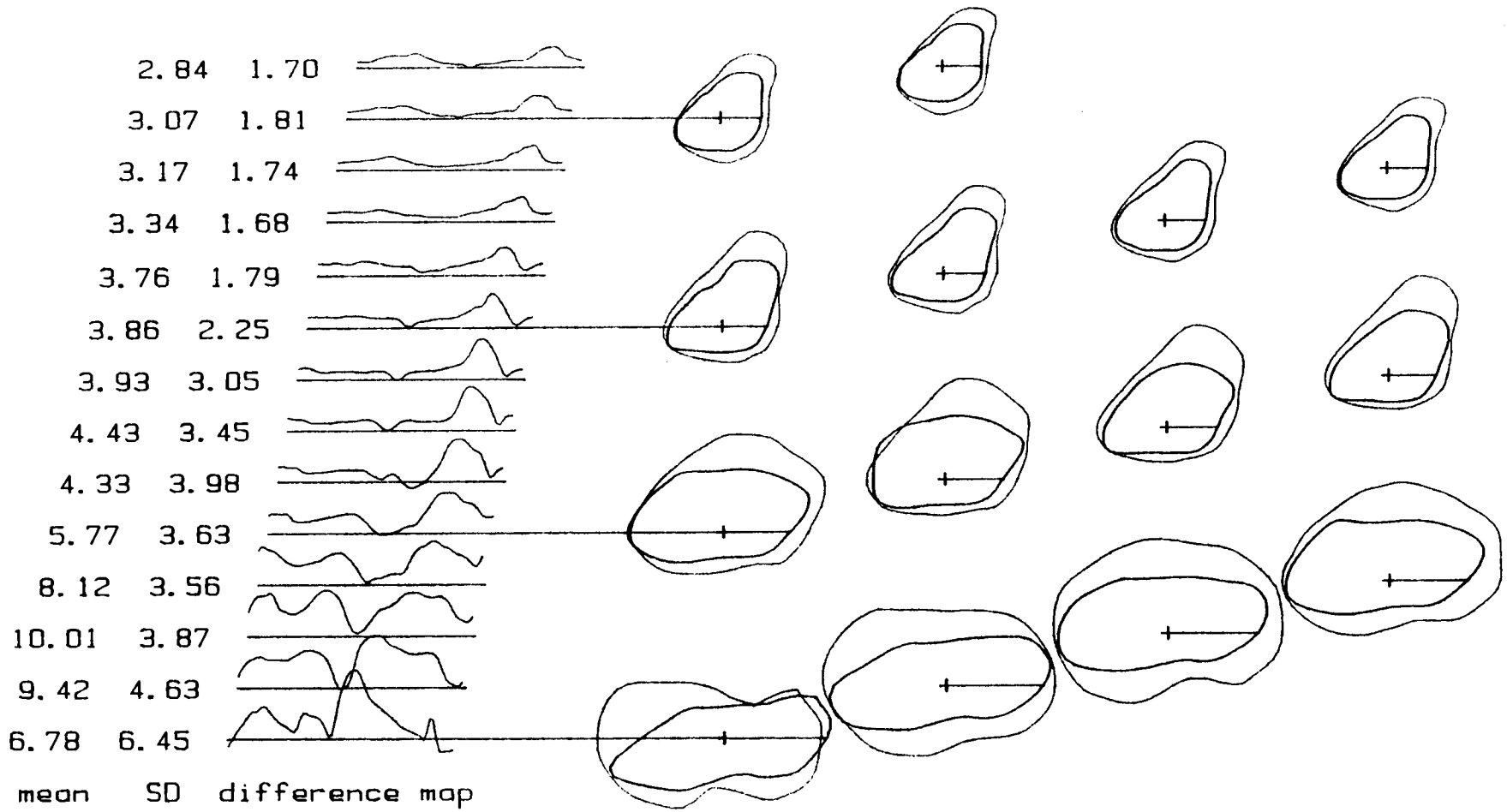

DL tibial CT shape verses uniform dilation tibia

Mean difference 5.20 mm
Standard Deviation 4.12 mm

Amputee CT cross sections are in blue
Z increment 7.00 mm

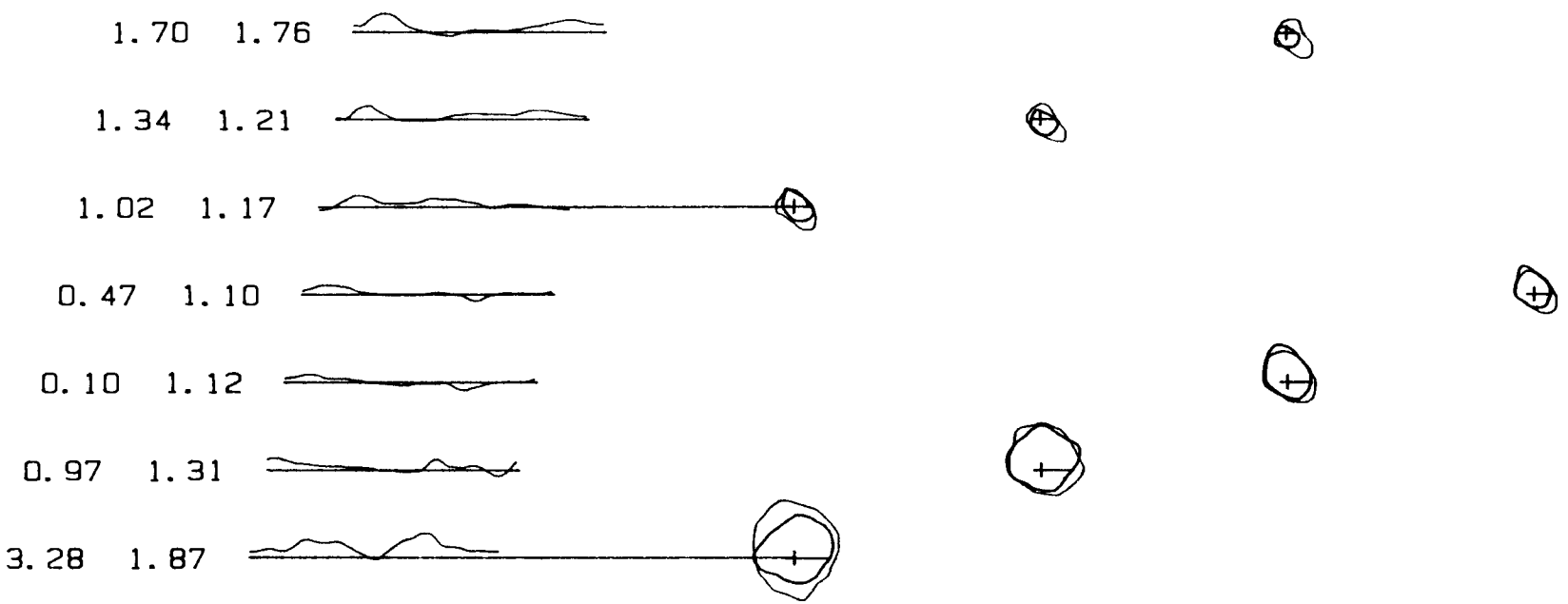

JD fibular CT shape verses non-orthogonal fibula

Mean difference 1.27 mm
Standard Deviation 1.69 mm

Amputee CT cross sections are in blue
Z increment 7.00 mm

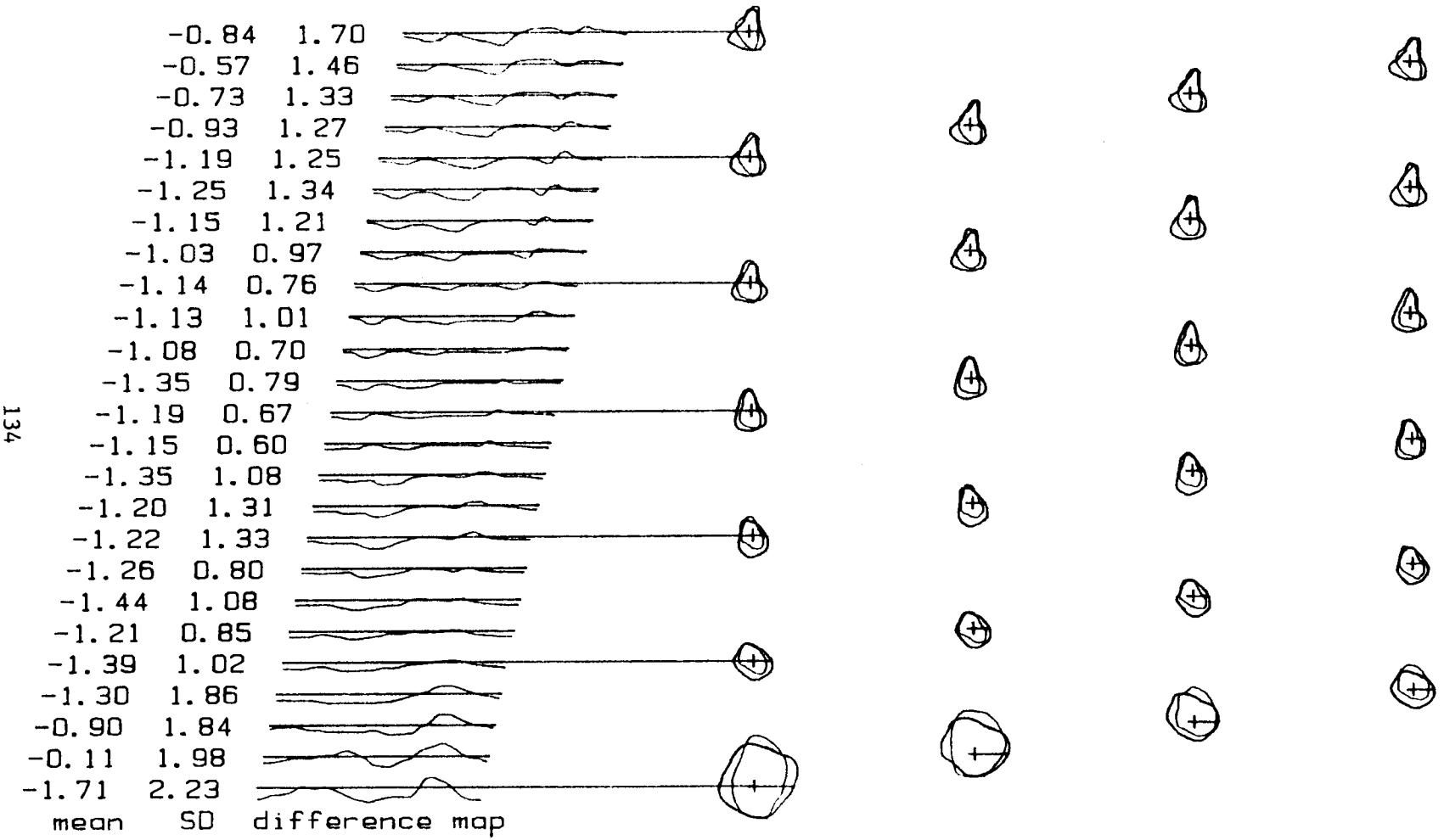

EH fibular CT shape verses non-orthogonal fibula

Mean difference -1.11 mm
Standard Deviation 1.33 mm

Amputee CT cross sections are in blue
Z increment 7.00 mm

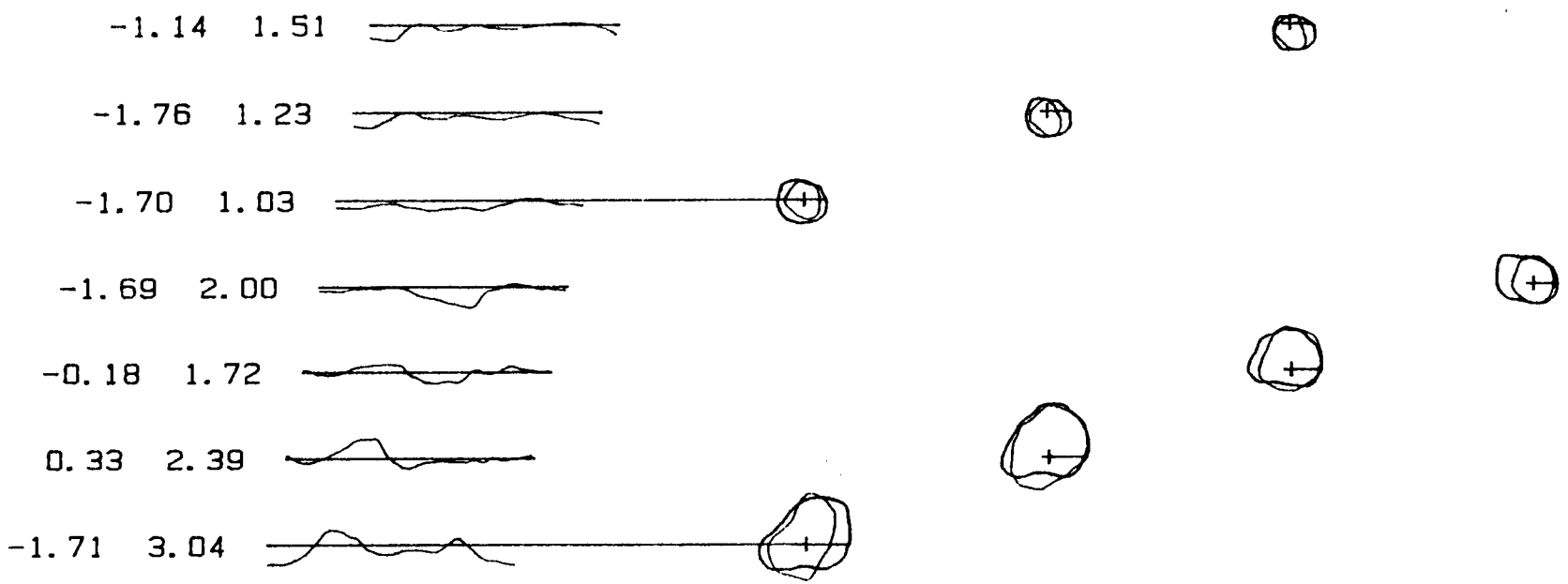

BW fibular CT shape verses non-orthogonal fibula

Mean difference -1.12 mm
Standard Deviation 2.11 mm

Amputee CT cross sections are in blue
Z increment 7.00 mm

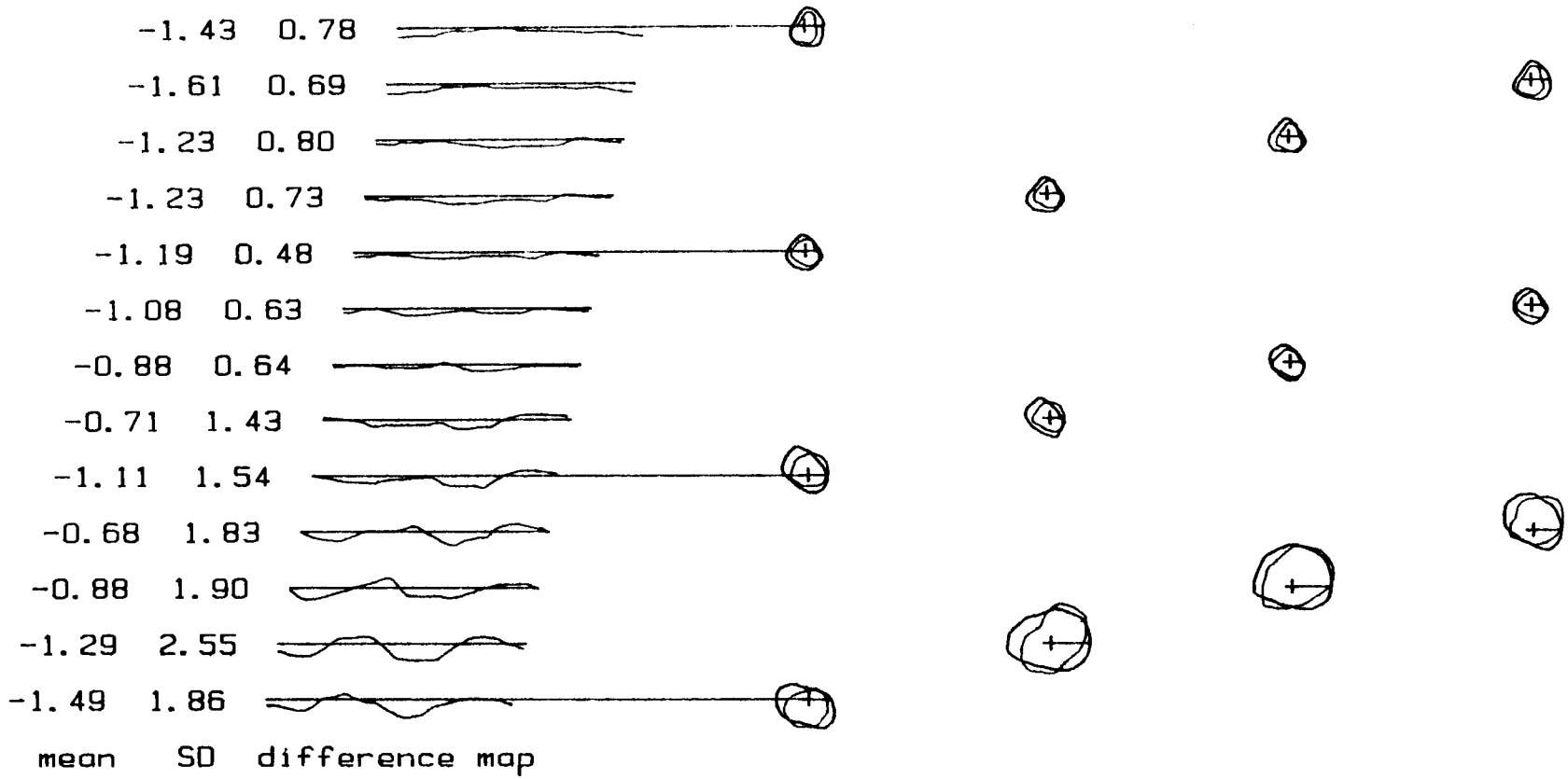

GS fibular CT shape verses non-orthogonal fibula

Mean difference -1.14 mm
Standard Deviation 1.40 mm

Amputee CT cross sections are in blue
Z increment 7.00 mm

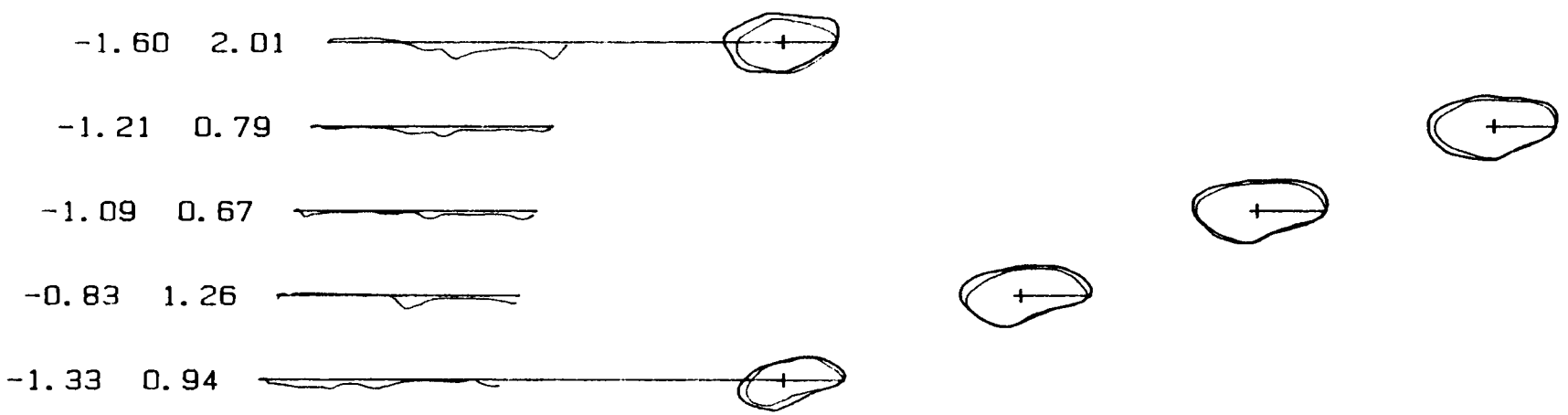

JO patellar CT shape verses ML uniform dilation patella

Mean difference -1.21 mm
Standard Deviation 1.26 mm

Amputee CT cross sections are in blue
Z increment 7.00 mm

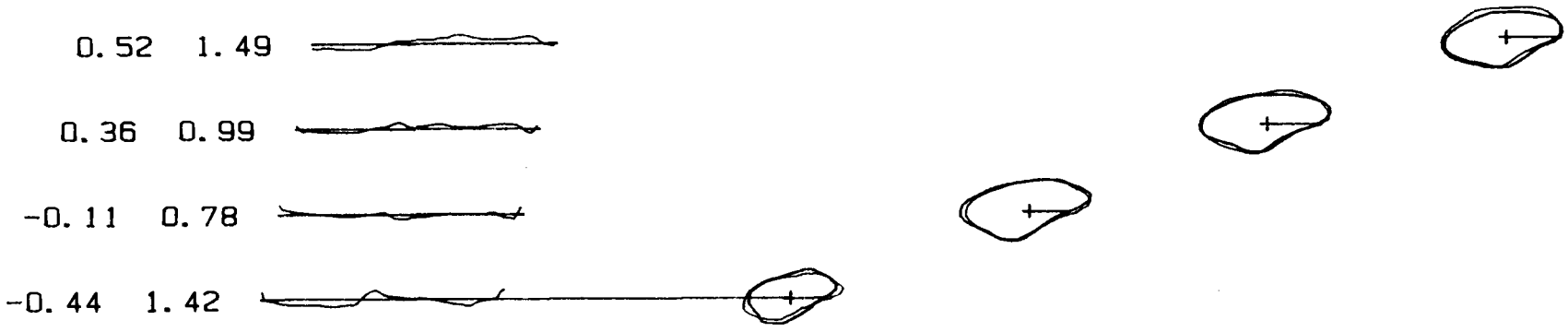

EH patellar CT shape verses ML uniform dilation patella

Mean difference 0.08 mm
Standard Deviation 1.27 mm

Amputee CT cross sections are in blue
Z increment 7.00 mm

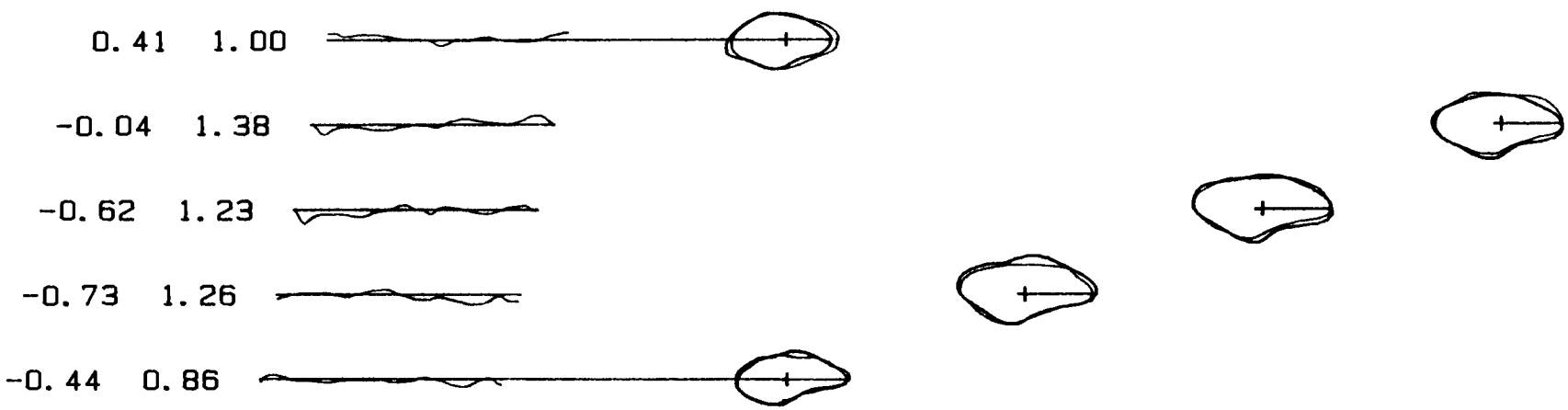

BW patellar CT shape verses ML uniform dilation patella

Mean difference -0.29 mm
Standard Deviation 1.23 mm

Amputee CT cross sections are in blue
Z increment 7.00 mm

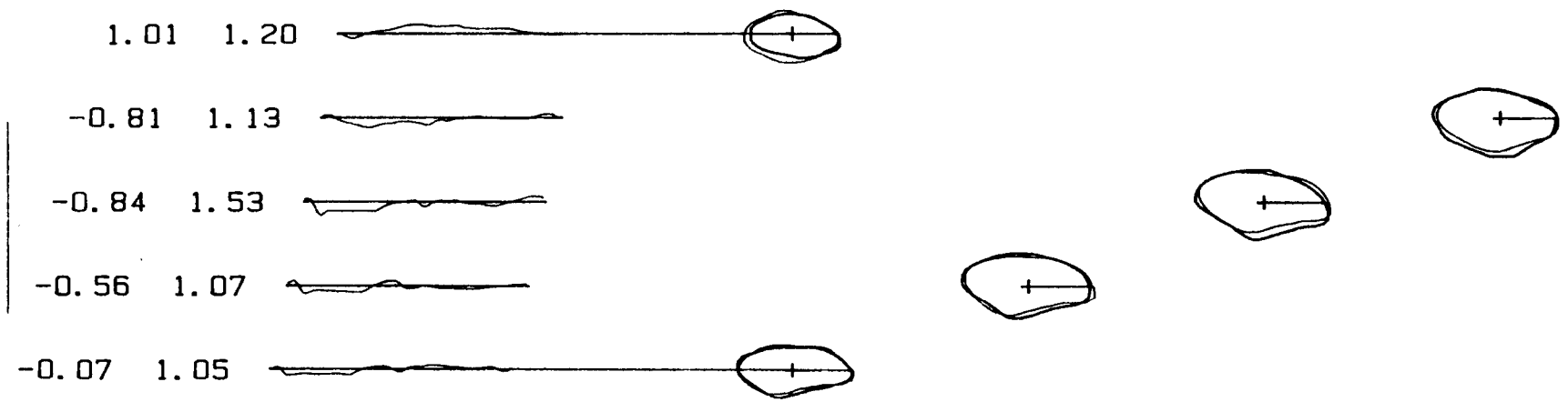

GS patellar CT shape verses ML uniform dilation patella

Mean difference -0.25 mm
Standard Deviation 1.39 mm

Amputee CT cross sections are in blue
Z increment 7.00 mm

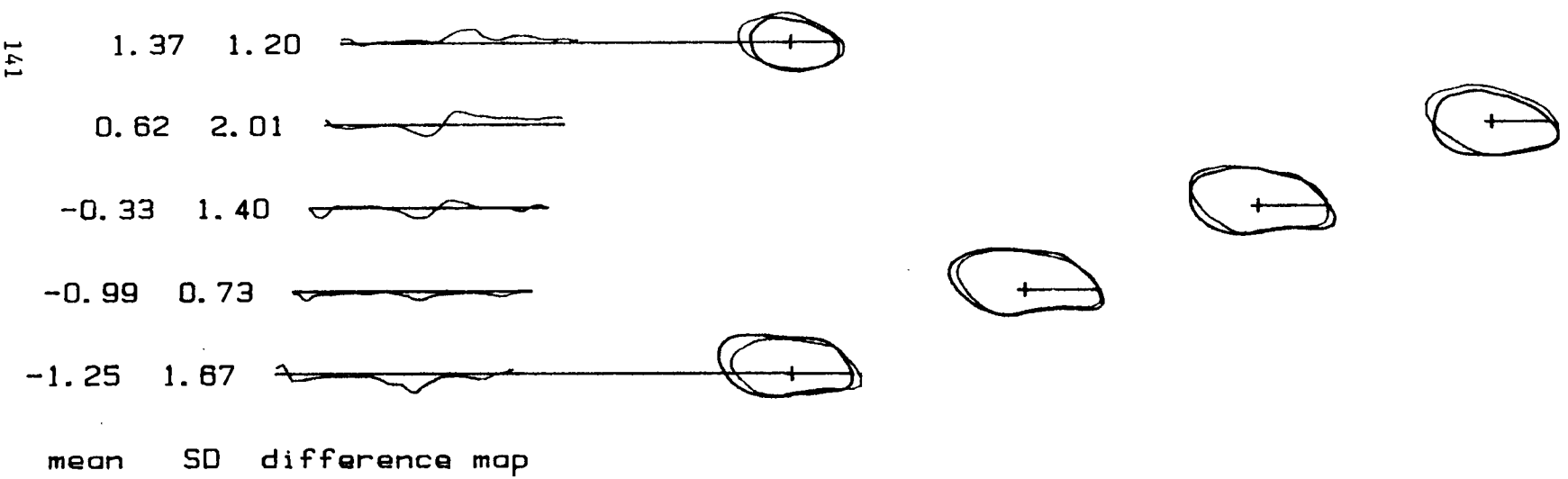

FD patellar CT shape verses ML uniform dilation patella

Mean difference -0.12 mm
Standard Deviation 1.77 mm

Amputee CT cross sections are in blue
Z increment 7.00 mm

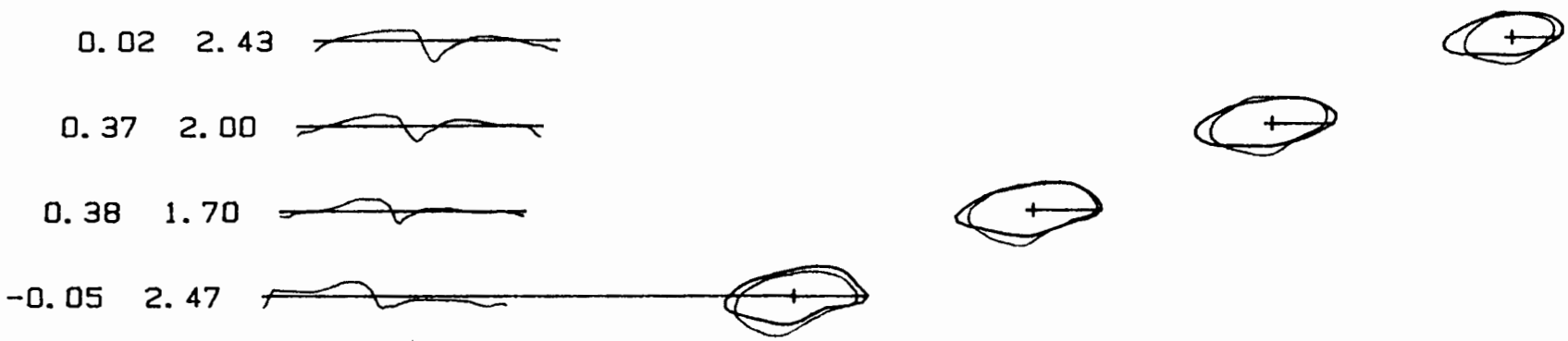

DL patellar CT shape verses ML uniform dilation patella

Mean difference 0.18 mm
Standard Deviation 2.18 mm

Amputee CT cross sections are in blue
Z increment 7.00 mm

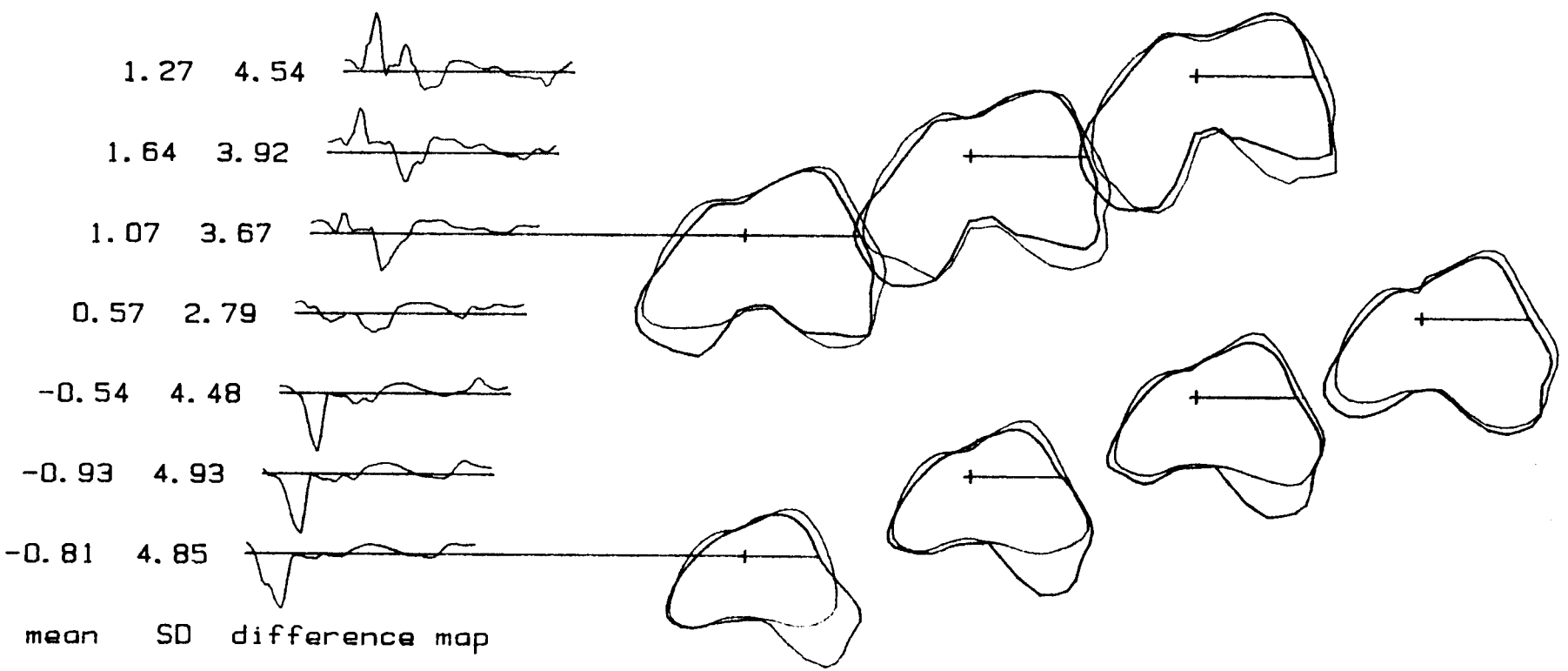

JD femoral CT shape verses uniform dilation femur

Mean difference 0.32 mm
Standard Deviation 4.34 mm

Amputee CT cross sections are in blue
Z increment 5.00 mm

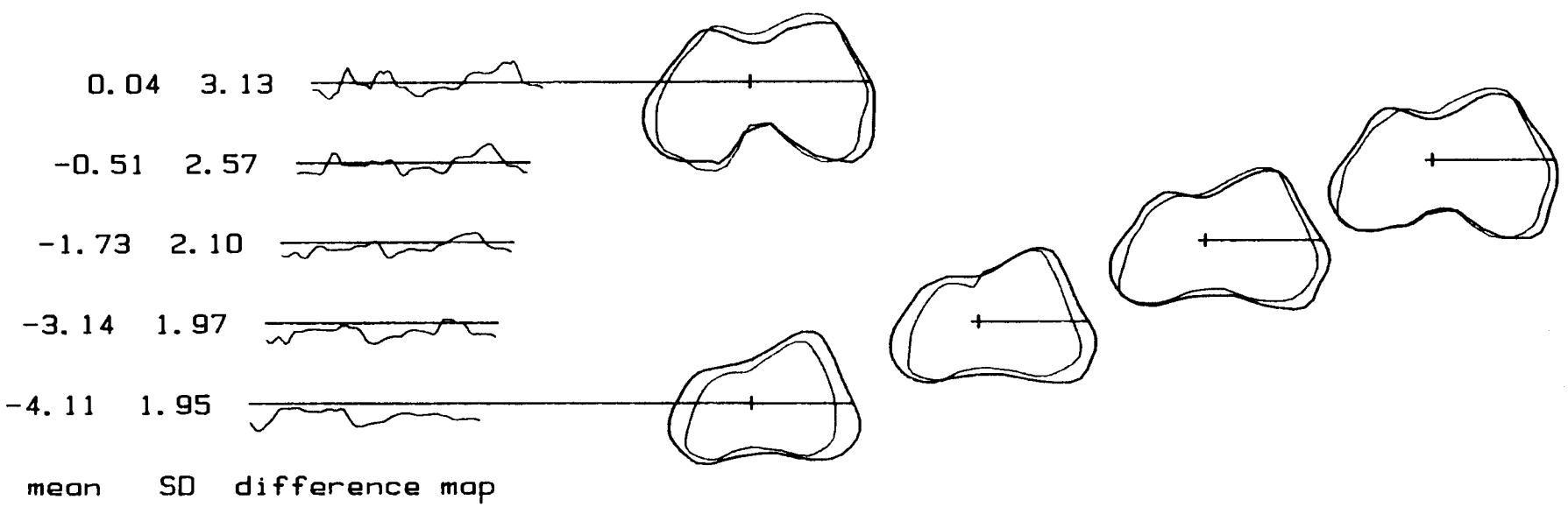

EH femoral CT shape verses uniform dilation femur

Mean difference -1.89 mm
Standard Deviation 2.85 mm

Amputee CT cross sections are in blue
Z increment 5.00 mm

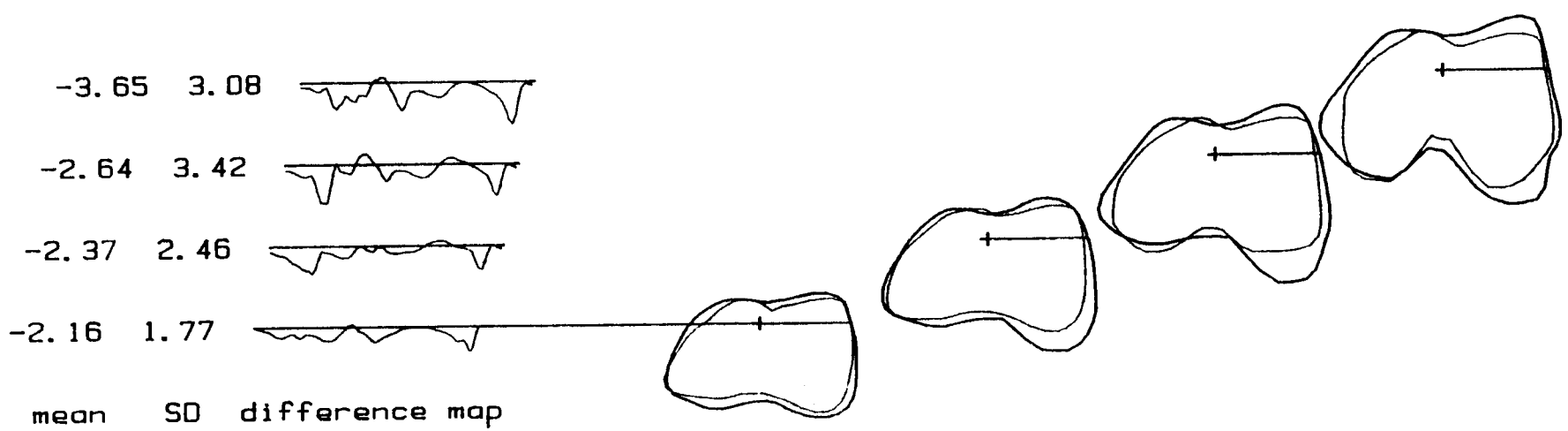

BW femoral CT shape verses uniform dilation femur

Mean difference -2.71 mm
Standard Deviation 2.82 mm

Amputee CT cross sections are in blue
Z increment 5.00 mm

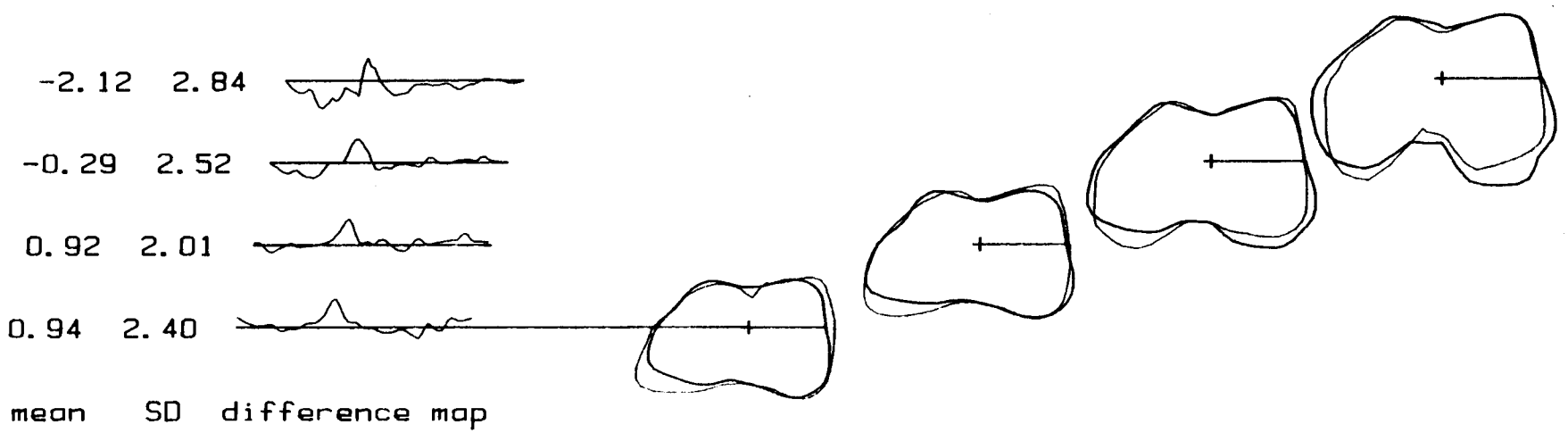

GS femoral CT shape verses uniform dilation femur

Mean difference -0.14 mm
Standard Deviation 2.76 mm

Amputee CT cross sections are in blue
Z increment 5.00 mm

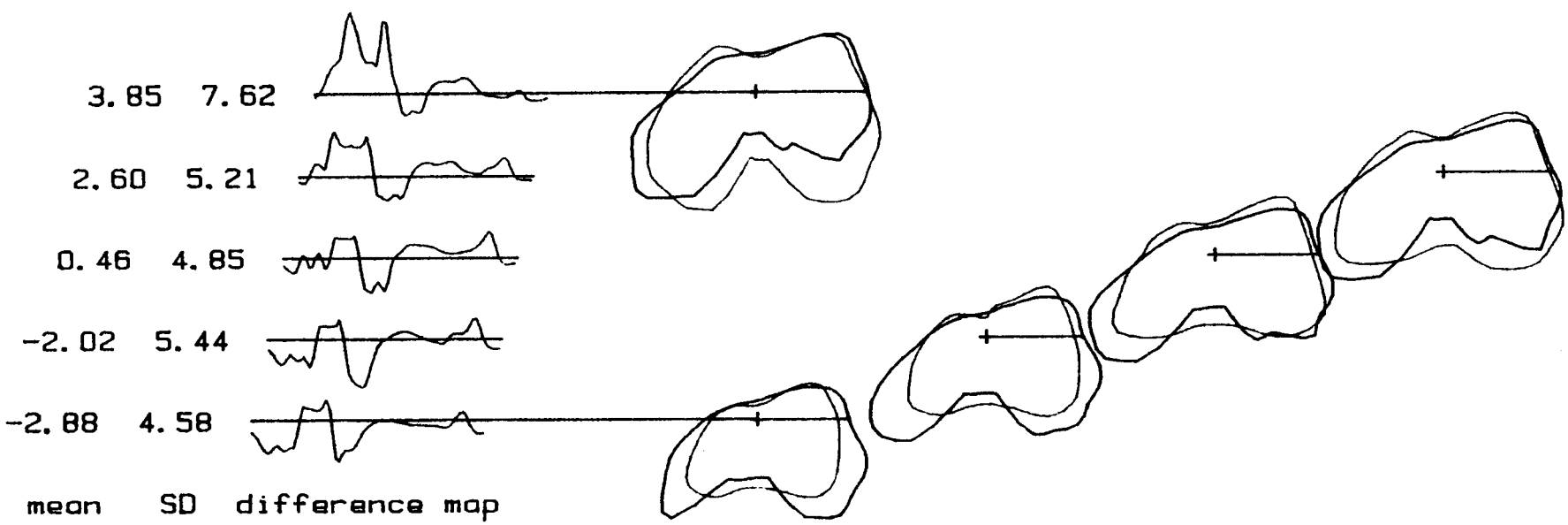

DL femoral CT shape verses uniform dilation femur

Mean difference 0.40 mm
Standard Deviation 6.21 mm

Amputee CT cross sections are in blue
Z increment 6.00 mm

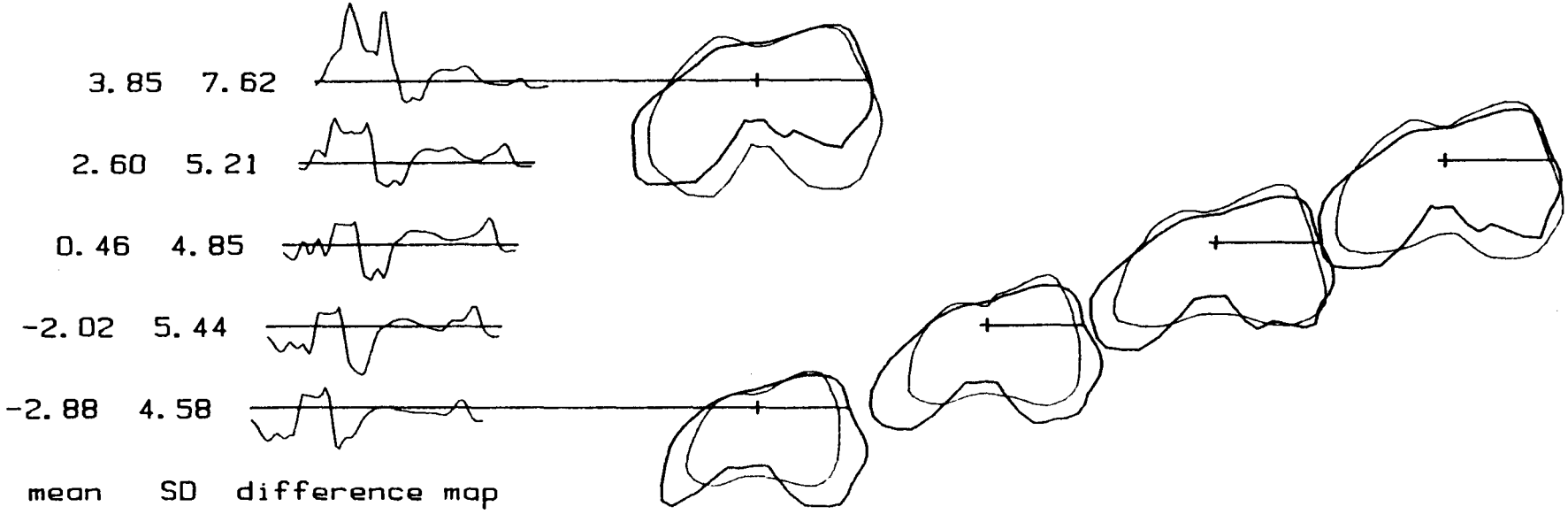

DL femoral CT shape verses uniform dilation femur

Mean difference 0.40 mm
Standard Deviation 6.21 mm

Amputee CT cross sections are in blue
Z increment 6.00 mm

Appendix III

Bone Shape Comprison Algorithm

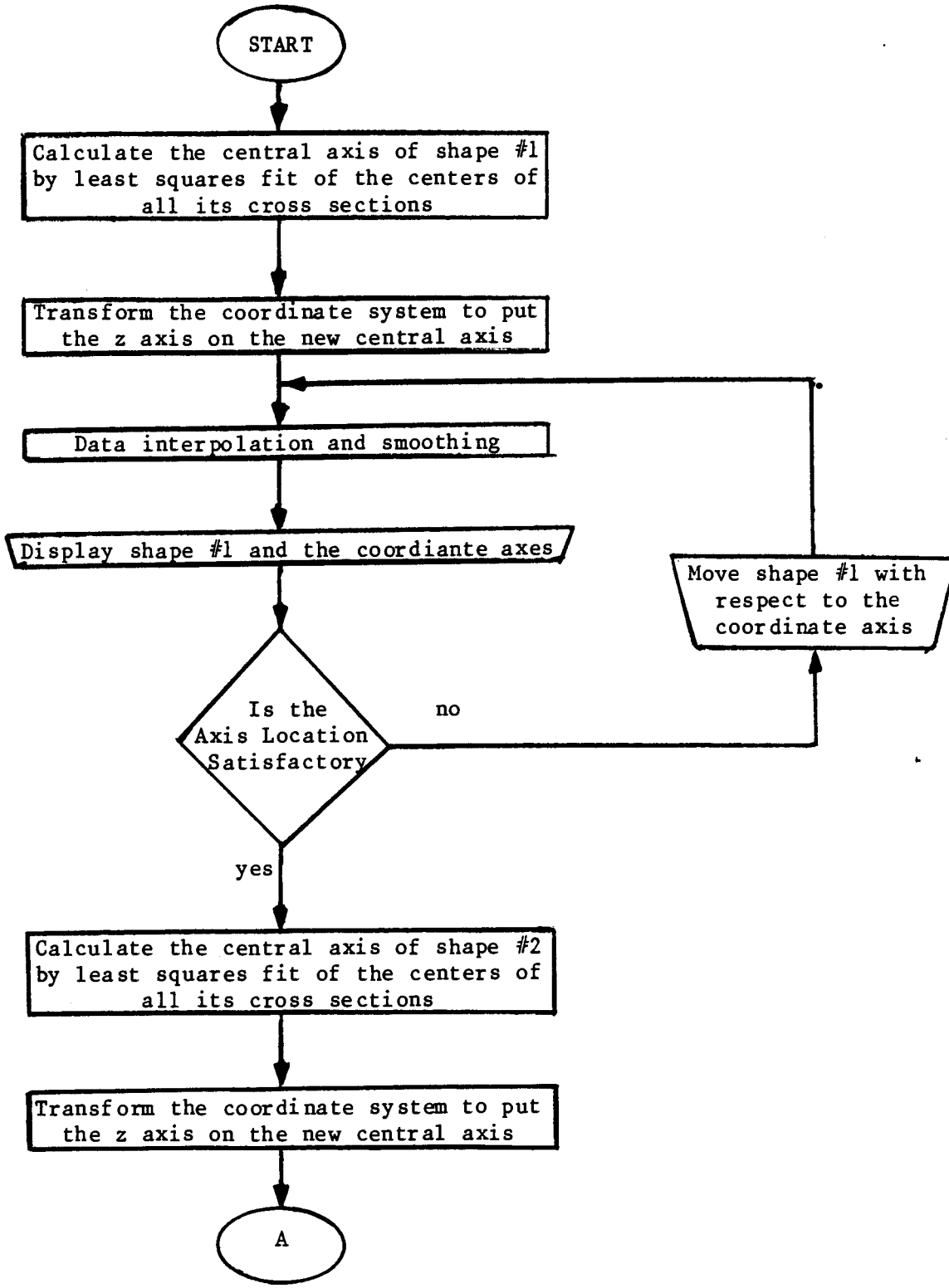

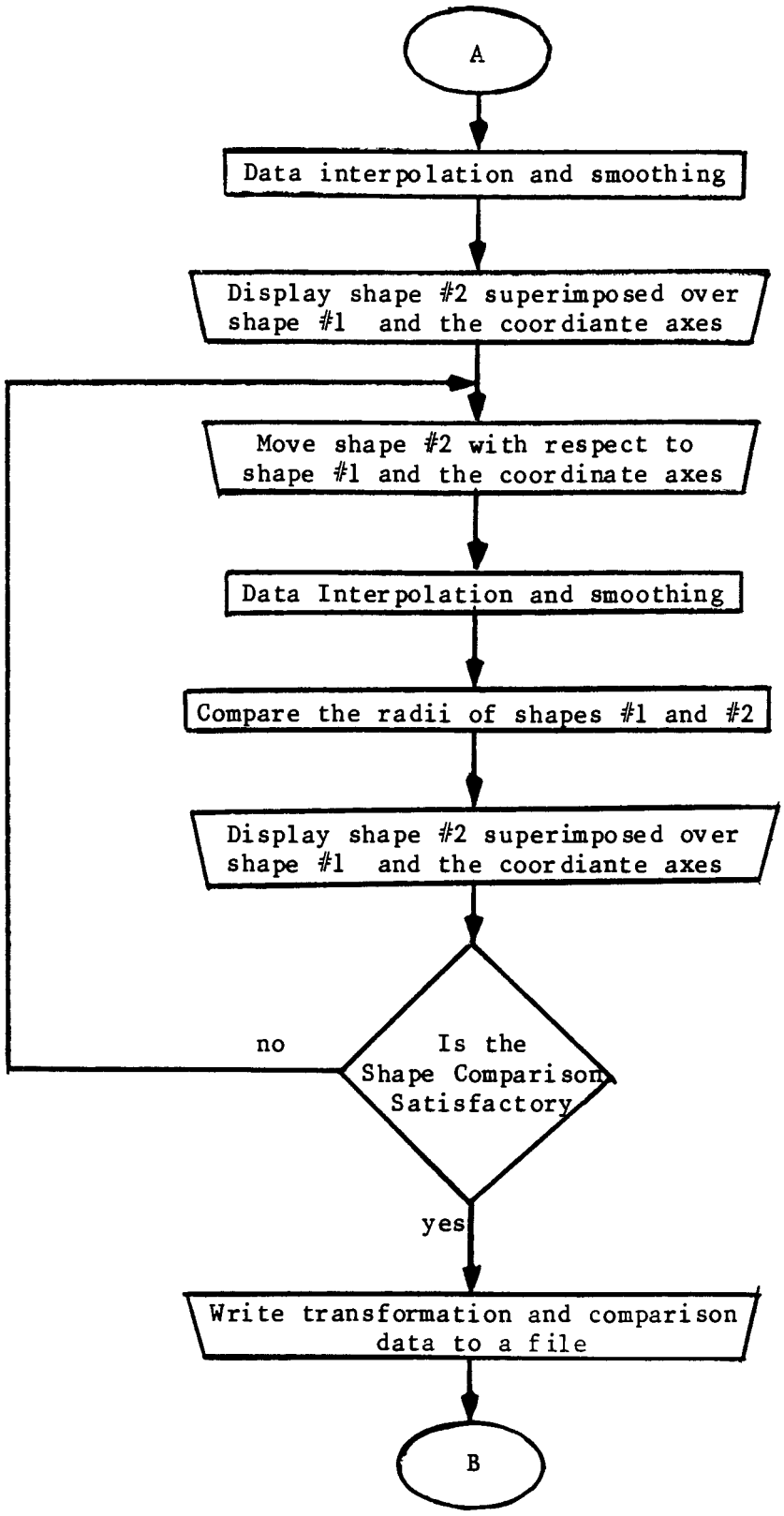
A
Data interpolation and smoothing
Display shape #2 superimposed over shape #1 and the coordiante axes
Move shape #2 with respect to shape #1 and the coordinate axes
Data Interpolation and smoothing
Compare the radii of shapes #1 and #2
Display shape #2 superimposed over shape #1 and the coordiante axes
Is the Shape Comparison Satisfactory
no
yes
Write transformation and comparison data to a file
B

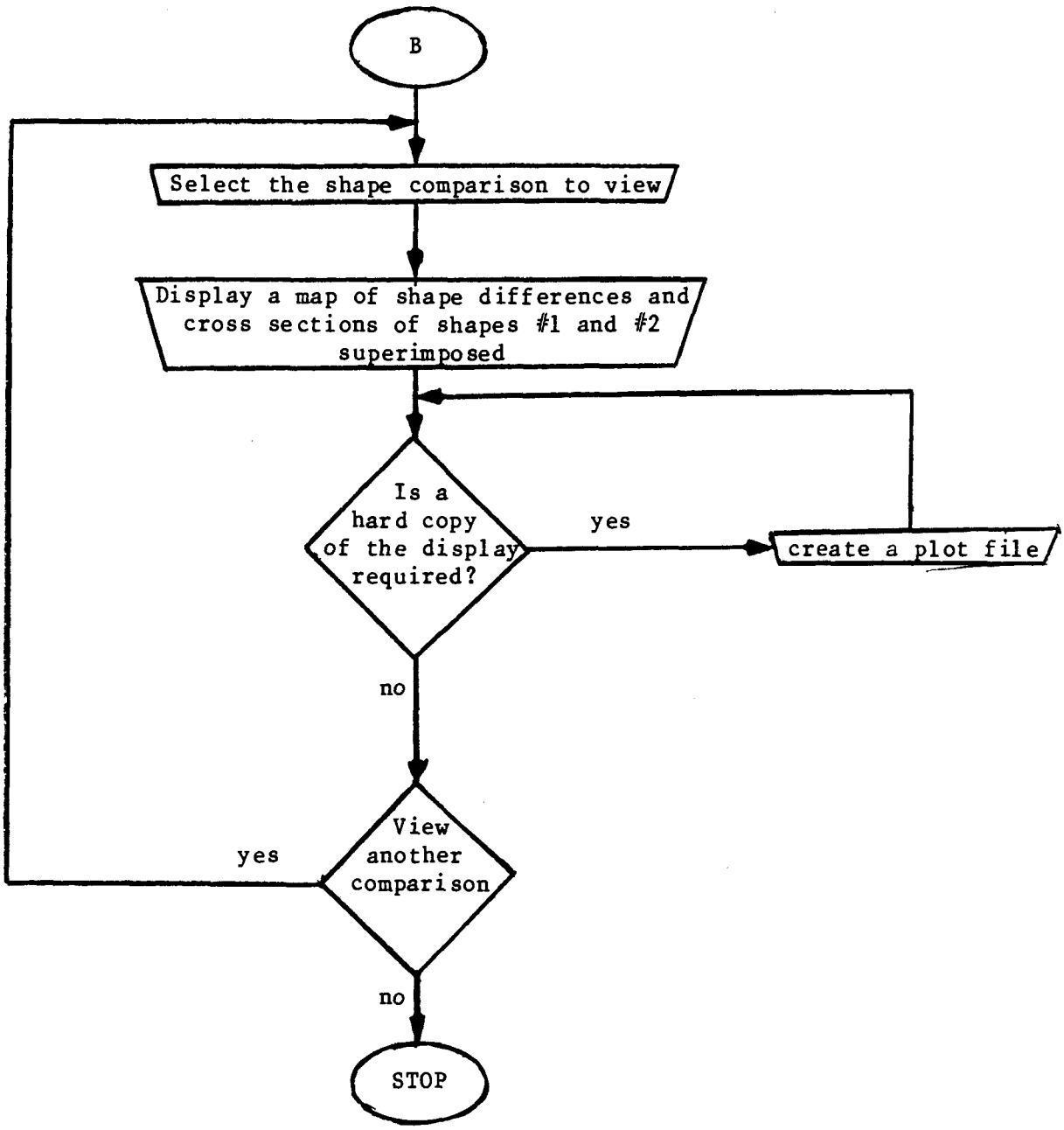
B
Select the shape comparison to view
Display a map of shape differences and cross sections of shapes #1 and #2 superimposed
Is a hard copy of the display required?
yes
create a plot file
no
View another comparison
yes
no
STOP

Data Interpolation and Smoothing

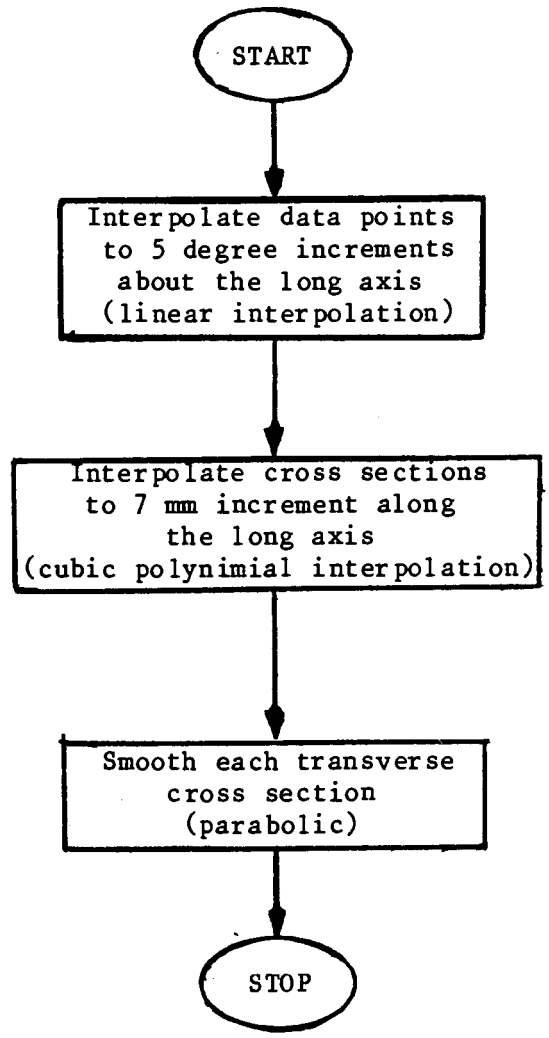

BIBLIOGRAPHY

Arnold J.S., Bartley M.H., Tont S.A., Jenkins D.P. - Skeletal Changes in Aging and Disease. Clin. Orthop. 49:17-38,1966

Ayoub M.A., Ayoub M.M., Ramsay J.D. - A Stereometric System for Measuring Human Locomotion. Human Factors 12(6):523-535,1970.

Barclay W. - Below-Knee Amputation - Prostheses. In: Prosthetic and Orthotic Practice, Ed: George Murdoch, Edward Arnold Ltd., London, p69-78,1969.

Boontje A.H. - Major Amputations of the Lower Extremity for Vascular Disease. Prosthetics and Orthotics International 4(2):87-89, 1980.

Breackey J.W. Prefabricated Below Knee Sockets for the Maturing Stump. Bulletin of Prosthetics Research,10-19:42-51,1973

Breimann R.S., Beck J..W., Korobkin M, et al. - Volume Determinations using Computed Tomography. AJR. 138:329-333,1982.

Christie J., Lamb D.W., McDonald J.M., Britten S. - A Study of Stump Growth in Children with Below Knee Amputations. J. Bone Jt. Surgery (Br) 61-B(4):464-465, 1979

Condie D.N. - Use of a Light Line in Silhouetting. In: Three Dimensional Shape Sensing and Reproduction of Limbs and Limb Remnants, University of British Columbia, 1973.

Cooper D. - Term Project, Computers in Biomedical Research - A pilot study, unpublished, 1982

Cumming G.R., Borysyk L., Bailey G., Garand T. - Calf X-ray Measurements Correlated with Age, Body Build and Physical Performance in Boys and Girls. J. Sports Med. 13:90-95, 1973

Davies R. - Bioengineering Centre, University College London, Roehampton Lane, London, SW15 5PR.

Ebskov B. - Choice of Surgery in Lower Extremity Amputation - Nationwide Survey. Prosthetics and Orthotics International 7(2):58-60, 1983.

Erickson M.F. - Aging Changes in the Medullary Cavity of the Proximal Femur in American Blacks and Whites. Am. J. Phys. Anthrop. 51:563-570, 1979.

Flodmark O. - Personal Communication, Department of Radiology, University of British Columbia,1984.

Foort J. - Status Report. Instant Sockets for Shank Amputees. Prosthetics and Orthotics Research and Development Unit, Manitoba Rehab. Hosp., Winnipeg, 1967.

Foort J. - personal communication, 1984.

Frobin W., Hierholzer E. - Rasterstereography: A Photogrammetric Method for Measurement of Body Surfaces. Photogrammetric Eng. and Remote Sensing, 47(12):1717-1724,1981.

Frobin W., Hierholzer E. - A Stereophotogrammetric Method for the Measurement of Body Surfaces using a Projected Grid. Proc. Soc. Photo-Optical Instr. Eng., 166:39,1978.

Gardner H.F. - Endoskeletal Structures for Lower-Extremity Prostheses. Bull. Pros. Res. BRP 10-13:113-119,1970.

Garn S.M., Rohmann G.G., Wagner B., Davila G.H., Ascoli W. - Population Similarities in the Onset and Rate of Adult Endosteal Bone Loss. Clinical Orthop. 65:51-60, 1969

Hannam A.G., Wood W.- Department of Dentistry, University of British Columbia, personal communication, November 1985.

Harada Y., Takemitsu Y., Imai M. - The Role of Contour Line Photography Using the Light Cutting Method and Moire Topography in School Screening for Scoliosis, In: Proceedings of International Symposium on Moire Fringe Topography and Spinal Deformity, Ed: Morland, Pope and Armstrong, Vermont, USA, 113-121, 1981.

Harada Y., Takemitsu Y., Imai M. - Follow-up Study on Hump Measurement in Idiiopathic Scoliosis Using Moire Fringe Topography, In: Proceedings of Second International Symposium on Moire Fringe Topography and Spinal Deformity, Ed: Drerup, Frobin and Hierholzer, Munster, West Germany, 149-154, 1982.

Hendee, W.R. - Medical Radiation Physics, Roentgenology, Nuclear Medicine and Ultrasound. 2nd Ed., Year Book Medical Publishers, Inc., Chicago, pp 353-389, 1979

Henderson J.M., Heymsfield S.B., Horowitz J., Kutner M.H. - Measurement of Liver and Spleen Volume by Computed Tomography. Radiology, 141:525-527,1981.

Herman G.T. - Applications of 3 dimensional Computer Graphics to surgical Planning and Evaluation. Proceedings of National Computer Graphics Association, 2:66-74, 1984.

Hierholzer E., Frobin W. - Automatic Measurement of Body Surfaces using Rasterstereography. In: proceedings of Optics in Biomedical Sciences sattelite meeting ICO-12,1981.

Hounsfield G. - Computerized Transverse Axial Scanning (Tmography): Part 1. Description of system. Br. J. Radil. 46:1016,1973.

Joel H.C. - The Corpograph - a Simple Photographic Approach to Three-Dimensional Measurements. Biostereometrics 74, Proceedings of the Symposium of Commision V, Washington, D.C., 1974.

Johnson E.M., Capowski J.J. - A System for the Three-Dimensional Reconstruction of Biological Structures. Computers and Biomedical Research 16:79-87,1983.

Katz K., Susak Z., Seliktar R., Najenson T. End-Bearing Characteristics of Patellar-Tendon-Bearing Prostheses - A Preliminary Report. Bull. Prosth. Res. (BPR 10-32), 16(2):55-68,1979.

Kawamura T., Wada J., Kotani M. - Computerized Moire Topography and Anterior Chest Wall Deformity, In: Proceedings of Second International Symposium on Moire Fringe Topography and Spinal Deformity, Ed: Drerup, Frobin and Hierholzer, Munster, West Germany, 241-247, 1982.

Kondraske G.V., Potvin A.R., Tourtellotte W.W., Syndulko K. - A Computer Based system for Quantification of Neurologic Function. IEEE Trans. Biomed. Eng. BME-31:404-414, 1984

Kuhl D., Edwards R. - Image Separation Radioisotope Scanning, Radiology,80(4):653,1963

Kuhl D., Hale J., Eaton W. - Transmission Scanning: A Useful Adjunct to Cnventinal Emission Scanning for Accurately Keying Isotope Deposition to Radiographic Anatomy. Radiology, 87:278,1966

Kuhn G.G. - Kondylen Bettung Munster am Unterschenkel Stumph 'KBM-Prothese'. Atlas d'Appareillage Prothetique, No. 14,1966.

Langrana N.A., Leppard D., Alexander H., Weiss A. - Kinematics of the Knee - A Computer Graphics Model. Amer. Soc. of Mechanical Engineers Journal. 40:1-8,1982.

Latamore G.E. - Creating 3-D Models for Medical Research, Computer Graphics World. 6:31, 1983.

Lawrennce R.B., Crawford H.V., Knox W., Davies R.M. - Thermoplastics for Prosthetic Application. In: Report from the Bioengineering Centre, University Collede London, Roehampton, London, pp 9-22,1981.

Leavitt L., Zuniga E., Calvert J., Conzoneri J., Peterson C. - Gait Analysis and Tissue-Socket Interface Pressures in Above-knee Amputees. Southern Medical Journal 65:10, 1972.

Ledley R., DiChiro G., Lussenhop A., Twigg H. - Computerized Transaxial X-ray Tomography of the Human Body. Science, 186:207,1974

Lew W.D., Lewis J.L. - An Anthropometric Scaling Method With Application To The Knee. J. Biomechanics 10:171-181, 1977

Lewis J.L., Lew W.D., Zimmerman J.R. - A Nonhomogeneous Anthropometric Scaling Method Based on Finite Element Principles. J. Biomechanics 13:815-824, 1980

Li D. - Personal Communication, Department of Radiology, Health Sciences Centre Hospital, University of British Columbia, 1984.

Lyquist E. - Recent Variants in the PTB Prosthesis. In: Prosthetics and Orthotics, Ed: George Murdoch, Edward Arnold Ltd., London, p79-88,1969.

Mandrup-Poulsen T., Jensen J.S. - Incidence of Major Amputations Following Gangrene of the Lower Limb. Prosthetics and Orthotics International 6(1):35-37, 1982.

Marsh J.L., Vannier M.W. - The 'Third' Dimension in Craniofacial Surgery. Plastic and Reconstructive Surgery 71(6):759-767,1983.

Martin R.B., Atkinson P.J. - Age and Sex Related Changes in the Structure of the Human Femoral Shaft. J. Biomechanics 10:223-232,1977

Meadows D.M., Johnson W.O., Allen B. - Generation of Surface Contours by Moire Pattern. Appl. Optics, 9:942-947, 1970.

Mehta M.H. - Moire Topography and Associated Asymmetries in Scoliosis, In: Proceedings of International Symposium on Moire Fringe Topography and Spinal Deformity, Ed: Morland, Pope and Armstrong, Vermont, 186-1189, 1981.

Micro Control Systems Inc., 143 Tunnel Road, Vernon, CT, 06066.

Morgan C.L. - Basic Principles of Computed Tomography. University Park Press, Baltimore,1983

Morrison J.B. - The Mechanics of the Knee Joint in Relation to Normal Walking. J. Biomechanics 3:51-61, 1970

Moss A.A.,Friedman M.A., Brito A.C. Determination of Liver, Kidney, and Spleen Volumes by Computed Tomography: an Experimental Study in Dogs. J. Comput. Assist. Tomography. 5:12-14,1981.

Moss A.A., Cann C.E., Friedman M.A., Marcus F.S.., Resser K..J., Beringer W. - Volumetric CT analysis of Hepatic Tumors. J. Comput. Assist. Tomogr. 5:714-718,1981.

Mysorekar V.R., Nanddedkar A.N. - The Soleal Line. The Anatomical Record 206:447-451,1983

Odendorf W. - Isolated Flying Spot Detection for Radiodensity Discontinuities - Displaying the Internal Structural Pattern of a Complex Object. IRE Trans. Biomed. Elec., BME 8:68,1961

Ohtsuka Y., Shinoto A., Inoue S. - Application of Moire Topography and Low-dose X-Ray Imaging to School Screening Program of Scoliosis. In: Proceedings of International Symposium on Moire Fringe Topography and Spinal Deformity, Ed: Morland, Pope and Armstrong, Vermont, 102-112, 1981.

Persson B.M., Liedberg E. A Clinical Standard of Stump Measurement and Classification in Lower Limb Amputees. Prosthetics and Orthotics International, 7:17-24,1983

Philadelphia - Proceedings of the Workshop on Locomotion and the Clinical Analysis of Gait. Dec. 6-8, 1976.

Pierquin L., Fajal G., Paquin J.M. - Prothese Tibiale a Emboitage Supracondylien. Atlas d'Appareillage Prothetique et Orthopadique,No.1,1964.

Pierquin L., Paquin J.M., Fajal G. - Discussion sur les Prostheses Tibiales. Atlas d'Appareillage Prothetique et Orthopadique,No.9,1965.

Pierrynowski M.R., Morrison J.B. - A Simplified Three-Dimensional Filming Technique. Abstract in Proceedings of the Can. Assoc. of Sports Sciences Conference, 1980.

Pierrynowski M.R. - A Physiological Model for the Solution of Individual Muscle Forces During Normal Human Walking. Ph.D. Thesis, Simon Fraser University, 1982.

Pierrynowski M.R., Morrison J.B. - A Physiological Model for the Solution of Individual Muscle Forces During Normal Human Walking: Theoretical Aspects. Math. Biosciences, 75:65-101,1985.

Pierrynowski M.R., Morrison J.B. - Estimating the Muscle Forces Generated in the Human Lower Extremity when Walking: A Physiological Solution. Math Biosciences, 75:43-68,1985.

Plato C.C., Purify F.E. - Age Sex and Bilateral Variability in Cortical Bone Loss and Measurements of the Second Metacarpal. Growth 46(2):100-112,1982

Polhemus Navigation Sciences Division, McDonnell Douglas Electronics Company,
P.O. Box 560 Colchester, Vermont, 05446

Pynsent P.B., Fairbank J.C.T., Clack F.J., Phillips H. Computer Recording of Anatomical Points in Three-Dimensional Space. J. Biomed. Eng.5:137-140,1983.

Raab F.H., Blood E.B., Steiner T.O., Jones H.R. - Magnetic Position and Tracking System. IEEE Transactions on Aerospace and Electronic Systems AES-15(5):709-718, 1979

Radcliffe C.W., Foort J. - The Patellar-Tendon-Bearing Below-Knee Prosthesis. Biomechanics Laboratory, School of Medicine, University of California, Berkeley, 1961.

Reid M.H. - Quantitative Sterology and Radiologic Image Analysis. Part I. Computerized Tomography and Ultrasound. Med. Phys. 9:346-360,1982.

Rice J.R. - Matrix Computations and Mathematical Software. Ed.: C.E. Stewart & F.A. Neal, McGraw-Hill Computer Science Series, New York, p45-46, 1981

Riseborough E.T., Barrett I.R., Shapiro F. - Growth Disturbences Following Distal Femoral Fracture Separations. J. of Bone and Jt. Surgery 65-A(7):885-893,1983

Ross W.D., Ward R. - Human Proportionality and Sexual Dimorphism. In: Sexual Dimorphism in Homo Sapiens, R. Hall (ed), Praeger, New York, 317-361, 1982.

Saito Y., Oshima T. - A New Three-Dimensional Measuring System for the Natural Hand and Foot. In: the proceedings of the Second International Conference on Rehabilitaion Engineering, Ottawa, Ontario, 151-152, 1984.

Saunders C.G. - Replication From 360 Degree Moire Sensing, In: Proceedings of International Symposium on Moire Fringe Topography and Spinal Deformity, Ed: Morland, Pope and Armstrong, Vermont, 122-131, 1981.

Saunders C.G. - Automatic Shape Definition Systems - A Review. Report to: Health and Welfare Canada, 6610-1255-51,1982.

Saunders C.G., Dean D. - A Software Package for Design and Manufacture of Prosthetic Sockets for Trans-Tibial Amputees. IEEE, in print, 1984.

Saunders C.G., Fernie G.R. - Automated Prosthetic Fitting. In: Procedings of the Second International Conference on Rehabilitation Engineering, Special Sessions, Ottawa, pp239-242,1984.

Saunders C.G., Panych L., Dean D. - Sculpting of 3-D Free Form Prosthetic Sockets Using Computer Graphics Techniques, in print, 1984.

Saunders C.G., Foort J., Bannon M., Dean D., Panych L. - Computer-Aided Design of Prosthetic sockets for Trans-Tibial Amputees. Prosthetics and Orthotics International, in print, 1985.

Saunders C.G. - A Three Dimensional Digitizer - MSc. Thesis, Electrical Engineering, UBC, March 1986.

Saunders C.G., Steinke T., Cooper D.G. - A Portable 3D digitizer for use in Prosthetic/Orthotic Applications. Abstract submitted to International Society for Prosthetics and Orthotics Fifth World Congress, Copenhagen, 1986.

Sevastrikoglou J.A., Eriksson U., Larson S.E. - Skeletal Changes of the Amputation Stump and the Femur on the Amputated Side. Acta Orthop. Scandinav. 40:624-633,1969

Scheid F. - Schaum's Outline Series, Theory and Problems of Numerical Analysis. McGraw-Hill, New York, p243-247, 1968.

Suzuki N., Yamashita Y., Yamaguchi Y., Armstrong G.W.D. - Measurement of Posture Using Moire Topography, In: Proceedings of International Symposium on Moire Fringe Topography and Spinal Deformity, Ed: Morland, Pope and Armstrong, Vermont, 122-131, 1981.

Takasaki H. - Moire Topography. Appl. Optics 9:1467-1472, 1970.

Takasaki H. - Moire Topography from its Birth to Practical Application. Optics and Lasers in Engineering. 3:3-14, 1982.

Theocaris P.S. - Moire Topography of Curved Surfaces. Expl. Mech. 7:289-296, 1967.

Turner-Smith A., Hawkin M., Osborne M. - Instrumentation for Shape Investigation - ISIS. Oxford Orthopaedic Engineering Centre Report,pp40-43,1982.

Udupa J.K. - Display of 3-D information in Discrete 3-D Scenes Produced by Computerized tomography, Proceedings of IEEE, 71:420, 1983.

Vannier M.W., Marsh J.L., Warren J.O. - Three dimensional CT reconstruction Images for Craniofacial Surgical Planning and Evaluation. Computer Graphics, 17:263, 1983.

Vannier M.W., Totty W.G., Stevens W.G., Weeks P.M., Dye D.M., Daum W.J., Gilula L.A., Murphy W.A., Knapp R.H. - Musculoskeletal Applications of Three-Dimensional Surface Reconstructions. Orhto. Clinics of North Amer. 16(3):543-555, 1985.

Van Gerven D.P. - Thickness and Area Parameters of Skeletal Involution in the Humerus, Femur, and Tibia. J. Gerontology 28(1):40-45, 1973

Wilson L.A., Lyquist E., Radcliffe C.W. - Air-Cushion Socket for Patellar-Tendon-Bearing Below-Knee Prosthesis. Tech. Rep. 55, Department of Medicine and Surgery, Veterans Administration, Washington, D.C.,1968.

Wilson L.A., Abrahamson M.A., Effeney D.J. - Improvement of the Air-Cushion Socket for Below-Knee Amputees. In: proceedings of the Second International Conference on Rehabilitaion Engineering, Ottawa,239-240,1984.

Windischbauer G. - Personal Communication, 1982.
Institut fur medizinische Physik Veterinarmed
Universitat Wien
Linke Bahngasse 11
A - 1030 Wien, Austria

Yamashita Y., Suzuki N., Oshima M., Yamaguchi Y. - Three-Dimensional Stereometric Measurement System Unsing Optical Scanners, Cylindrical Lenses, and Line Sensors, In: Proceedings Biostereometrics '82, San Diego, pp67-73,1982.